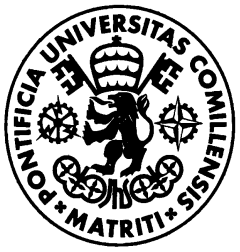

UNIVERSIDAD PONTIFICIA COMILLAS

ESCUELA TÉCNICA SUPERIOR DE INGENIERÍA (ICAI)

OFFICIAL MASTER'S DEGREE IN THE ELECTRIC POWER INDUSTRY

Master's Thesis

THE IMPACT OF STOCHASTIC VARIABILITY IN INSOLATION AND CAPITAL COST OF BATTERIES ON OPTIMAL MICROGRID DESIGN

Author: **Tim Schittekatte**

Supervisor: **Dr. Micheal Stadler**

Co-Supervisor: **Dr. Gonçalo Ferreira Cardoso**

Madrid, July 2015

Official Master's Degree in the Electric Power Industry (MEPI)
Erasmus Mundus Joint Master in Economics and Management of Network Industries (EMIN)

Master's Thesis Presentation Authorization

THE STUDENT:

Tim Schittekatte

.....

THE SUPERVISOR

Dr. Micheal Stadler

Signed: ..... Date: 06/30/15

THE CO-SUPERVISOR

Dr. Gonçalo Ferreira Cardoso

Signed: Gonçalo Cardoso Date: 06/30/2015

Authorization of the Master's Thesis Coordinator

Dr. Javier García González

Signed.: ..... Date: ...../ ...../ .....

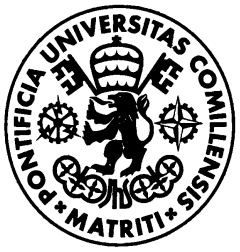

UNIVERSIDAD PONTIFICIA COMILLAS

ESCUELA TÉCNICA SUPERIOR DE INGENIERÍA (ICAI)

OFFICIAL MASTER'S DEGREE IN THE ELECTRIC POWER INDUSTRY

Master's Thesis

THE IMPACT OF STOCHASTIC VARIABILITY IN INSOLATION AND CAPITAL COST OF BATTERIES ON OPTIMAL MICROGRID DESIGN

Author: **Tim Schittekatte**

Supervisor: **Dr. Micheal Stadler**

Co-Supervisor: **Dr. Gonçalo Ferreira Cardoso**

Madrid, July 2015

UNIVERSIDAD PONTIFICIA COMILLAS

Abstract

Lawrence Berkeley National Laboratory
Energy Storage and Distributed Resources Department

Master in Economics and Management of Network Industries (EMIN)

The impact of stochastic variability in insolation and capital cost of batteries on optimal microgrid design

by Tim Schittekatte

In this research the impact of solar irradiation variability and battery prices on cost-optimal distributed energy resource (DER) investments is analyzed. A novel methodology is proposed to capture the impact on power demand charges caused by moving clouds in microgrids where photovoltaic (PV) arrays, electrochemical energy storage and generators are considered. This is done using a statistical approach to decouple accounting of energy and power demand economics, and allows events of different time lengths to be simultaneously analyzed. The methodology is implemented in the Distributed Energy Resources Customer Adoption Model (DER-CAM), and four case studies are performed.

In DER-CAM, a state of the art mixed integer linear model used to find cost- and CO_2-optimal DER portfolios of energy supply in decentralized energy systems, PV output is calculated using monthly average-hourly solar irradiation data. This approach fails to capture the effect of fast moving clouds and may sometimes lead to inaccurate results. The methodology introduced in this work estimates the variability of PV output and the resulting impact on power demand charges for different confidence levels taking into account that existing energy storage may offset drops in PV output if sufficiently charged, or that fast-ramping generator units may also be used for the same purpose. This formulation is embedded in the investment decision process, and is reflected in the optimal DER portfolio provided by DER-CAM.

Results obtained in the case studies suggest that in previous DER-CAM formulations the optimal capacity of PV was overestimated in cases where storage capacity was not sufficient to compensate for drops in PV output. Also it was found that the optimal capacity of on-site generators might have been slightly underestimated in some cases. The new model formulation depicts the economic value of PV more accurately while effectively capturing the synergic economic benefits of PV paired with electric storage.

Acknowledgements

First of all I would like to thank my supervisor Dr. Micheal Stadler for giving me the opportunity to conduct my thesis research at the Berkeley Labs. His guidance and support are greatly appreciated. I am also very grateful to my co-supervisor Dr. Gonçalo Cardoso. I could always pass by his office to shoot questions. The very frequent discussions we had, which at times almost reached a philosophical level, were of crucial importance for the development of this work. Thank you for your patience, advice and time, Gonçalo! Also I would like to thank the other people working at the Grid Integration Group at LBNL for their advice and encouragements.

I would like to thank as well Dr. Javier García González for coordinating the EMIN master and making my stay in Berkeley possible. I am very happy I got the opportunity to be part of this great program. I am grateful to the whole team at Universidad Pontificia Comillas and Université Paris-Sud for organising excellent courses. Also special thanks to Dr. Yannick Perez for taking care of the organisation in Paris and his support.

Furthermore I was very lucky to be part of an excellent generation of EMIN students, thank you for the good times. Thanks to Islam Abdin for the great collaboration the past two years and to Martin Roach for keeping me up to date with the latest microgrid related news! Also I would like to thank my friends and family back in Belgium, especially my parents. Thank you for your endless support, trust and giving me the freedom I need.

"Things always become obvious after the fact" - Nassim Nicholas Taleb

Contents

List of Figures

List of Tables

Abbreviations

LBNL	**L**awrence **B**erkeley **N**ational **L**aboratory
MILP	**M**ixed **I**nteger **L**inear **P**rogram
NLP	**N**on **L**inear **P**rogram
CHP	**C**ombined **H**eat **P**ower
I&P	**I**nvestment & **P**lanning
PV	**P**hoto**V**oltaic
GHI	**G**lobal **H**orizontal **I**rradiation
PbA	**L**ead **A**cid
LCOE	**L**evelised **C**ost **O**f **E**lectricity
DER-CAM	**D**istributed **E**nergy **R**esource - **C**ustomer **A**daptation **M**odel
HOMER	**H**ybrid **O**ptimisation **M**odel for **E**lectric **R**enewables
NREL	**N**ational **R**enewable **E**nergy textbfLaboratory
BLAST	**B**attery **L**ifetime **A**nalysis and **S**imulation **T**ool
ESM	**E**nergy **S**ystem **M**odel
GAMS	**G**eneral **A**lgebraic **M**odeling **S**ystem
AMPL	**A** **M**odelling **L**anguage for **M**athematical **P**rogramming
PDF	**P**robability **D**ensity **F**unction
CDF	**C**umulative **D**istribution **F**unction
CAPEX	**Cap**ital **Ex**penditures
OPEX	**Op**eration**a** **Ex**penditures
TOU	**T**ime **O**f **U**sage
LOLP	**L**oss **O**f **L**oad **P**robability
NPV	**N**et **P**resent **V**alue

Chapter 1

Introduction

1.1 Microgrid concept

With global economic development and population growth, energy demand is increasing at a fast pace. At the same time environmental concerns such as global warming and the depletion of fossil fuels are pushing forward the development and adaptation of renewable energy technologies. The investment cost of these easy scalable technologies, such as photovoltaics (PV), is decreasing fast. We are reaching a point in time where installing these technologies is becoming financially attractive, even without subsidies. Not only renewable technologies are becoming cheaper, this also holds for energy storage technologies. An example is the very recent launch of the Powerwall by Tesla, a battery to power homes and businesses, claiming to have the potential to revolutionise our daily energy use (WashingtonPost, 2015).

At the same time in some specific places the resiliency of the centralised electricity grid is questioned because of the threat of natural disasters (Greentechmedia, 2014) or malicious cyber attacks (Fathima and Palanisamy, 2015). Some critical systems such as hospitals, police department, and fire stations cannot be subjected to outages and the electricity grid cannot promise these will never occur.

Because of these opportunities and concerns the microgrid concept is gaining in popularity every day. A cheaper, more environmental friendly and more reliable alternative to the traditional centralised electricity grid can be offered this way. A microgrid is defined as group of interconnected loads and distributed energy resources (DERs) within

clearly defined electrical boundaries that acts as a single controllable entity with respect to the grid (Stadler et al., 2013). DER solutions include power generation and combined heat and power (CHP) generation using conventional fuel-fired technologies, but also renewable technologies and energy management strategies such as demand response, load shifting and peak-shaving, and storage (Miller et al., 2012).

A lot of research about microgrids has been carried out in the last years. The very recent works of Fathima and Palanisamy (2015) and Gamarra and Guerrero (2015) review the latest trends in the field. Broadly speaking, microgrid research could be split up into four domains as shown by Table 1.1. This work focusses on the investment and planning (I&P), also called sizing or dimensioning, of grid connected systems from the microgrid owners' point of view.

	Operations	Investment and planning
Grid connected		Focus of this work
Standalone		

TABLE 1.1: Classification of research in microgrids

It should be noted that the boundaries between these four domains are not strict. The design and operation are somewhat interdependent: the optimal design depends on the way that the system will be operated and the optimal operation depends on the system design (Hittinger et al., 2015). The approach for designing the optimal grid connected system will share similarities with the approach used for standalone microgrid if outages of the central grid are considered and the cost of power not served is very high. Also most grid connected systems have the option to operate independently.

Today in the majority of the cases the most cost effective solution is to have a microgrid which is still connected to the traditional electricity grid (Türkay and Telli, 2011). Only in very remote places having a completely decentralised energy system can be cheaper than grid extensions (Mahapatra and Dasappa, 2012). In the case microgrids are still connected to the grid this connection offers reliability, where this is not the case for isolated systems. Mainly because of that reason the economics of both systems differ substantially (Hafez and Bhattacharya, 2012).

As mentioned earlier, the focus of this work is laid on investment and planning decision support tools for grid connected microgrids. These tools give as an output the optimal quantities of the considered technologies to be installed in the microgrid and a provisional

planning for their operation. This planning or dispatch is further optimised in real-time by an operations tool or controller for microgrids wherefore the sizes of the installed technologies are input parameters.

Different microgrids will have different optimal sizes of technologies to be installed and different ways to be operated. Without optimal utilization of sources the cost of investment in a microgrid might not be justified. A lot of parameters need to be taken into account. The most important input parameters for an I& P model are the expected loads to be served, the electricity tariff applied, the local weather conditions and the operational and financial characteristics of the considered technologies. Objectives could differ from project to project, commonly the objective is to minimise the total cost but also minimising emissions, maximising resiliency or a combination of these might be the reason for installing a microgrid. Different ways have been proposed in the literature to solve this sizing problem, they could be split up in three groups: simulation models, linear programming (LP) models and non-linear programming (NLP) models. Almost all models using linear and non-linear programming are mixed integer.

Next to the research domain concerned about the operations and investment and planning of microgrids, siting could be considered as a third category. Siting deals with the problem where to locate microgrids on the distribution grid to minimise losses and to deliver the maximum power quality to the load. This problem is looked at from both the microgrid owners and the utility points of view, while in the other domains the problem is mostly tackled only seen from the viewpoint of the microgrid owner. Villarreal et al. (2014) state in a report by the Californian Public Utilities Commission that siting is a critical factor related to bringing down the cost of microgrid deployment, for two reasons:

1. Microgrid benefits can be optimized through properly locating the microgrid in or near areas of the macro-grid that experience congestion or other capacity or grid balancing issues; and,

2. Microgrid costs can be reduced through siting in preferred locations, such as near existing distributed generation, in particular, combined heat and power or where grid infrastructure upgrades are not required.

Tariffs could be seen as the interface between the microgrids and the utility to guide the investments in the right direction so a win-win situation is created for both parties. To do so tariffs should unbundle attributes (energy and power) and provide fine temporal and spatial granularity (Rocky Mountain Institute, 2014).

1.2 Motivation of the thesis topic

In this thesis the emphasis is laid on PV generation modelling in a mixed integer linear programming method used as a decision support tool for the dimensioning of microgrids. The main advantage of a linear programming approach over the other approaches is the fact that an optimal solution can be found relatively easily. The main disadvantages is that more assumptions and simplifications need to be made in order to keep the computational time reasonable. The different approaches and their pro and cons are discussed in more depth in the next chapter.

The idea is that the way how PV generation is modelled could have an impact on the optimal microgrid design. An impact on the investment decision regarding PV itself, generator sets and in particular regarding stationary storage can be expected. A simplification in linear programming models is that the granularity is often hourly and typical days are used to represent a longer period. This way, variability, especially sub-hourly variability of PV generation, is hard to take into account.

An example of hourly averaged solar radiation data is shown by the bottom graph on Figure 1.1. The global horizontal irradiance (GHI) is the total amount of shortwave radiation received from above by a horizontal surface (OpenEI, 2015). As can be seen from comparing the bottom graph with the ones above, by using averaged hourly values a lot of information gets lost.

If hourly solar radiation is used, the short-term stochastic component of the variability of insolation due to fast moving clouds is filtered out. Several papers report changes by more than 60-70% with averaging times from 1 minute to 180 minutes of insolation on partly clouded days (NERC, 2009; Mills and Wiser, 2010). The problem becomes even more prominent if typical days are used to represent a month. This way not only variability within an hour is filtered out, but also the variability between different hours occurring at the same time of the day in a month is smoothed out.

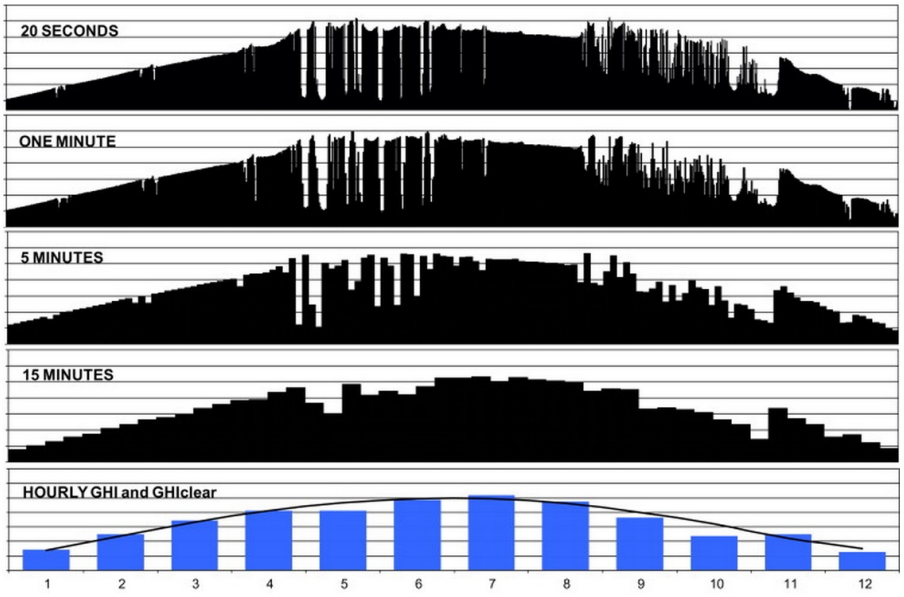

FIGURE 1.1: Comparing global horizontal irradiance (GHI) for all selected Δt sampling rates for a particular site. The bottom plot reports hourly GHI model input and clear sky background (Perez et al., 2011).

On one hand, this variability in insolation and subsequently in PV generation does not have necessarily a big impact on volumetric charges to be paid to the utility in the case of a grid-connected microgrid with PV installed. The differences per hour are averaged out. On the other hand, impacts on the anticipated demand or power charges could be significant. As stated by Neubauer and Simpson (2015): " *behind-the-meter solar power generation decreases energy costs, but solar intermittency due to cloud cover may cause the peak load—and thereby demand charges—to remain unaffected*". By using averaged out solar data the potential of a PV installation to reduce demand charges, and thus the total value added by PV to the microgrid, might be overestimated.

These sudden drops PV output do not necessarily cause spikes in purchases and thus potentially an increase in demand charges. Either a battery or a very fast ramping onsite generator could be used to smooth out this introduced variability in the net demand of the microgrid. There will be a trade-off in this case of which the outcome depends on many parameters, such as tariffs, load shape and technology costs and state of operation. The probability of occurrence of these variations is linked to the demand charges and the state of charge or state of operation of these local devices. The idea is that by taking this effect in account, bigger batteries in terms of maximum power output and/or energy capacity could be proven to be more optimal, also their average state of charge might be

higher or generator sets will be obliged to be online more often. An other outcome could be that investment in PV becomes less attractive. Also wear and thus the operational life of batteries and to a lesser extend generator sets could be affected if these are used to dampen this variability.

Hittinger et al. (2015) observe this problem and found that in a diesel/PV/PbA battery standalone system with a large amount of solar, switching from 1-h to 1-min resolution increases the levelised cost of energy (LCOE) by only 3%. But the optimal amount of batteries to be installed for this system at a 1-min resolution is more than double (236%) the optimal amount at a 1-h resolution. In that same paper it is stated that by examining systems at a 1-h resolution, any microgrid modelling package will overestimate the capabilities of energy storage in the presence of fluctuating PV, and underestimate the amount of storage required.

1.3 Objective

The objective of this thesis is to propose an original mathematical formulation to take into account short-term variability of PV generation in a microgrid investment and planning decision support tool using a MILP approach without sacrificing too much computational time. Also the sensitivity of the investment decisions to the capital cost of batteries is investigated.

Chapter 2

Literature review

This chapter consist out of three parts. It starts with an introductory section describing the relation between solar radiation and PV production. Next, a summary is given about the literature describing the statistical properties of solar radiation, of which a more detailed overview can be found in Appendix A. The last part of this chapter describes different approaches for solving a microgrid sizing problem and discusses their pro and cons.

2.1 Photovoltaic generation and solar radiation

A PV systems consist out of a photovoltaic array which collects light photons falling on its electrons. DC current is generated this way which can be boosted with DC-DC converters and then inverted to AC current. A maximum power point tracker(MPPT) is employed to enable the PV to extract maximum energy from the sun. At last, the power is filtered with a low-pass filter to eliminate unwanted harmonics (Fathima and Palanisamy, 2015).

The critical input for a PV systems are light photons emitted by the sun. It is important to point out the difference between solar radiation, irradiance and insolation as these terms might cause confusion. Solar radiation and irradiance are in this text used as synonyms and express the rate of energy that is being delivered to a surface area at any given time. Its units are Watts per square meter (Sargosis, 2014). That means that

for any given surface area A, there exists a specific amount of power P that is being delivered to that area in photonic form. The equation is shown below:

$$Irradiance = \frac{Power}{Area} \left[\frac{W}{m^2}\right]$$

Insolation is the total amount of energy that has been collected on a surface area within a given time. While the irradiance denotes the instantaneous rate in which power is delivered to a surface, the insolation denotes the cumulative sum of all the energy striking the surface for a specified time interval (Sargosis, 2014). The resultant insolation equation is as follows:

$$Insolation = \frac{Power * Time}{Area} \left[\frac{Wh}{m^2}\right]$$

In order to estimate the power output of PV panels in a precise manner more than just the observed insolation is needed, a simulation model is necessary. An example of such a simulation model is the one developed by Sandia National Laboratories, which is described in the paper of Fanney et al. (2009). In that paper they compare the measured to the predicted PV module performance using this model. The difference between measured and predicted annual energy predictions varied between 1% and 8%. The input of the simulation model are the technical characteristics of the PV module, the irradiance collected by the module and the module's operating temperature. The irradiance collected by the module depends on five factors (Bourges, 1991):

- The location of the PV module, more precisely the geographic latitude
- The time of the year and day; which determines the solar declination and hence the angle of incidence
- Local climates introducing atmospheric effects on solar radiation, the most important being clouds
- The orientation and tilt angle of the PV panels
- The coefficient of reflection of the ground in the local environment

The total or global irradiance collected by the module consists out of three components: a direct or beam component, a diffuse component and a ground-reflected component (in the case of tilt panels) (Bourges, 1991). Figure 2.1 illustrates the three components for a solar panel with a tilt angle β.

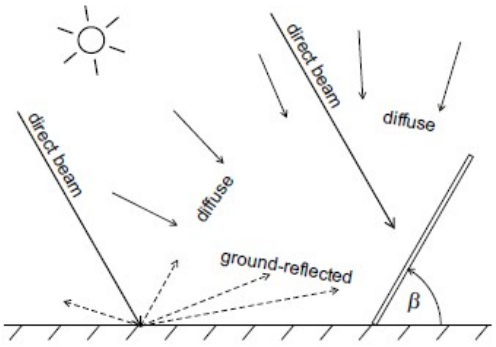

FIGURE 2.1: The three components of solar radiation collected by a tilt PV panel (AssignmentPoint, 2015)

By knowing the direct and diffuse horizontal surface irradiance, the ground reflection coefficient and the configuration of the panels (orientation and tilt angles) the global irradiance collected by the photovoltaic panels can be estimated. Different methodologies are described in the literature to perform this estimation, examples are: anisotropic sky models (Fanney et al., 2009), simpler correlation models (Bourges, 1987) or more complex approaches using artificial neural networks (Dahmani et al., 2014). Next to the irradiance collected by the PV module, also the PV module's operating temperature is an important parameter. The PV module's operating temperature has an influence on the efficiency of the PV module and can be calculated by an algorithm given values of the solar radiation, ambient temperature, wind speed, and the manner in which the modules are mounted. An example of an algorithm to estimate the operating temperature is also presented in the already mentioned paper by Fanney et al. (2009).

It is mainly the variability in the global solar radiation that will cause variability in the PV output. In the papers of Mills (2010) and Marquez et al. (2012) the relation between the variability of solar radiation and the output of different PV plants is analysed. A smoothing of the rapid ramps relative to the expected ramps is found. This smoothing effect is more pronounced for larger PV plants. Figure 2.2 illustrates the findings.

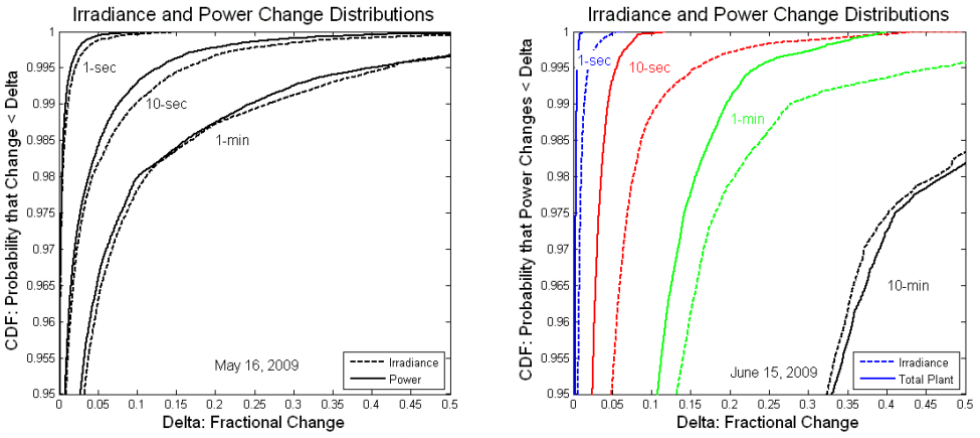

FIGURE 2.2: Cumulative distributions (95th to 100th percentiles) of irradiance and PV power changes over various time periods during a single day from a 30-kW PV system (left) and a multi-MW PV system (right) show a reduction in variability between single point measurements (irradiance) and PV plant output (power/ total plant) (Mills, 2010)

Mills and Wiser (2010) and Marquez et al. (2012) argue that the PV plant output is generally proportional to solar radiation. The stochastic variability in solar insolation is not exactly equivalent to the stochastic variability in actual PV plants due to: 'within-plant' smoothing that can occur relative to variability of insolation at a point, changes in PV plant efficiency with temperature, PV tracking systems, and diverse PV panel orientations other than horizontal for non-tracking PV systems. In microgrids the PV installations considered are generally small in size (a capacity installed lower than 1 MW). In these cases it is reasonable to use the same tools to asses variability in PV output as the ones used for solar insolation variability, an analysis which is done more frequent in the literature (Skartveit and Olseth, 1992; Gansler et al., 1995; Tovar-Pescador et al., 2001; Assuncao et al., 2003; Vijayakumar et al., 2005; Woyte et al., 2007; Tovar-Pescador, 2008; Mills and Wiser, 2010; Zhang, 2014; Fernández-Peruchena and Bernardos, 2015). Taking the remarks mentioned into account it could be said that the variability of solar radiation can be seen as an upper bound of the variability of the PV output (Mills and Wiser, 2010).

2.2 Statistical analysis of solar radiation

From the literature review of statical analysis of solar radiation, which can be found in Appendix A, it is concluded that it is possible to model the stochasticity of solar radiation on different time-scales fairly well. To do this a lot of different methodologies

are proposed. In the literature, distributions of short term solar radiation are conditioned for the optical air mass and/or the average hourly solar radiation, while in this work the short term solar radiation will be conditioned for the month and the hour of the day to be conform with the formulation of the used mixed integer linear program. Although these are different variables for which solar radiation is conditioned, similar distributions could be observed. This claim needs to be verified by additional research.

An interesting application of the models described in Appendix A could be to verify if the short term variability in irradiance in one place is comparable to the short term variability in irradiance in another place. It seems to be necessary to assess this question because, even within the same climate zone different behaviour of sub-hourly variability in solar radiation is observed (Fernández-Peruchena and Bernardos, 2015). Also, obtained distributions from the same site conditioned for different values, e.g. a different hour in a different month, could be compared. This way, by having a better insight in the distributions of sub-hourly variability the analysis can be made less data demanding, but this is not the major focus of this work.

2.3 Optimal microgrid design

In this section a short overview is presented of existing models and papers related to optimal microgrid design. As already mentioned in the introduction, research in microgrids could be split up in four domains as shown by Table 1.1. This work focusses on the investment and planning of grid connected systems domain. Three approaches can be distinguished to solve these microgrid sizing problems. Table 2.1 gives an overview of the different approaches and selected related work.

Method	Related models/papers
Simulation models	HOMER, ESM, RETScreen, BLAST, Gitizadeh and Fakharzadegan (2014)
MILP models	DER-CAM, Chen et al. (2012)
NLP models	Chen et al. (2011), Logenthiran et al. (2012)

TABLE 2.1: Different methods for optimal sizing of microgrids

In the next section an overview is given of the models and papers listed in Table 2.1. There are several commercial products available using a simulation approach while for the optimization approaches, especially non-linear optimization, this is not the case.

One of the main reasons, next to their increased complexity, is that in order to be able to solve a large-scale optimization problem robust commercial modelling environments, such as GAMS (General Algebraic Modeling System) are necessary. Licensing issues can arise when software build on these commercial solvers wants to be commercialised.

2.3.1 Simulation models

HOMER

In the area of microgrid modelling a tool called HOMER (Hybrid Optimization Model for Electric Renewables) is often cited in the literature. HOMER is a system modelling program, and utilizes a time-series approach to solve the microgrid I&P problem (Hittinger et al., 2015). HOMER has built in algorithms to simulate thousands of different systems for every hour of the year, over multiple year life cycles. HOMER then ranks the considered systems by financial performance and technical feasibility (HOMER, 2015). Originally it was developed by the National Renewable Energy Laboratory (NREL). HOMER Energy, the company that distributes the software, reports over 100,000 users in 193 countries (Koohi-Kamali et al., 2014).

Examples of possible applications of HOMER are discussed in a paper by Hafez and Bhattacharya (2012). In that paper HOMER is used for the optimal design of a hybrid, renewable energy based microgrid with the goal of minimizing the lifecycle cost, while taking into account environmental emissions. Four different cases including a diesel-only, a fully renewable-based, a diesel-renewable mixed, and an external grid-connected microgrid configuration are investigated, to compare and evaluate their economics, operational performance and environmental emissions.

ESM

The Energy System Model (ESM) is an engineering-economic simulation model that inputs a set of data about a location (solar potential, expected load, and financial information), determines the optimal microgrid configuration, and calculates the operation of the system. The model can input different amounts of diesel generation, solar PV, and batteries and is flexible enough that it can take any combination of these as input, including cases where only one or two of these components are present (Hittinger, 2013).

In a recent paper by Hittinger et al. (2015) is stated that ESM is very similar to HOMER, but improves upon the battery models used in that model. Five flaws are summed up concerning the battery modelling approach used in HOMER: lack of battery capacity fade in the operational mode, overly optimistic lead acid battery lifetimes, lack of temperature effects, use of constant round-trip efficiency and modelling resolution of 1h. An interesting conclusion of this paper is that the optimal technology choice for electrochemical energy storage is dependent of the way storage will be used. Aqueous Hybrid Ion (AHI) and lead acid (PbA) batteries are compared. It is found that AHI only has an advantage in systems where frequent cycling is valuable, while PbA is a better choice if batteries are more used as a back-up.

BLAST

BLAST stands for the Battery Lifetime Analysis and Simulation Tool and is also developed by the NREL. BLAST is an optimal peak load reduction control algorithm for energy storage systems and can be applied to historic solar power data and meter load data from multiple facilities for a broad range of energy storage system configurations. For each of these scenarios, the peak load reduction and electricity cost savings are computed. From the results, favorable energy storage system configurations are identified that maximize return on investment via minimizing the payback period (Neubauer and Simpson, 2015). In contrast with HOMER only the optimal size of the storage devices will be determined, not the dimensions of other possible DERs to be installed.

In the paper by Neubauer and Simpson (2015) BLAST is used to determine the optimal battery energy and power capacity for different load profiles using the energy storage system to perform demand charge management. The paper also investigates whether the optimal battery system specifications are sensitive to a fixed capacity of PV installed on-site or no PV installed on-site. Surprisingly, no influence of the installation of PV on the optimal energy system configuration was found. It should be noted that the capacity of PV to be installed was not optimized simultaneously with the optimal battery size. A fixed capacity of PV installed, more specifically a PV installation with a capacity equal to half of the peak load, was assumed.

RETScreen

The Renewable Energy Project Analysis Software (RETScreen) was developed from RETScreen International, Canada and is operated by Natural Resources Canada. It is the most downloaded tool of all simulation tools with more than 383,000 users spread across 222 countries (Fathima and Palanisamy, 2015). RETScreen is an Excel-based program to manually analyse clean energy projects based on e.g. calculated payback periods. This is done by defining different system configurations that can include several technologies such as renewables and CHP. Results include economic and environmental performance indicators, allowing a quick assessment of different solutions (Stadler et al., 2014). RETScreen is in comparison to HOMER, ESM and BLAST a statistical model, which does not perform time-series simulations (Lambert et al., 2006).

Paper by Gitizadeh and Fakharzadegan (2014)

Gitizadeh and Fakharzadegan (2014) determine the optimal battery capacity for a grid connected PV system. A mixed integer linear programming model (MILP) is formulated for the optimal battery scheduling and battery degradation cost is taken into account. The amount of PV installed is fixed and a loop is done over the energy capacities of batteries between 3 and 30 kWh. The ratio of the maximum power output and the energy capacity of the battery is assumed to be 1. It could be argued that in this paper a hybrid approach is used. The battery scheduling is optimized, while for finding the optimal size of the battery a simulation is used.

Two time-varying pricing structures, a time-of-use rate without specifying demand charge and a time-of-use rate with demand charge were considered in the study. Results show that sizing determination of the battery highly depends on the exact pricing structure. In addition, non-ideal modelling of battery ageing confirms that considering the real conditions of battery operation is necessary to achieve reliable sizes of battery storage systems.

2.3.2 Linear programming

DER-CAM

Since 2000 the Microgrid Team at the Lawrence Berkeley National Lab (LBNL) has been developing the Distributed Energy Resources Customer Adaptation Model (DER-CAM). DER-CAM is a mixed integer linear program (MILP) that defines optimal adoption and use of DERs in a microgrid or building complex. Its optimization techniques find both the combination of equipment and its operation over a typical year that minimizes the site's total energy bill or CO2 emissions, typically for electricity plus O&M cost and fuel purchases, as well as amortized equipment purchases (Stadler et al., 2014). DER-CAM is coded in GAMS.

Historically the emphasis of the development of the tool has been primarily on the grid connected investment and planning version (Marnay et al., 2008; Stadler et al., 2013; Cardoso et al., 2014). Also a version focused on real-time operation exists. In the investment and planning version outages of the macrogrid can be considered in order to design a truly resilient microgrid.

Paper by Chen et al. (2012)

A method based on the cost-benefit analysis for optimal sizing of an energy storage system in a microgrid is presented in the paper by Chen et al. (2012). In this paper the considered microgrid consists of a PV system, a wind turbine system, two microturbines, a fuel cell, and an energy storage system. Only the energy capacity of the battery (lithium-ion) is optimized, the maximum power output is fixed as 50% of the energy capacity. Also the installed capacities of the other technologies are fixed. The main problem is formulated as a MILP, which is solved in AMPL (A Modelling Language for Mathematical Programming).

This model presented by Chen et al. (2012) allows for a lot less flexibility than DER-CAM. A strong point of the model is that time series and feed-forward neural network techniques are used for forecasting the wind speed and solar radiations respectively and therefore the expected forecast errors are taken into account in the optimization.

2.3.3 Non-linear programming

In a large amount of papers the microgrid sizing problem is formulated as a non-linear optimization problem (Fathima and Palanisamy, 2015; Gamarra and Guerrero, 2015). If the models is large scale, e.g. if the optimization of the capacities of several technologies is considered, optimal solutions are hard to obtain.

For such problems, heuristic search techniques have been established since 1940s. Heuristics includes trial and error solution finding strategies for complex problems within real time limits when classic optimization techniques are not able to find the optimal solution. The aim is to find efficiently good, but feasible solutions within time limits. In the 1980s and 90s metaheuristic algorithms were developed (Fathima and Palanisamy, 2015). The point of metaheuristics is that they can combine more than one heuristic method: the first one can be used to find a primary solution and later another heuristic method can be used in order to find a better solution (Gamarra and Guerrero, 2015).

Gamarra and Guerrero (2015) classify these metaheuristic algorithms as either population based methods, trajectory based methods or bio-inspired methods. The most popular algorithms in the class of population based methods are genetic algorithms (GA) and particle swarm optimization (PSO). Trajectory meta-heuristics use a single-solution approach focused on modifying and improving a single candidate solution during the search process. An example is simulated annealing (SA). Bio-inspired metaheuristics mimic nature for solving optimization problems, evolutionary algorithms are part of this class.

Paper by Chen et al. (2011)

In this paper a methodology is presented to optimally size the energy storage system in a microgrid. The problem is formulated as a large-scale, mixed-integer, combinatorial, and non-linear programming method. A matrix real-coded genetic algorithm (MRCGA) is used to solve it. The quality of the optimization is estimated according to the net present value (NPV).

The considered low voltage microgrid is grid connected and consists out of AC and DC loads, two fuel cells, a microturbine, PV and stationary storage. Only the energy capacity and maximum power output of the battery technology (two different technologies

are considered) are optimized while taking into account their operation. A typical year of data is used and no static electricity tariff, but a dynamic market price for electricity is assumed.

Paper by Logenthiran et al. (2012)

In this work the investment decisions of an integrated microgrid are optimized. An integrated microgrid is an architecture in distributed power systems, in which several microgrids are interconnected with each other for superior control and management of the distributed power systems. Right coordination among DER in microgrids, and proper harmony among the microgrids are taken into consideration in this paper.

The problem is formulated as a non-linear mixed-integer optimization, the sum of capital and annual operational costs of DERs is minimized while respecting a variety of system and unit constraints. These constraint include the reliability of the system, quantified as an upper boundary of the expected loss of load probability (LOLP). An evolutionary strategy was developed to solve the problem.

2.3.4 Discussion of the different approaches

Each of the three approaches discussed in the previous section has its advantages and disadvantages. This subsection focusses on two tools: the simulation model HOMER and the mixed integer linear programming model DER-CAM. Of all the models discussed these can be considered the most extensive and customizable. In both models a wide selection of different technologies with varying sizes can be considered. Regarding the non-linear programming models, as their computational effort needed increases strongly with the consideration of an additional technology or feature no models are found as complete as HOMER and DER-CAM. Also for non-linear programming models, as the models becomes larger, assuring that the optimal solution will be found becomes harder.

An advantage of linear programming over simulation is the fact that by using a linear programming approach, the truly optimal system design can be determined without relying on the user. In a simulation model only specific capacities (not a continuous capacity range) entered by the user are taken into account. There could bebetter optimized configurations that are not being considered (Litchy et al., 2012). In other words

more experience with the microgrid sizing problem is required when using a simulation model in order to obtain reasonable outcomes. Especially when a large amount of different technologies are considered this can become an issue. Mendes et al. (2011) put it as: *"DER-CAM solves a three-level assignment problem in opposition to the two-level assignment problem being solved by HOMER."*

Using a simulation approach instead of an optimization approach also has an impact on the way the dispatch is done. Especially when storage technologies and demand charges with a monthly ratchet are considered this issue becomes prominent. The dispatch is of great importance because optimal design is dependent on the way that the system will be operated. For example in the case of DER-CAM the obtained planning or dispatch is optimal, all information is taken into account. The dispatch and the sizing of technologies are optimized simultaneously, while in most simulation models rule-based heuristics need to be used, which are not necessarily always generating the optimal dispatch. An issue with a linear programming approach might be that this way perfect forecasts are assumed and thus the added value of storage for the microgrid can be overestimated. This drawback is limited by assuming daily cycling and typical day load profiles.

A disadvantage of using a linear programming approach mentioned by Hittinger et al. (2015) is that this approach normally accounts for neither the importance of uncertainty in load and variable renewable energy nor the risk aversion towards unserved load seen in the design of actual microgrids. This risk of unserved load is mainly an issue for standalone microgrids and is solved in DER-CAM by considering macrogrid outages and putting a price on power not served. The other issues mentioned can be solved by using stochastic optimization, with the drawback that computational time increases very fast with the consideration of more scenarios. The uncertainty in renewable energy generation is the focus of this work and an alternative to stochastic optimization in the specific case of gird-connected systems is presented.

Another issue with linear programming is the fact that it is difficult to model non-linear relationships between decision variables. Some non-linear physical phenomena can be linearised but accuracy might be lost. An example of this are efficiencies of generators or batteries which are dependent of their operation. In some cases this hurdle can be

solved by formulating the relationship in a creative linear way using additional binary variables, but again at the expense of additional computational time.

To conclude it can be said that a trade-off exists between complexity of the component modelling and the ability to search for optimal systems and system operation (Hittinger et al., 2015). While a simulation model, such as HOMER, maybe outperforms a linear programming model, such as DER-CAM, in terms of individual component modelling, the ability of a linear programming model to search for optimal systems is superior. What model to prefer over the other depends on the relative importance of these two attributes for a specific case study. It should be noted that as computational power and algorithms are expected to improve significantly in the future the best approach on the middle long term might become non-linear programming models. These have the capabilities to solve the challenges faced by simulation and linear programming models today.

2.3.5 Selection of the model

In this thesis the Distributed Energy Resource Customer Adaptation Model (DER-CAM) is used to build upon. It is opted to use DER-CAM because it is the state-of-the-art linear programming model used for microgrid sizing problems. The model is already under constant development for more than 15 years and applied throughout several dozen case studies (Marnay et al., 2008; Stadler et al., 2013, 2014; Cardoso et al., 2014; Steen et al., 2015; Milan et al., 2015). One of the strengths of DER-CAM, as already mentioned, is that it is one of the most extensive models in its domain. DER-CAM has the possibility to consider a very wide range of technologies and the capability to optimized simultaneously their capacities to be installed taking into account their operation and the interdependencies. This is a serious advantage over simulation models.

The way the model is formulated is very modular, it is easy to include and exclude particular features and to add new ones. In the last years several projects have been conducted in order to add features or update certain modules of I&P DER-CAM. Examples are an electrical vehicle (EV) model including uncertainty in electric vehicle driving schedules by Cardoso et al. (2014), a more precise representation of thermal storage by Steen et al. (2015) and the consideration of non-linear CHP efficiency curves by Milan et al. (2015).

In this thesis a similar extension to DER-CAM is proposed with the emphasis laid on PV electricity generation. The idea is that the way how PV generation is modelled could have an impact on optimal microgrid design. An impact on the investment decisions regarding PV itself, generator sets and in particular regarding stationary storage is expected.

Chapter 3

Mathematical formulation of DER-CAM

3.1 Short overview of the model

Two different types of the DER-CAM model exist which have different purposes; *Operations* DER-CAM and *Investment and Planning* (I&P) DER-CAM. The main difference between both is the time scale and the consideration of investments. Operations DER-CAM is an optimization model to dispatch the available distributed energy resources (investments are fixed) in a microgrid in the most efficient way by considering weather and load forecasts. In this model week-ahead, day-ahead and close to real time scheduling can be done.

The goal of the I&P DER-CAM is to find out in what DERs to invest. Figure 3.1 gives a schematic overview of the model. As can be seen a lot of parameters are taken into account to make this investment decision. The most important parameters are load profiles (split up into electricity, heating and cooling), electricity tariffs, weather conditions and technical and operational characteristics of the considered DERs. The model plans the dispatch of the DERs in an optimal way and determines at the same time the optimal combination of DERs to invest in to make this dispatch feasible. Two versions of I&P DER-CAM exists; a 3-day deterministic version and a 7-day version with the option to allow for stochasticity in several input parameters. Time steps in both versions are one hour.

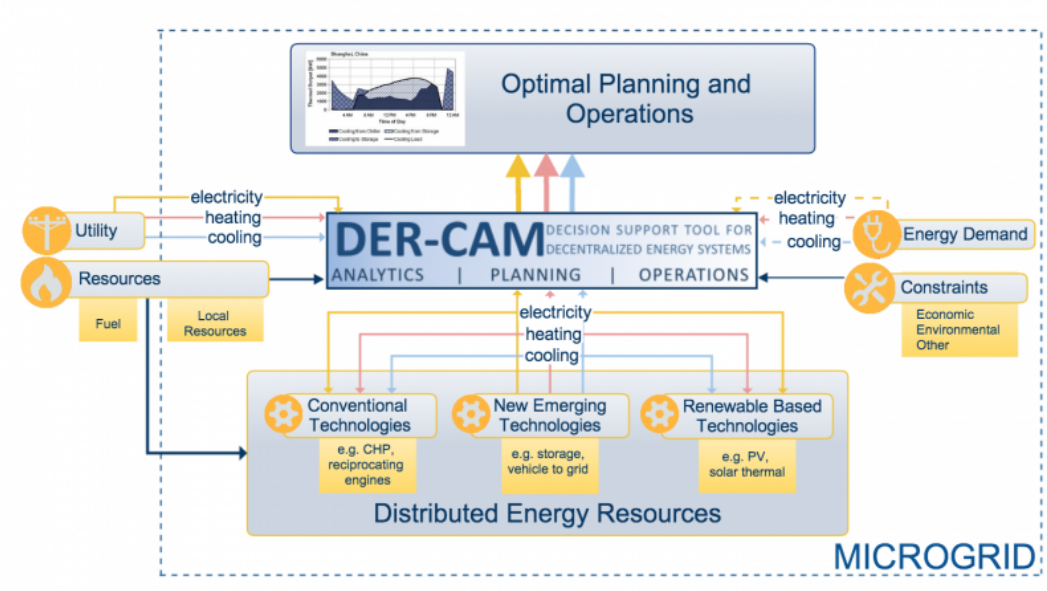

FIGURE 3.1: Schematic overview of DER-CAM (LBNL Grid Integration Group, 2015)

The 3-day version considers 3 different day-types within a month: a week day, a weekend day and optionally a peak day or special day. The number of days per day-type is an input. Days are not interlinked, this has an effect on the scheduling of for example stationary storage. In total 36 days are seen as representative for the whole lifetime of the investments. In the 7-day version one week is used to represent a month and the days within a week are interlinked. In total 84 days are considered this model. The 7-day model is a better representation of reality but the computation time is longer. There is trade-off between complexity and computation time. In this thesis the 3-day version of DER-CAM, which is offered as a software as a service (SaaS) [1], is used.

3.2 Mathematical formulation

The formulation of DER-CAM given in this section is based on the paper of Cardoso et al. (2014), one of the most recent papers making use of DER-CAM. Slight adjustments are made because in that paper the stochastic version of DER-CAM is used, while in this thesis the deterministic version is employed. Figure 3.2 gives a high-level overview of the structure of the formulation. In this work the economic objective function is used. DER-CAM also has the capability to use an environmental (minimizing CO_2) or a dual-objective function.

[1] Available at https://microgrids2.lbl.gov/

```
MINIMIZE:
   Total energy costs:
       energy purchase cost
       + amortized DER technology capital cost
       + annual O&M cost
SUBJECT TO:
   Energy balance:
       energy purchased + energy generated exceeds demand
   Operational constrains:
       generators, etc, must operate within installed limits
       heat recovered is limited by generated waste heat
   Regulatory constrains:
       minimum efficiency requirements
       maximum emission limits
   Investment constrains:
       maximum payback
   Storage constrains:
       electricity stored is limited by battery size
       heat storage is limited by battery size
```

FIGURE 3.2: High-level formulation of the DER-CAM version used (Cardoso et al., 2014)

In the following sections the mathematical formulation of the considered version of DER-CAM is described. It should be noted that this formulation does not include all the features available in DER-CAM, only the ones most relevant for this work are included.

In the DER models used in DER-CAM some technologies are modelled as continuous and others as discrete. This distinction has to do with the way their capacities are modelled: the optimal capacity of discrete technologies is determined as a discrete number of units, whereas the capacity of continuous technologies is determined by a continuous variable. If a technology is available in a small enough module and the capital cost can be easily scaled by using a fixed and variable term, the optimal capacity to be installed is modelled as a continuous variable. Modelling the installed capacity as a continuous variable decreases computational time significantly.

3.2.1 Indices

h	hour {1, 2,..., 24}
n	hours previous to the current hour {0, 1, . . . , h}
p	period on-peak, mid-peak, off-peak
t	day-type {1, 2, 3}
m	month {1, 2,..., 12}

s	season {winter, summer}
u	end-use {electricity only (eo), cooling (cl), refrigeration (rf), space heating (sh), water heating (wh), natural gas only (ng)}
c	set of continuous generation technologies {photovoltaic panels (PV), solar thermal panels (ST), and absorption chillers (AS)}
g	set of discrete generation technologies { internal combustion engines (ICE), microturbines (MT), gas turbines (GT), and fuel cells (FC)}
k	set of storage technologies {stationary electrical storage (ES), and thermal storage (TH)} (capacities are also modelled as continuous variables)
j	set of all generation technologies ($g \cup c$)
i	set of all technologies ($j \cup k$)
r	demand response type {low, med, high}

3.2.2 Parameters

Load

$CLoad_{m,t,h,u}$	customer load in kW in month m, day-type t, during hour h and for end-use u

Market data

$RTEnergy_{m,t,h}$	regulated tariff for electricity purchase in month m, day-type t, during hour h, $/kWh
$RTEExport_{m,t,h}$	regulated tariff for electricity export in month m, day-type t, during hour h, $/kWh
$RTPower_{s,p}$	regulated noncoincident demand charge under the default tariff for season s and period p, $/kW
$RTCCharge_{m}$	regulated tariff customer charge in month m, $
$MktMCRate_{m,h}$	marginal carbon emissions from marketplace generation in month m and hour h, kg/kWh
$NGBSF_{m}$	basic service fee for natural gas in month m, $

$NGPrice_m$	price of natural gas in month m, $/kWh
$NGCRate$	carbon emissions rate from generation technology j, kg/kWh
$DRPrice_{r,u}$	cost of demand response measure of type r and end-use u, $/kWh
$CTax$	tax on carbon emissions, $/kg

Technology data

$Annuity_i$	annualized capital cost of DER technology i, $
$DERlifetime_i$	expected lifetime of technology i, a
$DERcapcost_j$	turnkey capital cost of generation technology j, $/kW
$CFixcost_{c,k}$	fixed capital cost of DER technology modeled as continuous, $
$CVarcost_{c,k}$	variable capital cost of DER technology modeled as continuous, $/kW or $/kWh
$DERmaxp_g$	nameplate power rating of discrete generation technology g, kW
$DEROMfix_i$	fixed annual operation and maintenance costs of technology i, $/kW
$DEROMvar_j$	variable operation and maintenance costs of technology i, $/kWh
$DERhours_j$	maximum number of hours generation technology j is permitted to operate during the year, h
$DERCostkWh_{j,m}$	production cost of technology j during month m, $/kWh
$S(j)$	set of end-uses that can be met by technology j
COP_a	absorption chillers coefficient of performance
COP_u	central microgrid chillers coefficient of performance
α_j	amount of useful heat (in kW) that can be recovered from unit kW of electricity generated by technology i
η_j	electrical efficiency of generation technology j
$ScEff_{c,m,h}$	solar radiation conversion efficiency of continuous generation technology c, in month m, and hour h
$ScPeakEff_c$	theoretical peak solar conversion efficiency of continuous generation technology c

Storage parameters

$\overline{SOC_k}$	maximum state of charge of storage technology k
$\underline{SOC_k}$	minimum state of charge of storage technology k
$SCEff_{c,m,h}$	charging efficiency of storage technology k
$SDEff_k$	discharging efficiency of storage technology k
ϕ_k	losses due to self-discharge in storage technology k
$\overline{EPratio_k}$	maximal ratio of the energy capacity over maximal power output of storage technology k
$\underline{EPratio_k}$	minimal ratio of the energy capacity over maximal power output of storage technology k

Other parameters

$BAUCost$	total energy costs in the business-as-usual case, obtained by running the model with DER investments disabled, $
$IntRate$	interest rate on DER investments, %
$PBPeriod$	maximum payback period allowed on the integrated DER investment decision, a
$ScArea$	available area for solar technologies, m^2
$Solar_{m,h}$	average fraction of maximum solar irradiance received, during hour h of month m
β_u	amount of heat (kW) generated from unit kW of natural gas purchased for end-use u

3.2.3 Decision variables

$psb_{m,t,h}$	binary decision of purchasing or selling electricity in month m, day-type t, and during hour h
$URLoad_{m,t,h,u}$	electricity purchased from distribution utility company in month m, day-type t, and during hour h to meet end-use u costumer loads, kW
$Pur_{c,k}$	customer purchase binary decision of continuous generation technology c, or storage technology k

$cap_{c,k}$	installed capacity of continuous generation technology c or maximum power output (and input) of storage technology k, kW
$Ecap_k$	installed energy capacity of storage technology k, kWh
$InvGen_g$	number of units of discrete generation technology g installed by the customer
$GenU_{j,m,t,h,u}$	energy generated by technology j, in month m, day-type t, and during hour h to meet end-use u customer loads, kW
$GenS_{j,m,t,h}$	energy generated to export by technology j, in month m, day-type t, and during hour h, kW
$ebiou_{k,m,t,h}$	binary charge/discharge decision at the microgrid for storage technology k, in month m, day-type t, and during hour h
$SInput_{k,m,t,h}$	energy input from the microgrid to storage technology k, month m, day-type t, and during hour h, kWh
$SOutput_{k,m,t,h}$	energy output to the microgrid from storage technology k, month m, day-type t, and during hour h for end use u, kWh
$NGP_{m,t,h}$	natural gas purchase in month m, day-type t, and during hour h, kWh
$RecHeat_{j,m,t,h}$	amount of useful heat recovered from power generated by technology j, in month m, day-type t, and during hour h, kW
$ALoad_{m,t,h}$	amount of heat used to drive absorption chillers in month m, day-type t, and during hour h, kW
$CDRLoad_{r,m,t,h,u}$	customer load not met due to demand response of type r, during month m, day-type t, and during hour h, for end-use u costumer loads, kW

3.2.4 Economic objective function

$$
\begin{aligned}
\min \mathrm{C} = & \sum_{m} RTTCharge_{m} \\
& + \sum_{m}\sum_{t}\sum_{h}\sum_{u} URLoad_{m,t,h,u} * (RTEnergy_{m,t,h} + CTax * MktMCRate_{m,h}) \\
& + \sum_{s}\sum_{m\in s}\sum_{p} RTPower_{s,p} * max\Big(\sum_{u\in eo,cl,rf} URLoad_{m,(t,h)\in p,u}\Big) \\
& + \sum_{m} NGBSF_{m} \\
& + \sum_{m}\sum_{t}\sum_{h}\sum_{u} NGP_{m,t,h,u} * (NGPrice_{m} + CTax * NGCRate) \\
& + \sum_{j}\sum_{m}\sum_{t}\sum_{h}\Big(GensS_{j,m,t,h} + \sum_{u} GenU_{j,m,t,h,u}\Big) \\
& * (DERCostKWh_{j,m} + DEROMvar_{j}) \\
& + \sum_{g}\sum_{m}\sum_{t}\sum_{h}\Big(GensS_{j,m,t,h} + \sum_{u} GenU_{j,m,t,h,u}\Big) * \frac{NGCRate}{\eta_{j}} * CTax \\
& + \sum_{g} InvGen_{g} * DERmaxp_{g} * (DERcapcost_{g} * AnnuityF_{g} + DEROMFix_{g}) \\
& + \sum_{i\in c,k} (CFixcost_{i} * Pur_{i} + CVarcost_{i} * (Cap_{i} + ECap_{i})) \\
& * (AnnuityF_{i} + DEROMFix_{i}) \\
& + \sum_{r}\sum_{m}\sum_{t}\sum_{h}\sum_{u} CDRload_{r,m,t,h,u} * DRPrice_{r,u} \\
& - \sum_{j}\sum_{m}\sum_{t}\sum_{h} GenS_{j,m,t,h} * RTEExport_{m,t,h}
\end{aligned}
\tag{3.1}
$$

The objective function formulated by Equation 3.1, which is also represented in a simplified way on Figure 3.2, consists out of three big parts: the cost of energy purchased, O&M cost of the DERs and amortised investment cost of the DERs. The first five elements of the summation are payments to be made to the utility companies offering electricity and gas. The electricity bill in most systems consists out of a fixed customer charge or connection fee, time-of-use volumetric electric charges and time-of-use demand or power charges. The gas bill consists out of a fixed charge for the connection and volumetric charges. In this formulation the cost of gas is split up in two parts: the natural gas directly used for heating loads and natural gas as a fuel for DERs. Natural gas used as the fuel for DERs are accounted for as an operational costs of the DERs burning natural gas. In some systems additional charges needs to be paid to account for the emissions, this feature is enabled by setting a tax on carbon emission. The sixth and seventh

element of the summation account for the operations, maintenance and environmental cost of the installed DERs. The following two elements of the summation represent the annualised investment costs in DERs. The investment cost calculation is split into two parts: one formulation for continuous generation and storage technologies and another formulation for discrete generation technologies. The last two elements of the objective function represent the cost of demand response and the income of electricity sold.

3.2.5 Microgrid constraints

The microgrid constraints are formulated by the following equations:

$$\begin{aligned} &Cload_{m,t,h,u} - \sum_{r} CDRload_{r,m,t,h,u} + \frac{SInput_{k,m,t,h}}{SCEff_k} \\ &= URLoad_{m,t,h,u} + \sum_{j} GenU_{j,m,t,h,u} + SOutput_{k,m,t,h,u=(eo)} * SDEff_k \\ &\forall\ m,t,h\ u{=}\{eo\} \wedge k{=}\{ES\} \end{aligned} \tag{3.2}$$

$$\begin{aligned} &Cload_{m,t,h,u} - \sum_{r} CDRload_{r,m,t,h,u} + \frac{SInput_{k,m,t,h}}{SCEff_k} + Aload_{m,t,h} \\ &= \sum_{j} GenU_{j,m,t,h,u} + \frac{SOutput_{k,m,t,h,u}}{SDEff_k} \\ &\quad + \beta_u * NGP_{m,t,h,u} + \sum_{g} RecHeat_{g,m,t,h,u} \forall\ m,t,h\ u{=}\{sh,wh\} \wedge k{=}\{TH\} \end{aligned} \tag{3.3}$$

$$Cload_{m,t,h,u} = GenU_{j,m,t,h,u} + URLoad_{m,t,h,u} * COP_u\ \ \forall\ m,t,h{:}u \in \{cl,rf\} \tag{3.4}$$

$$Cload_{m,t,h,u} = NGP_{m,t,h,u} \forall\ m,t,h{:}u \in \{ng\} \tag{3.5}$$

$$\sum_{u} GenU_{g,m,t,h,u} + GenS_{g,m,t,h} \leq InvGen_g * DERmaxp_g \forall\ g,m,t,h \tag{3.6}$$

$$cap_i\ \leq Pur_i * M\ \ \forall\ i\ \in \{c,k\} \tag{3.7}$$

$$\begin{aligned} &\sum_{u} GenU_{c,m,t,h,u} + GEnS_{c,m,t,h}\ \leq cap_c * \frac{ScEff_{c,m,h}}{ScPeakEff_c} * Solar_{m,h} \\ &\forall\ m,t,h\ : c \in \{PV,ST\} \end{aligned} \tag{3.8}$$

$$\sum_{c} \frac{Cap_c}{ScPeakEff_c}\ \leq ScArea\ : c \in \{PV,ST\} \tag{3.9}$$

$$SInput_{k,m,t,h} \leq ebiou_{k,m,t,h} * \mathbf{M}\ \ \forall\ k,m,t,h \tag{3.10}$$

$$\sum_u SOutput_{k,m,t,h,u} \leq (1 - ebiou_{k,m,t,h}) * \mathbf{M} \ \ \forall\, k, m, t, h \tag{3.11}$$

$$ECap_k * \underline{SOC_k} \ \leq \sum_{n=0}^{h} \Big(SInput_{k,m,t,n} - \sum_u SOutput_{k,m,t,n,u} \Big) * (1 - \phi_k)^{h-n} \leq ECap_k * \overline{SOC_k} \ \ \forall\, k, m, t, h \tag{3.12}$$

$$SInput_{k,m,t,h} \leq Cap_k \ \ \forall\, k, m, t, h \tag{3.13}$$

$$\sum_u SOutput_{k,m,t,h,u} \leq Cap_k \ \ \forall\, k, m, t, h \tag{3.14}$$

$$\overline{EPratio_k} * Cap_k \leq ECap_k \ \ \forall\, k \tag{3.15}$$

$$\underline{EPratio_k} * Cap_k \geq ECap_k \ \ \forall\, k \tag{3.16}$$

$$GenU_{j,m,t,h,u} = Aload_{m,t,h} * COP_a \ \ \forall\, m, t, h : j = \{AC\} \wedge u = \{cl, rf\} \tag{3.17}$$

$$\sum_u RecHeat_{g,m,t,h,u} \leq \alpha_g * \Big(\sum_u GenU_{g,m,t,h,u} + GenS_{g,m,t,h} \Big) \ \ \forall\, g, m, t, h \tag{3.18}$$

$$\sum_m \sum_t \sum_b \Big(\sum_u GenU_{g,m,t,h,u} + GenS_{g,m,t,h} \Big) \ \leq InvGen_g * DERmaxp_g * DERhours_g \ \ \forall\, g, m, t, h \tag{3.19}$$

$$\sum_u URLoad_{m,t,h,u} \leq psb_{m,t,h} * \mathbf{M} \ \ \forall\, m, t, h : u = \{eo, cl, rf\} \tag{3.20}$$

$$GenS_{j,m,t,h} \leq (1 - psb_{m,t,h}) * \mathbf{M} \ \ \forall\, j, m, t, h \tag{3.21}$$

$$AnnuityF_i = \frac{IntRate}{\Big(1 - \frac{1}{(1+IntRate)^{DERLifetime_i}}\Big)} \ \ \forall\, i \tag{3.22}$$

$$C \leq BAUCost + \sum_g InvGen_g * DERmaxp_g * DERcapcost_g * AnnuityF_g + \sum_{i \in c,k} (CFixcost_i * Pur_i + CVarcost_i * Cap_i) * AnnuityF_i - \frac{\sum_g InvGen_g * DERmaxp_g * DERcapcost_g + \sum_{i \in c,k} (CFixcost_i * Pur_i + CVarcost_i * Cap_i)}{PBPeriod} \tag{3.23}$$

$$RecHeat_{j,m,t,h,u} = 0 \ \ \forall\, j, m, t, h : u \notin S(j) \tag{3.24}$$

$$GenU_{j,m,t,h,u} = 0 \ \ \forall\, g, m, t, h : j \neq \{ST\} \wedge u \in \{sh, wh, ng\} \tag{3.25}$$

$$GenS_{c=(ST),m,t,h} = 0 \ \ \forall\, m, t, h \tag{3.26}$$

$$URLoad_{m,t,h,u} = 0 \ \ \forall\, m, t, h : u \in \{sh, wh, ng\} \tag{3.27}$$

- Equations 3.2, 3.3 , 3.4 and 3.5 state the energy balance equations for the different end-uses, respectively for electricty, space and water heating, cooling and refrigeration and natural gas.

- Equation 3.6 ensures that for all discrete technologies installed the total production at any time step is always lower than the maximum capacity per unit multiplied by the number of units installed. If no capacity of a certain type of discrete technology is installed the total production will always be equal to zero.

- Equation 3.7 is used to set the value of the binary variable which indicates if there will be invested in a particular technology modelled as continuous to take into account the fixed investment cost in the objective function. **M** is an arbitrary large quantity.

- Equations 3.8 and 3.9 are valid for PV and solar thermal. The first constraint ensures the sum of energy used on-site and sold at any time step is lower than the energy produced by the technology at that time step. If there is no curtailment the sum of the energy used on-site and sold will be equal to the energy generated. The way how $ScEff_{c,m,h}$ is obtained is described in more detail in Appendix B. Equation 3.9 forces the total area occupied by photovoltaic panels and solar thermal to be smaller than the maximum area available. This constrains the weighted sum of the capacities of these two technologies to be installed.

- The operational constraints of stationary electrical storage and heat storage are formulated by Equations 3.10, 3.11, 3.12, 3.13 and 3.14. Equations 3.10 and 3.11 make sure that at any time step the storage device is either charging or discharging, one action excludes the other. By Equation 3.12 the energy stored or state of charge of the storage device is forced to be within its limits. Also losses are taken into account by this equation. Equations 3.13 and 3.14 are used to ensure the maximum power input and output limits of the storage devices are respected.

- Equations 3.15 and 3.16 constrains the ratio of the energy capacity and the maximum power output of the storage technologies installed.

- Equations 3.17 sets the microgrid chiller conversion of heat to cooling.

- Equation 3.18 will be activated if there are discrete technologies installed with CHP capabilities. It states that the recovered heat at a time step which can be

used for space or water heating is less or equal than a fraction α_g of the electricity produced by all generators with CHP capabilities at that time step.

- By Equation 3.19 the total amount of hours a discrete technology can be used to generate electricity in a year is capped.
- Equations 3.20 and 3.21 ensure that at any time step the microgrid is either buying electricity or selling electricity, these actions cannot happen simultaneously. **M** is an arbitrarily large number.
- Equation 3.22 determines the annualized capital cost of DER investments.
- Equation 3.23 states that the investments done need to paid back for by operational savings (obtained in comparison to a business as usual case) in a period that does not exceed the maximum payback period.
- Equations 3.24, 3.25, 3.26 and 3.27 are boundary conditions that ensure the proper links between different technologies and the loads they can meet.

Chapter 4

Implementation of stochastic cloud cover in DER-CAM

4.1 PV modelling

Currently the solar radiation profiles fed into 3-day I&P DER-CAM are hourly averages based on historical data of the particular site. Solar radiation is modelled as being dependent of the hour of the day and the particular month. An example of currently used solar profiles in DER-CAM is shown on Figure 4.1[1].

The solar profile as shown on Figure 4.1 has a very similar to the shape of the profile shown by the bottom graph of Figure 1.1 in the introduction. Currently only the diurnal variability of solar irradiation due to the position of the sun, which is deterministic, is taken into account in 3-day I&P DER-CAM. The stochastic component of the variability of solar insolation due to moving clouds is not yet incorporated. As mentioned in the introduction, not including this effect might overestimate the potential of PV to reduce demand charges.

In the 7-day stochastic I&P version there is the possibility to insert certain scenarios for solar radiation. This way there is the possibility to include more variability in the modelling but as the time steps are still hourly, no variability on a sub-hourly scale is considered.

[1]Data retrieved from: http://solardat.uoregon.edu/index.html, special thanks to Dr. Frank Vignola

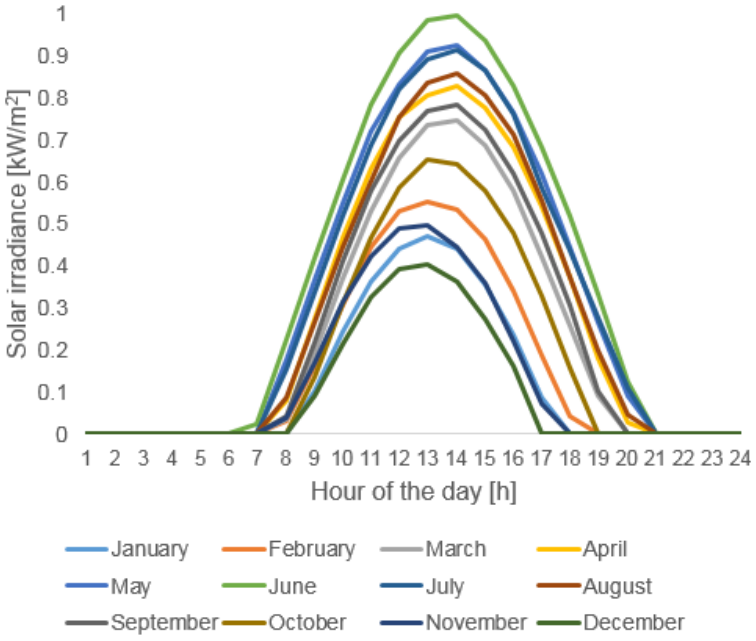

FIGURE 4.1: Example of a solar profiles currently used in DER-CAM

HOMER also uses hourly time steps for solar radiation. Solar radiation values are obtained for each hour of the year by using the Graham algorithm. This algorithm uses as an input monthly solar values of a specific location which are made available by NASA. Tests show that synthetic solar data produce virtually the same simulation results as the real data (HOMER, 2015). By simulating a whole year with hourly time steps supra-hourly variability in insolation is even better captured than in the 7-day I&P version with a limited number of scenarios.

As discussed in the introduction, the financial impact of this variability in PV generation for a grid connected microgrid will be mainly reflected by the demand charges. The demand charges for a microgrid are very sensitive to how on-site technologies, in particular the battery (if there is one installed) are operated. As HOMER is a simulation software the dispatch of the battery is done by a rule-based heuristic. Awerbuch (2015) mentions in the support of HOMER that peak shaving is one of the options that can be chosen as a battery dispatch strategy in HOMER, just as grid arbitrage is another one. In DER-CAM both main objectives of the battery in a grid-connected system; peak shaving and grid arbitrage, are simultaneously taken into account. As both have a direct financial implication and the problem is not solved sequentially but in a linear programming manner, there is no problem in doing so.

This difference in both approaches to do the dispatch of the battery is an additional argument why DER-CAM is a better alternative to investigate the impact of short-term stochastic variability of PV generation on optimal grid design. The study conducted by Neubauer and Simpson (2015) utilising BLAST, briefly mentioned in the previous chapter, is also very relevant in this context. In that paper the optimal configuration of the battery to be installed is determined with and without the presence of on-site PV generation. The strong point in that work is that data with a granularity of 1-min is used to do the simulation, thus capturing sub-hourly variability. The weaker points are that the capacity of PV to be installed is not optimised, a fixed capacity is assumed, and that the dispatch of the battery is not optimal. The battery is only used for demand charge management and not for grid arbitrage.

No work was found in the literature simultaneously optimizing the capacities of different technologies in a grid-connected microgrid taking into account their operation while including the potential impact of short-term variability of PV on the demand charges.

4.2 Stochastic variability

After going through the literature and analysing short-term radiation data it became clear that in order to incorporate stochastic cloud variability in DER-CAM the problem should be split up in two. The criteria to base the categorisation on is the duration of cloud cover. At one end of the spectrum clouds can be present during a whole day and on the other end of the spectrum there are fast moving clouds, of which the duration of its impact is in the order of minutes.

From a microgrid owner's perspective both situations, a cloudy day and fast moving clouds, can lead to an increase in expected demand charges. This increase in demand charges can be avoided in a different way for both situations as the dispatch will be different. The assumption made is that in the case of long-lasting cloud cover, in the order of a couple of hours to a full day, all on-site generators can be used to limit the increase in demand charges. In the case of fast moving clouds the response to avoid spikes in electricity purchased because of unexpected drops in PV output needs to be faster. It is assumed that batteries with enough energy content and power output or online on-site fast ramping generators can be used for this purpose.

4.3 Analysis of solar radiation data

This section starts with going back to the solar profile shown by Figure 4.1. It can be seen on that figure that at 2 pm in June the average radiation is very close to 1000 W per m^2, the theoretical maximum if reflection is not taken into account, while at 1 pm in December the average radiation is around 400 W per m^2. It should be noted that to calculate the average radiation at for example for 11 am data from 10 am to 11 am is considered. Figure 4.2a and 4.2b show the distribution of the solar radiation between 1 pm and 2 pm in June in more detail. The graph on the left uses fifteen minute data while the graph on the right uses hourly data. Figure 4.3a and 4.3b show the same information but now for solar radiation data registered between 12 am and 1 pm in December.

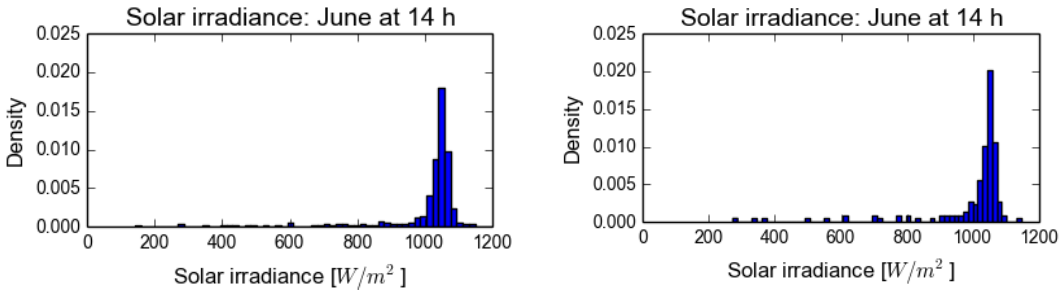

(A) 15-min data (B) Hourly data

FIGURE 4.2: Probability density function of solar radiation between 1 and 2 pm in June

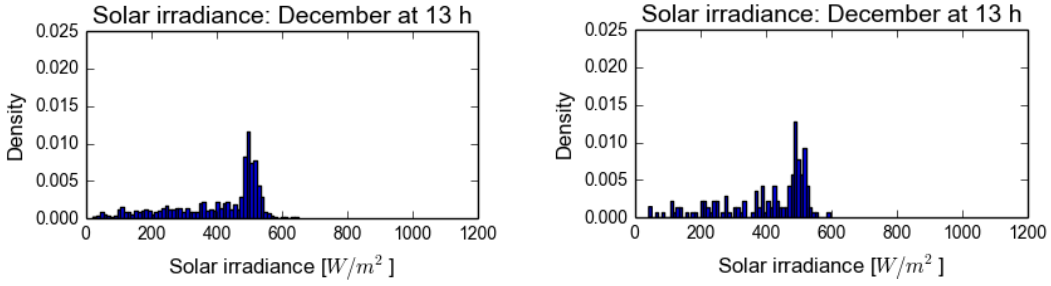

(A) 15-min data (B) Hourly data

FIGURE 4.3: Probability density function of solar radiation between 12 am and 1 pm in December

The difference between data from June and December is very clear; not only the averages, but also the distributions differ significantly. In the case of June there is a clear peak around 1000 W per m^2, while for December the distribution is wider. It could be said that the difference in average has more to do with deterministic factors, such as the

position of the sun, while the difference in distributions more has to do with stochastic factors or cloud cover. The potential increase in demand charges will be caused by the tails to the left. By only using the average value of solar radiation in DER-CAM this effect is not captured.

The distributions using 15-min data or hourly data do not differ significantly on first sight. The main difference is that tails to the left are 'smoother' in the case 15-min data is used, which is as expected. It should be noted that also the peaks are slightly higher if hourly data is used. Both effects are caused by averaging out the data. Figure 4.4 and 4.6 illustrate the implication of using data with these different time intervals in a clearer way.

Figure 4.4 summarizes Figures 4.1 and 4.3. Solar profiles are shown using the averages as on Figure 4.1 and different percentiles using the cumulative distributions which can be easily obtained from the probability density functions shown on Figure 4.3. The convention used in this work is that with the *'x'* percentile confidence interval for irradiance is meant that for *'x'* % of the population of samples a higher irradiance was observed than that value.

One subtle, but import remark needs to be made concerning the 15-min data. The different percentile levels for 15-min data are not obtained by using the cumulative distribution containing all the 15-min samples of a particular hour of a particular month. Only the lowest 15-min irradiance per observed hour in the data was collected to obtain this cumulative distribution. The reason for this is that demand charges -as is described in the next chapter in more detail- are for most systems today calculated using the highest demand during a month averaged over a 15-min interval. In other words only the 15 minutes per hour with the lowest irradiance are relevant in this context. In the datasets used in this work 4 measurements of irradiance were done per hour, every 15 minutes. Actually by using the sample with the lowest irradiance of these 4, the lowest irradiance during 15 minutes of that hour will be slightly underestimated as the 15 minutes lasting measurements are not done continuously. It is not expected that this will strongly influence the results. The same analysis can easily be done if demand charges were calculated using the highest power purchased from the utility averaged over a 5-min interval.

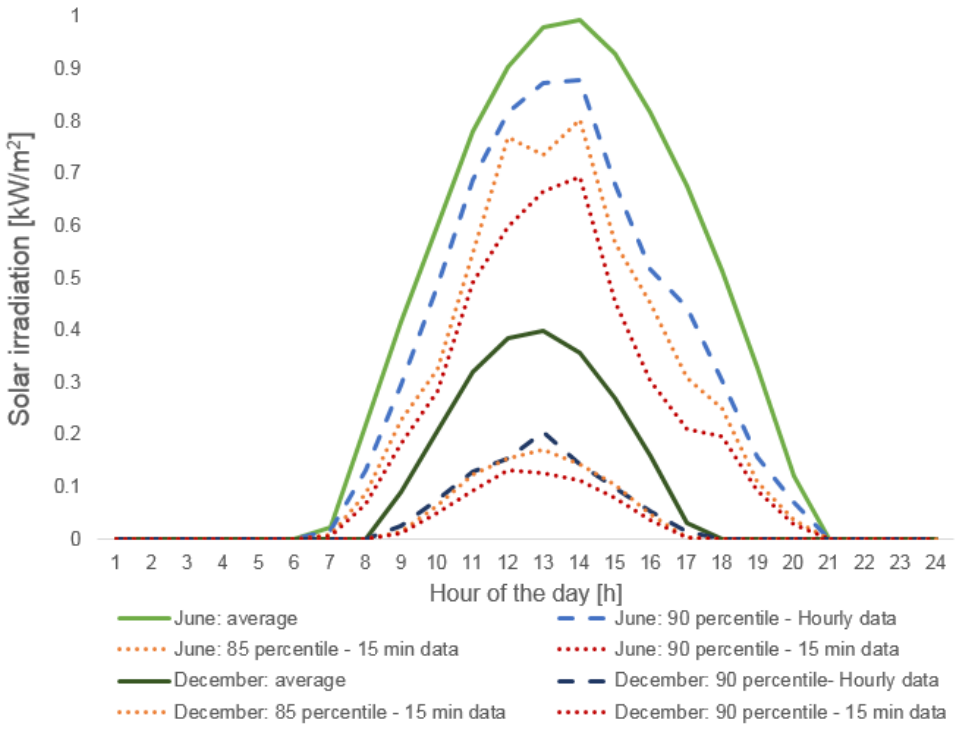

FIGURE 4.4: Solar profiles using 5 years of data from a site in Moab, Utah

If radiation would be constant within an hour there would be no difference observed looking at the curves of e.g. the 90th percentile using hourly data and that same percentile using 15-min data. A large difference between these two profiles indicates high variability on a sub-hourly scale can be seen on Figure 4.4. For June there is a big gap between the 90 percentile profiles using hourly and fifteen minutes data. Even the profile using the 85th percentile with 15-min data is consistently under the profile using 90th percentile with hourly data. For December the gap between both curves is a lot smaller, this confirms that sub-hourly variability is less present in this month.

The dynamics shown on Figure 4.4 are very data dependent, therefore the same graph is shown on Figure 4.6[2] but now using five years of data of a site in Green River situated in Wyoming. On Figure 4.5 the two locations are indicated. Green River is a less suitable place for a PV installation as can be seen on both Figure 4.5 and in more detail on Figure 4.6.

For the site in Green River the gap between the average radiation and the 90th percentile using hourly data is much wider than it is the case for the site in Utah. The reason

[2]Data retrieved from: http://solardat.uoregon.edu/index.html

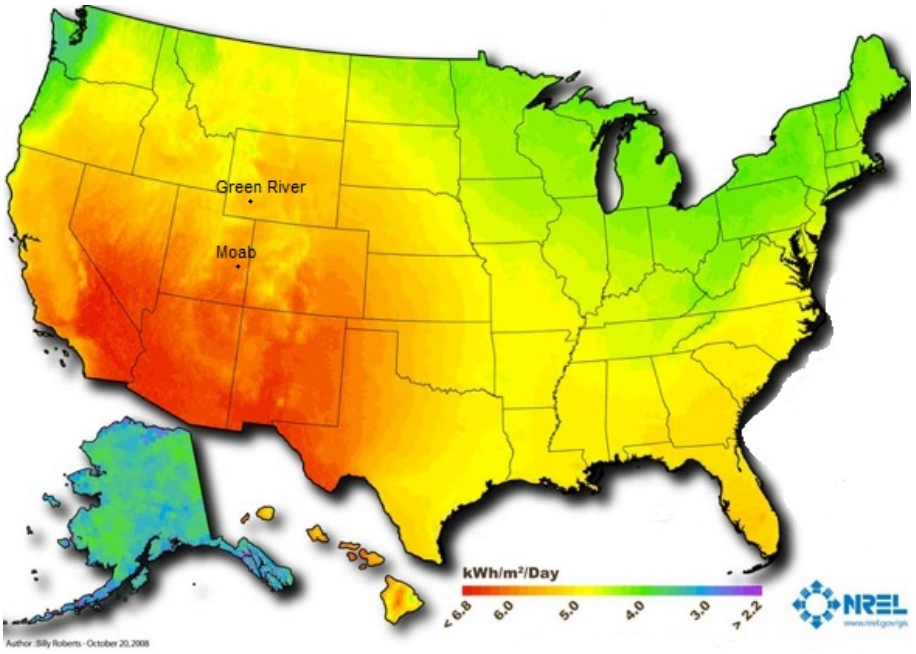

FIGURE 4.5: Average daily solar insolation per square meter in the US for a tilt collector (Roberts, 2008)

is that in Green River even for the month with the highest radiation on average still a lot of longer lasting cloud cover is present. Also the gap between the 90th percentile using hourly and 15-min data is large, indicating the presence of sub-hourly variability in June. For December the differences between the curves showing the 90th percentile using hourly or fifteen minute data are very small, this points out that for that month the sub-hourly variability is very small.

The conclusion from this analysis that can be made is that at the moment of the year when PV output is expected to be the highest, or in other words when the PV system will add the most value to the microgrid, the effect of sub-hourly variability is the strongest.

4.4 Supra-hourly cloud cover

The proposed method to take into account a cloudy day in DER-CAM is straightforward. By introducing a small change in the code solar radiation profiles become day-type dependent. The idea is to use a cloudy day radiation profile for one day in the month and scale the average solar profile up to respect the -expected- energy balance.

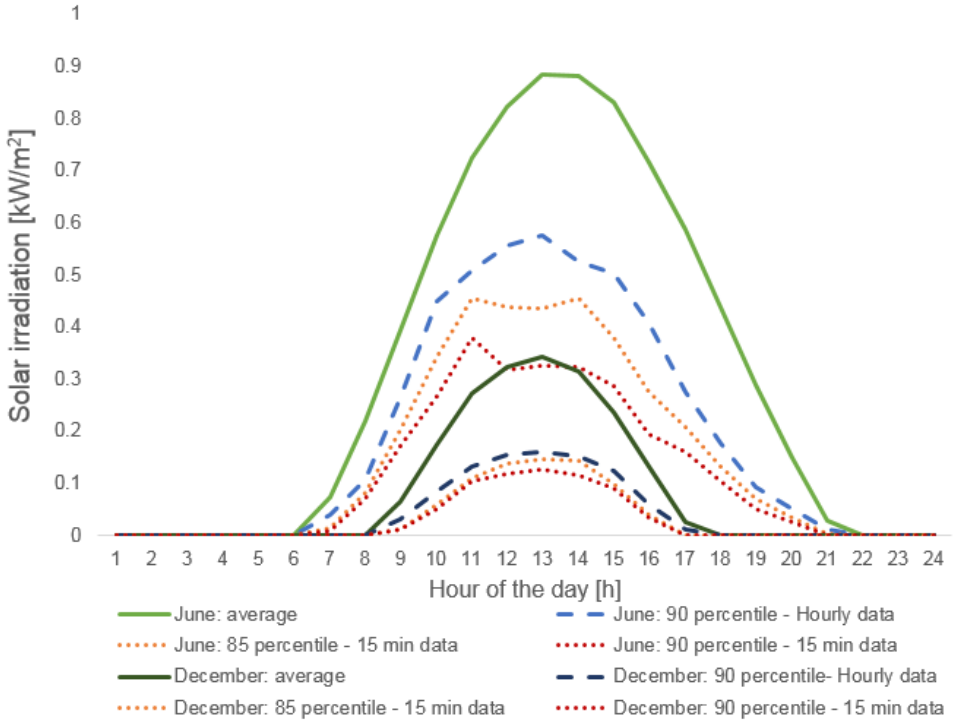

FIGURE 4.6: Solar profiles using 5 years of data from a site in Green River, Wyoming

Only including one cloudy day per month is enough because it is assumed that the variability in PV output will only affect demand charges and these are calculated per month. Two questions need to be answered before this approach can be incorporated into DER-CAM. Firstly, how will a cloudy day radiation profile be estimated and secondly, which load profile is associated with this day modelled as cloudy. These questions cannot be answered independently. The reason for this is that what is really important in this case is the net load, which is obtained by subtracting the PV generation from the original load.

The problem is that the load and radiation are input parameters and the actual size of the PV installed is a variable, so the expected PV output is a variable as well. Therefore the net load to be expected is a variable. Thus retrieving information about this net load and use it as an input creates non-linearities and does not comply with the formulation of DER-CAM. The only way to do this would be iterative runs, which leads us too far.

This is not the focus of this thesis but a study could be done how solar radiation and load correlate for a certain site. On first sight it is expected for sites located in a warmer climate that load - which in that case consists for a large fraction of cooling

load - will be lower when solar radiation is lower, so they compensate each other. It is also expected that the installation of PV is favourable at those locations because of the warmer climates. In colder climates this compensation does not hold because if irradiance is lower, load -which in that case consists for a large fraction of heating load- could be expected to be higher. But this effect is less important because PV will be less favourable at that location in the first place.

Not much literature was found describing this correlation explicitly. In a paper by Al-Hasan et al. (2004) the previous statement about warm climates is confirmed, it is stated that that the peak load matches the maximum incident solar radiation in Kuwait. Also Perez et al. (2003) found that "*thanks to the natural PV-load correlation characterizing many commercial buildings, customer-sited PV also capture value from billed load demand reduction*". It is actually the validity of this statement of Perez et al. (2003) which is investigated in this work.

It is proposed to model this cloudy day by using the 90th percentile (lowest 10%) of hourly radiation data for a particular hour in a particular month. The load profile during that cloudy day will be matched with the peak day load profile. The peak day load profile for a month is the profile obtained by averaging out the three days with the highest daily load per month observed in a series of 1 year of historical load data [3]. This approach could be regarded as conservative because it is not expected that low irradiance and high load will coincide for sites for which PV generation is important.

On Figure 4.7 an example of the considered solar profiles is shown. It can be seen that the scaled average solar irradation profile is slightly higher than the average solar profile because of the consideration of one cloudy day during which radiation is lower than average. As mentioned in the previous chapter, DER-CAM uses 3 days to model a month: weekdays, weekend days and peak days. In the cases that are run in the next chapter the scaled average radiation profile will be used for weekdays and weekend days, while for the one peak day the 90th percentile solar radiation profile is used.

[3] This is just one method to obtain the peak day load profile, other methodologies are possible to preprocess the load data such as a percentile approach similar to the way solar data is preprocessed in this work.

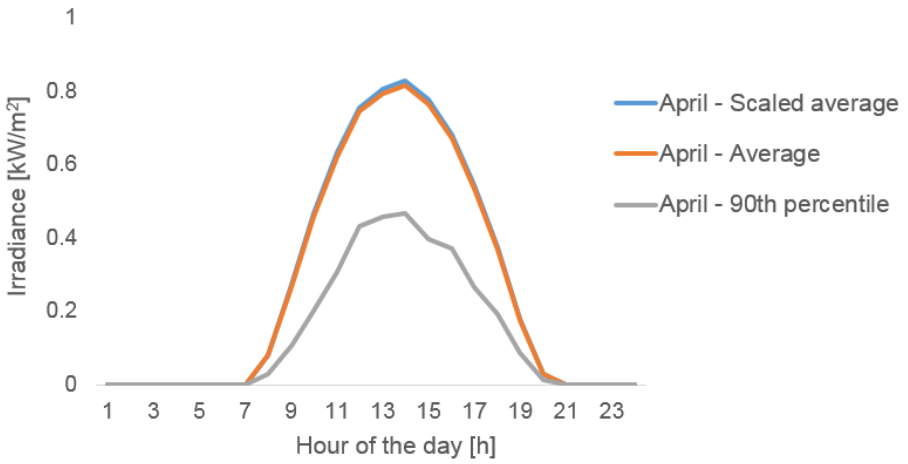

FIGURE 4.7: Different solar radiation profiles for April using hourly data from a site in Moab, Utah

4.5 Sub-hourly cloud cover or fast moving clouds

It could seen from for example Figure 4.4, shown in the section of this chapter where solar radiation data was analysed, that not all the variability of solar radiation is captured when using hourly data. Especially when the radiation is expected to be highest, thus adding the most value to the system, the sub-hourly variability is most present. Also during those months in summer in most places demand charges are the highest, as is the case in California (PG&E, 2015). The natural phenomenon underlying this sub-hourly variability are fast moving clouds.

These fast moving clouds are taken into account using a statistical approach to decouple accounting of energy and power demand economics, and allow events of different time lengths to be simultaneously analysed. The methodology introduced estimates the variability of PV output and the resulting impact on power demand charges for different confidence levels. Because of the sudden - in most cases hard to anticipate upon - changes these fast moving clouds cause of PV output not all on-site installed generation technologies will be able to react fast enough to dampen the drop in PV generation and thus spike in electricity purchased they cause. This peak in electricity purchased, especially when the capacity of PV installed is large, might be the one determining the demand charge for that particular month and thus have a strong influence on the electricity bill.

It is assumed that existing energy storage may offset drops in PV output if sufficiently charged, or that fast-ramping generator units may also be used for the same purpose. This formulation is embedded in the investment decision process, and is reflected in the optimal DER portfolio provided by DER-CAM.

4.5.1 Adjustment to the objective function

The impact of sub-hourly variability is modelled as purely financial, more precisely as an additional term to the energy purchased used to calculate the demand charges at every time step. Modelling this additional term this way no additional volumetric charges will be accounted for. The demand charges are an element of the objective function shown by Equation 3.1 in the previous chapter. The demand charges are allowed to have different values for different TOU periods and seasons. Equations 4.1 shows the change in the objective function:

$$\begin{aligned} \min \mathrm{C} = \ldots \\ + \sum_{s} \sum_{m \in s} \sum_{p} RTPower_{s,p} * \\ max\Big(\sum_{u \in eo,cl,rf} URLoad_{m,(t,h) \in p,u} + \boldsymbol{\delta_{m,(t,h) \in p} * \alpha_{m,(t,h) \in p}} \Big) \\ \ldots \end{aligned} \tag{4.1}$$

$\delta_{m,t,h}$ is a strict positive continuous variable and could be defined as the potential increase in power purchased at a particular time step due to fast drops in PV generation. $\alpha_{m,t,h}$ is a binary parameter set to 1 if the microgrid is coupled with the macrogrid and 0 otherwise. $\delta_{m,t,h}$ is multiplied by $\alpha_{m,t,h}$ because when the microgrid is islanded, demand charges will not be affected by sub-hourly variability in electricity purchased [4].

4.5.2 Battery as the technology to mitigated the power drops

In this section we assume only stationary batteries to be able dampen the short-term drop in PV generation. $\delta_{m,t,h}$, introduced in Equation 4.1, is in this case dependent of following parameters and variables:

$Ecap_{ES}$	the energy capacity of the battery installed, kWh

[4] Instead, depending on the circumstances, it could be necessary to curtail load

Cap_{ES}	the maximum power output (and input) of the battery installed, kW
$SOutput_{ES,m,t,h,u=\{eo\}}$	the power output of the battery in month m , day-type t, during hour h, kW
$GenU_{PV,m,t,h,u=\{eo\}}$	the PV output used on-site in month m , day-type t, during hour h, kW
$\underline{SOC_{ES}}$	the minimum state of charge of the battery, %
$SDEff_{ES}$	the discharge efficiency of the battery, %
$SOC_{ES,m,t,h}$	the state of charge of the battery in month m , day-type t, during hour h, kWh
$PVOutput_{m,t,h}$	the expected PV output at in month m , day-type t, during hour h, kW

Please note that the solar radiation is now assumed to be day-type depended as was discussed in the previous section. All variables and parameters listed up, except for the last two variables, were already defined in the previous chapter for the mathematical formulation of DER-CAM. $SOC_{ES,m,t,h}$, the state of charge of the battery at a time step is now formulated explicitly to make the interpretation of the proposed equations clearer. For the same purpose the variable $PVOutput_{m,t,h}$, defined as the maximum PV generation at a time step, is created. Following equations show the formulation of the these two newly introduced variables.

$$SOC_{k,m,t,h} = SOC_{k,m,t,h-1} + SInput_{k,m,t,h} - \sum_{u} SOutput_{k,m,t,h,u} - SOC_{k,m,t,h-1} * \phi_k \quad \forall\, k,m,t,h \neq 1 \tag{4.2}$$

$$SOC_{k,m,t,1} = SOC_{k,m,t,24} \quad \forall\, k,m,t \tag{4.3}$$

$$PVOutput_{m,t,h} = cap_{PV} * \frac{ScEff_{PV,m,h}}{ScPeakEff_{PV}} * Solar_{m,t,h} \quad \forall\, m,t,h \tag{4.4}$$

Equation 4.2 states that the state of charge at a time step is equal to the state of charge at the previous time step minus the power output at that time step or plus the power input at that time step minus the losses because of self-discharging. Equation 4.3 ensures that the state of charge at the first hour of the day is the same as at the last hour of

the day. This is a necessary simplification because of the way the 3-day I&P DER-CAM version is formulated. In the 7-day I&P DER-CAM this simplification is not introduced as one entire week is used to represent a month. By using a representative week the optimization horizon of the battery is extended from one day to that whole week.

Equation 4.4 states that the maximum PV generated at a time step is equal to the capacity of PV installed multiplied by the radiation and the irradiance conversion rate at that time step divided by the peak efficiency. The energy generated by the PV installation can be used to serve on-site load, can be sold to the macrogrid or can be curtailed. If the loads are served and selling of energy generated by the PV installation from the microgrid to the macrogrid is not possible or the selling limit is exceeded, the excess energy will be curtailed.

In order to determine $\delta_{m,t,h}$ one new variable and two new parameters are introduced. The values for the parameters are obtained from statistical analysis and how these are exactly determined will be explained in more detail later in this chapter.

$BPotential_{m,t,h}$	variable indicating the potential of the battery to dampen the drop in PV generation in month m , day-type t, during hour h, kW
$\Delta^{M}_{m,t,h}$	parameter indicating the magnitude of the sub-hourly drop in PV generation as a percentage of the expected PV output in month m , day-type t, during hour h, %
$\Delta^{D}_{m,h}$	parameter indicating the duration of the sub-hourly drop in PV generation as a fraction of an hour in month m and during hour h, possible values or 0.25, 0.5, 0.75 and 1

The following equation is used to determine $\delta_{m,t,h}$:

$$\begin{aligned}\delta_{m,t,h} \geq \Delta^{M}_{m,t,h} * PVOutput_{m,t,h} - (PVOutput_{m,t,h} - GenU_{PV,m,t,h,u=\{eo\}}) \\ - BPotential_{m,t,h} * SDEff_{ES} \ \forall\, m,t,h\end{aligned} \tag{4.5}$$

With:

$$BPotential_{m,t,h} \leq Cap_{ES} - SOutput_{ES,m,t,h,u=\{eo\}} \ \forall\, m,t,h \tag{4.6}$$

$$BPotential_{m,t,h} \leq \frac{1}{\Delta^{D}_{m,h}} * \Big(\frac{SOC_{ES,m,t,h-1} + SOC_{ES,m,t,h}}{2} - ECap_{ES} * \underline{SOC_{ES}} \Big) \quad \forall\, m,t,h \tag{4.7}$$

Equations 4.5 ensures that $\delta_{m,t,h}$ will be equal or bigger than the right hand side of the equation if this right hand side is positive and zero if this right hand side is negative. $\delta_{m,t,h}$ will not be greater than the right hand side when this would imply an extra cost which is minimised by the objective function. A positive value of $\delta_{m,t,h}$ will not always imply an increased demand charge, only when it coincidences with an already high value of electricity purchased at that time step an increase can occur.

In other words by formulating the effect of sub-hourly variability in irradiance this way it is assumed that at every hour PV is generating electricity a drop occurs with a certain magnitude $\Delta^{M}_{m,t,h}$ and duration $\Delta^{D}_{m,h}$. At some hours this drop will not have an effect on demand charges because the sum of this drop at the time step and the electricity purchased at the time step is not close to the maximum demand in that billing cycle. At other moments this drop can have an impact on demand charges if this sum exceeds the maximum electricity purchased in that billing cycle. In that case there is the option to let this increase happen or prevent it by selling or curtailing more PV or having a battery with the potential to dampen it.

In the case that no energy generated by PV is curtailed or sold the difference between $PVOutput_{m,t,h}$ and $GenU_{PV,m,t,h,u=\{eo\}}$ will be zero. If this is not the case selling or curtailing energy generated by PV at a time step will lower the chances of having an increase in demand charges. Another way to dampen the drop in PV output and thus the potential increase in demand charges is by a battery, quantified by $BPotential_{m,t,h}$. It should be noted that no direct cost is associated by using the battery to dampen the drop in PV generation. It is import to note that Equation 4.5 does not model real electricity discharged by the battery, it only checks for the potential to do so. The energy balance does not chance.

Equations 4.6 and 4.7 constrain the use of the battery to dampen the drop in PV output at a time step. Equation 4.6 constrains the battery in terms of power, it states that the power a battery can deliver a time step to dampen the drop is lower or equal than the maximal power output minus the power the battery is already delivering if the battery

is discharging at that moment. Equation 4.7 constrains the battery in terms of energy, it states that enough energy must be available in the battery in order to be able to discharge to dampen the drop. Because the drop can have a duration shorter than an hour the accessible energy content in the battery is divided by the duration as a fraction of an hour. Subtracting the minimum state of charge of the battery from the average state of charge between two time steps in that equation forces the state of charge to be higher than the minimum state of charge at all times. The average state of charge of the previous and the actual time step is used as the energy content available, the reason for this is that it is unknown when this sub-hourly drop will occur within the hour.

4.5.3 Consideration of online fast ramping on-site generators

Next to the battery there is also the option to dampen the drops in PV generation with extra generation by an available generator. The requirement would be that the on-site generator is online and fast ramping, otherwise the reaction speed would be an issue. There will be an additional fuel cost associated with this additional generation of electricity, while it is modelled to be costless to use the battery for the same purpose. This additional fuel cost δfc is added to the objective function, as shown by the following equation:

$$\begin{aligned} \min \text{ C} = & \ ... \\ & + \sum_{s} \sum_{m \in s} \sum_{p} RTPower_{s,p} \\ & * max\Big(\sum_{u \in eo,cl,rf} (URLoad_{m,(t,h) \in p,u}) + \boldsymbol{\delta_{m,(t,h) \in p} * \alpha_{m,(t,h) \in p}} \Big) \\ & + \boldsymbol{\delta fc} \\ & ... \end{aligned} \tag{4.8}$$

Several variables and parameters, which were already introduced in the previous chapter, are related to dampening the drop by an online fast ramping on-site generator:

$GenU_{g,m,t,h,u}$	the output of a generator g in month m , day-type t, during hour h for end use u, kW
$InvGen_g$	number of units invested in of generator technology g, integer
$DERmaxp_g$	the maximum power output per unit of a generator technology g, kW

$DERCostkWh_{g,m}$	production cost of a discrete generator technology g (including the efficiency and fuel cost) in month m, $/kWh
$RTEnergy_{m,t,h}$	regulated tariff for electricity purchase in month m, day-type t, during hour h, $/kWh

Also a new variable and two new parameter are introduced:

$GPotential_{g,m,t,h}$	variable indicating the potential of generation technology g to dampen the drop in PV generation in month m , day-type t, during hour h, kW
γ_g	parameter indicating if a generation technology g is fast ramping (1) or not (0), binary
CL	confidence level related with the chosen magnitude and duration of the sub-hourly drops in PV generation, %

By introducing this option an additional term is added to Equation 4.5:

$$\begin{aligned}\delta_{m,t,h} \geq \Delta^{M}_{m,t,h} * PVOutput_{m,t,h} - (PVOutput_{m,t,h} - GenU_{PV,m,t,h,u=\{eo\}}) \\ - BPotential_{m,t,h} - \sum_{g} \boldsymbol{GPotential_{g,m,t,h}} \;\; \forall\, m,t,h\end{aligned} \tag{4.9}$$

With $GPotential_{g,m,t,h}$ being determined by the following equations:

$$GPotential_{g,m,t,h} \leq GenU_{g,m,t,h,u} * \boldsymbol{M} * \gamma_g \;\; \forall\, g,m,t,h \tag{4.10}$$

$$GPotential_{g,m,t,h} \leq InvGen_g * DERmaxp_g - \sum_{u} GenU_{g,m,t,h,u} \;\; \forall\, g,m,t,h \tag{4.11}$$

And δfc is estimated by the following equation:

$$\begin{aligned}\delta fc = (1 - CL) * \sum_{g}\sum_{m}\sum_{t}\sum_{h} \Delta^{D}_{m,h} * GPotential_{g,m,t,h} \\ * (DERCostkWh_{g,m} - RTEnergy_{m,t,h})\end{aligned} \tag{4.12}$$

Equation 4.9 states that the possible increase in demand charges because of the drop in PV generation now can be dampened when PV is curtailed or sold, or by a battery respecting its constraints or by a fast ramping generator respecting its constraints.

Equations 4.10 and 4.11 formulate how $GPotential_{g,m,t,h}$ is constraint. Equation 4.10 ensures that the generators must be online and fast ramping to be considered, with **M** an arbitrarily large number. And Equation 4.11 ensures that the power outputted by the generators stays at all time under their maximum power output.

Equation 4.12 estimates the additional fuel cost if a generator is used to dampen the drop in PV. Because of the probabilistic nature of this approach in combination with a MILP it is hard to calculate exactly the additional fuel cost. A choice of confidence level for the modelled sub-hourly drops in PV generation needs to be made, which complicates this calculation. This confidence level is directly related with the magnitude and duration of the drop at every time step, which is explained in more detail the next section. The higher the confidence level the more conservative a microgrid owner's attitude towards short-term variability. A higher confidence level will imply a larger, but shorter drop.

Equation 4.9 is build up assuming, as already mentioned, that at every time step this drop in PV occurs. Although in reality a drop of that magnitude or larger will occur with a probability of 1 minus the confidence level. The reasons for modelling the drop as such are: first, when it occurs it will be very hard to foresee and second, a drop will not have an impact at every time step, even if it is not dampened as explained in the previous section. Only at 'critical' time steps, when the purchase of electricity is already high and/or the capacity of PV installed is large, this drop will matter. At every time step the microgrid should have the potential to dampen the drop if a drop at that time step would impact the demand charges more than the cost incurred by having this capability.

So by accounting an additional fuel cost every time step the generator has to possibility to dampen this drop would be assuming a drop with that magnitude and duration always occurs, which is not the case. A drop of that duration and magnitude (or larger) will only occur with the probability of 1 minus the confidence interval, therefore the operational cost is multiplied by this probability in Equation 4.12.

It should also be taken into account that in this section only drops in PV outputs were considered, but also spikes in PV output will occur. If no drop would be dampened by a battery or a generator these drops and spikes will average out. On the other hand if the drops are dampened by a battery, the battery will process more energy, thus more losses will occur and energy will not average out completely. There would be a small increase

in electricity purchased or generated on-site. This small increase will come with a cost which is not taken into account. Also if the drops are dampened by a generator this energy balance is not averaged out any more. This dampening by a generator comes with a cost which is taken into account, but also less electricity will need to be bought from the grid. To average out again the total energy the volumetric electricity cost is subtracted from the operational cost of the generator in Equation 4.12. In most cases when a static electricity tariff is applied the operational cost of the on-site generator will be higher than de volumetric electricity price. In other words, by formulating Equation 4.12 as such, load following behaviour of the generator is assumed.

Equation 4.12 is an estimation, by using this approach it is not possible to exactly obtain the additional cost. Case studies done explicitly to estimate this estimation of the cost show that is negligible in comparison to the total cost. Only when fuel for on-site generation would become extremely expensive this cost will matter. One of the reasons for the fact this cost is negligible is that the minimum load the on-site generators is already very high, thus the additional power that can be provided for this purpose is small and thus also the additional fuel cost.

4.6 Determination of the power drop $\Delta_{m,t,h}$

4.6.1 Monthly demand ratchet

The difficulty in incorporating short-term radiation in 3-days I&P DER-CAM is the fact that in most systems the demand charge ratchet is monthly. This means that the demand charges for the whole month will be determined by the maximum power purchase during one particular 15 (or 5) minute interval in that month. In 3-days I&P DER-CAM, three day-types are used to represent a month. It is hard to model expected demand charges using this approach. A non-linear measure such as a demand charge is not modelled correctly if averages are used. For that reason the energy generated by PV and the reliability of the power supply of PV were decoupled as explained in the previous sections.

If daily demand charges would be in place instead of monthly demand charges, obtaining values for the drop in radiation would be simplified. In that case expected values (in

the mathematical sense) for the drop in radiation relative to the inserted solar radiation could be used. Although by using this approach demand charges could be slightly underestimated. The net electricity purchased could be around the same level during several hours dependent on the relation between demand and PV generation. The occurred drop in net purchase for a complete day will be larger on the long run than the expected drop during each hour separately.

In the case of monthly demand charges and the way 3-day I&P DER-CAM is formulated, the best approach seems to be using different confidence levels quantifying the attitude of the microgrid designer towards short-term fluctuations in solar radiation. A modelled drop in solar radiation has two dimensions: a magnitude and a duration. The larger the magnitude the shorter the duration and vice versa. In this work it is chosen to fix the magnitude of the drop and subsequently to determine the duration.

4.6.2 The magnitude of the power drops

The magnitudes of the drops are found using the cumulative probability distribution of 15-min historical data conditioned for the hour and the month. The same procedure is valid for 5-min data. Following steps explain how this is done:

1. Collecting of 15-min historical solar radiation data (5 years in this case)
2. Sorting the data per hour per month (12x24 groups)
3. Removal of night hours by deleting the groups of which the average irradiance is lower is below the threshold (e.g. 10 W/m^2)
4. For each hour belonging to a group store the 15-min data sample with the lowest irradiance, this is how the distributions of 15-min data shown on Figures 4.2a and 4.3a are obtained
5. Sort these 15-min samples (from high to low)
6. The sample at the the confidence interval percentile represents the magnitude of the drop for that confidence level
7. The PV drop in percentage is calculated as: $\frac{\text{expected irradiance} - \text{irradiance of that sample}}{\text{expected irradiance}}$. For the day-types week and weekend the expected radiation is the scaled up average

hourly irradiance and for the peak day the expected radiation is the 90th percentile of the hourly data for that hour of that month.

Figure 4.8 shows the irradiance profile for the daylight hours of the different months of the year. The profiles for the weekdays and weekend days, which is the scaled average hourly profile, and for the peak days, which is the 90th percentile of the hourly values, are shown. Also the assumed irradiance during the sub-hourly drops for confidence intervals varying from 70 % up to 95% are shown. Night hours are left out of this Figure.

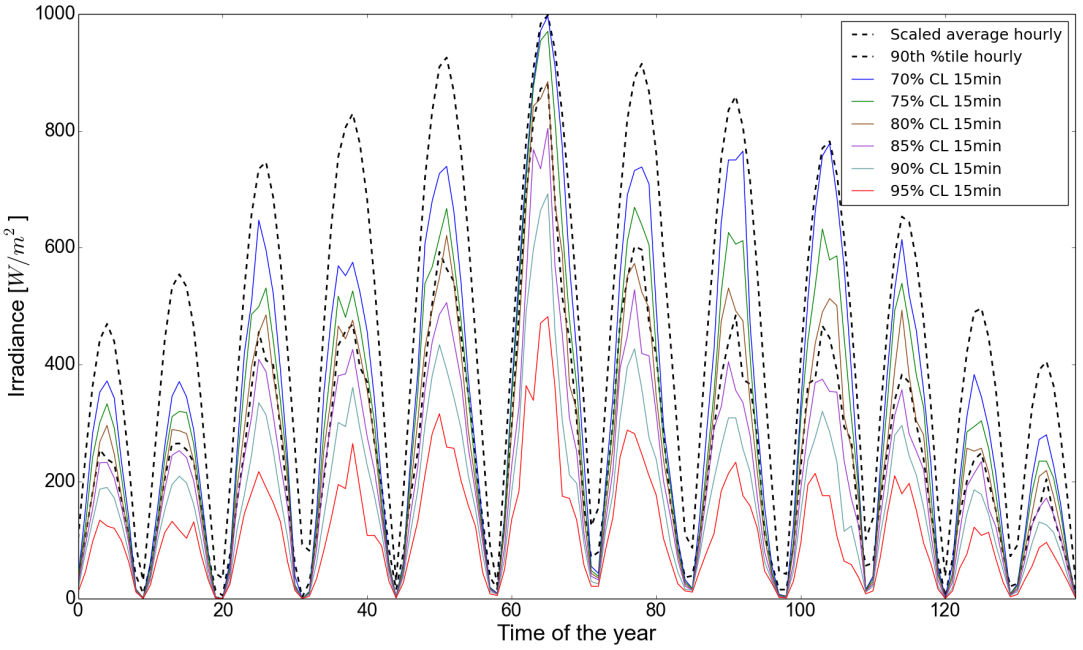

FIGURE 4.8: Different radiation profiles throughout the year (one daylight hours profile to represent a month) using 15-minute and hourly data from a site in Moab, Utah

It should be noted that the information shown on Figure 4.4 is actually included in Figure 4.8. It can be seen from Figure 4.8 that in several months the 90th percentile of hourly data approximately corresponds with the 80th percentile using 15-min data, this confirms the existence of sub-hourly variability for this site. The difference in irradiance between the 90th percentile using hourly data and that same percentile using 15-min is significant, especially during the months with highest average irradiance. This means the sub-hourly variability is the strongest when PV adds the most value to the microgrid.

Figure 4.9 shows the actual inserted values for $\Delta^{M}_{m,'week',h}$, used in Equation 4.9, with confidence intervals varying from 70 % up to 95%. Please not that for day-type weekends the values are the same. For the peak day-type the values are different as they are relative

to the 90th percentile or 'cloudy day' irradiance profile. Negative values for $\Delta^{M}_{m,t,h}$ would not have an impact. $\delta_{m,t,h}$ is defined as a positive continuous variable and will be equal to zero if $\Delta^{M}_{m,t,h}$ is negative.

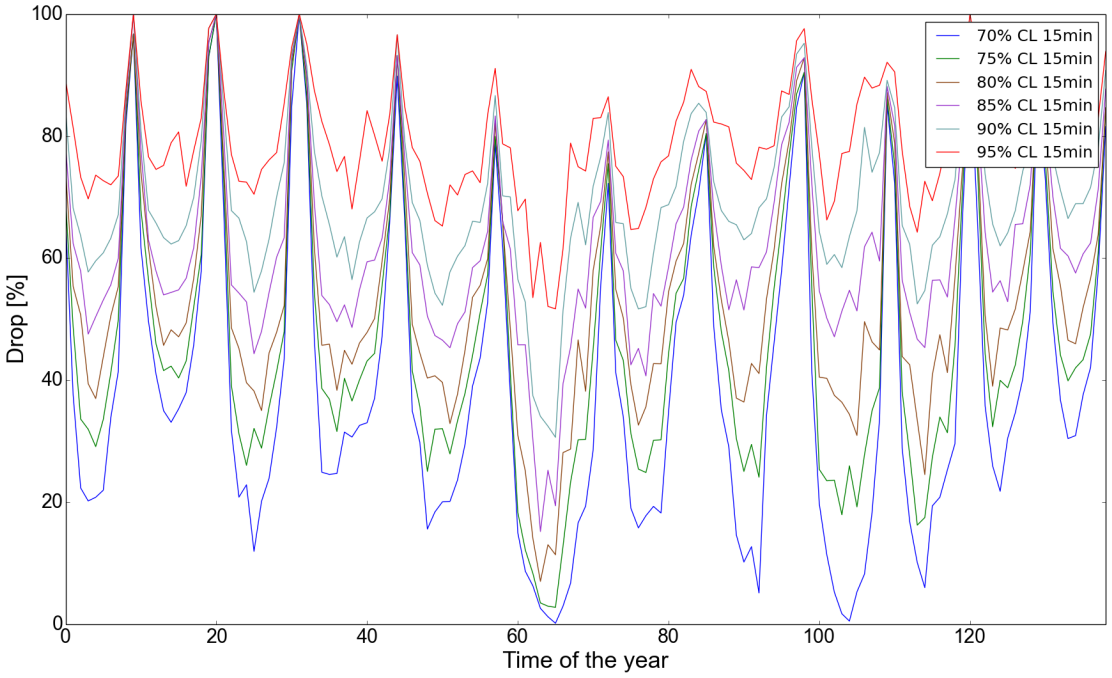

FIGURE 4.9: Obtained values for $\Delta^{M}_{m,'week',h}$ for different confidence intervals throughout the year (one daylight hours profile to represent a month) using 15 minute data from a site in Moab, Utah

The extreme high values of $\Delta^{M}_{m,'week',h}$, in some cases almost 100 %, occur in the early morning and the late evenings. This high values indicate that at those moments of the day the power supply by PV is very unreliable. The more towards the middle of the day, when the irradiance is maximal, the lower the drop in relative to the average in most cases. In other words, the U-shape of the monthly curves means that the variability or stochasticity in cloud cover in relative terms is weaker towards the middle of the day, which intuitively makes sense.

The very high values in the early morning and late evening actually do not impact the system significantly. At those moments the irradiance is already very low thus a large drop relative to the average at that time is still a small drop in absolute values. The opposite is true for the hours in the middle of the day. Figure 4.10 allows an easier interpretation of the implication of the values of $\Delta^{M}_{m,'week',h}$. The actual assumed drop in irradiance in absolute values is shown, which are calculated as $\Delta^{M}_{m,'week',h} * PVOutput_{m,'week',h}$. Again the values are the same for the 'weekend' day-type but

different for the 'peak' day-type as these are calculated relative to the 'cloudy day' irradiance profile. This drop in irradiance could also be seen as temporary capacity loss of the PV installation.

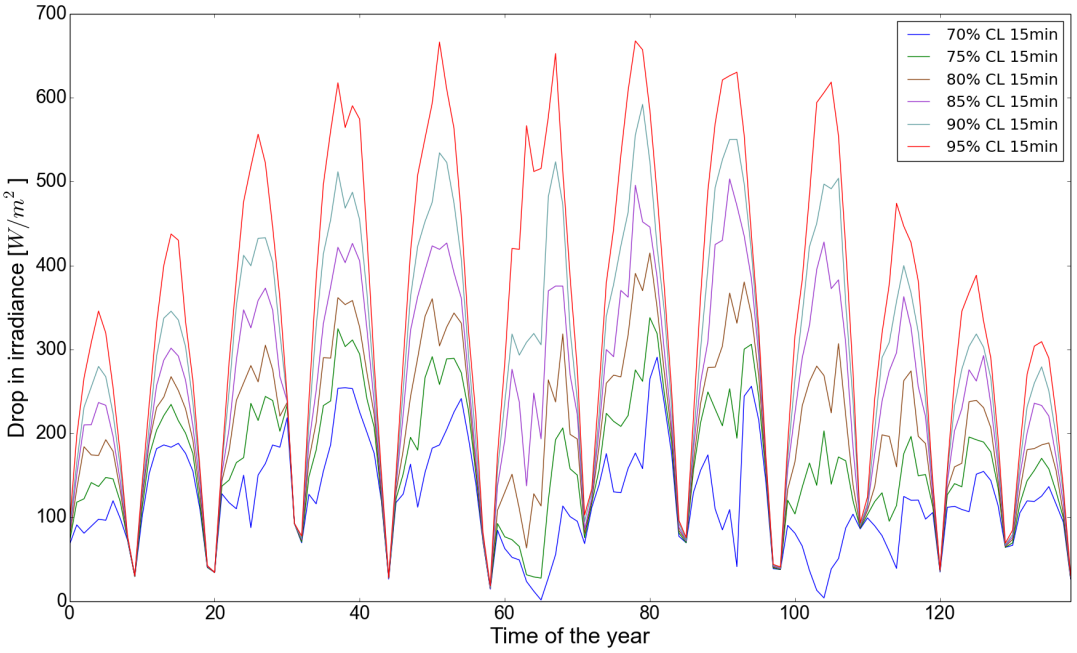

FIGURE 4.10: Absolute drop in irradiance relative to the average irradiance throughout the year (one daylight hours profile to represent a month) using 15-data from a site in Moab, Utah

4.6.3 The duration of the power drops

The modelled drops in irradiance, as already mentioned in the previous section, have two dimensions: a magnitude and a duration. It was chosen to fix the magnitude by the choice of a confidence level and afterwards to determine the duration which is related to the magnitude. A general rule of thumb would be the larger the assumed drop, the shorter its duration.

The methodology used to find the durations per hour per month is explained by the following steps:

1. The hours for which the irradiance of at least one 15-min sample is under the value of the irradiance at the chosen the confidence level are collected and grouped per hour per month.

- e.g. for March at 3 pm with a confidence level of 85% the magnitude of the irradiance is 450 W/m^2 using 15-minute data. In this case all historical hours for March at 3 pm during which at least for 15 minutes the irradiance was under 450W/m^2 are collected.

2. For these collected hours it is counted for how many hours the irradiance was under the irradiance of the chosen the confidence level for only 15-min, 30-min, 45-min or the full hour.

   - e.g. for March at 3 pm there were 30 hours collected after step 1. In 40% of the cases for only 15-min the irradiance was under the 450 W/m^2, in 30% of the case 30-min were under this threshold, in 20 % of cases 45-min were under this threshold and for the remaining 10% the full hour was under the threshold

3. Using the frequency of occurrence of the different durations per group obtained in the previous step, the cumulative probability is calculated.

   - e.g. following the same example of step two, the percentage value for 15-min would be 40%, for 30-min 70% (40%+30%), for 45-min 90% (40%+30%+10%) and always 100% for 1 hour.

4. A threshold is set related to the cumulative probability and is the same for all hours of all months. This threshold will determine the final duration $\Delta^D_{m,t,h}$. The higher this threshold the more conservative and thus the longer the assumed durations of the drops in irradiance.

   - e.g. if the threshold for cumulative probability is set at 50% then in the case of March at 3 pm $\Delta^D_{m,h}$ is equal 0.5 (fraction of an hour) or 30 minutes

Figure 4.11 shows the obtained cumulative probabilities after step 3 for the same data set used in the previous section for the 85% confidence level. Also the threshold of 50% is shown on this graph. A 50% threshold is chosen because this way the median of the duration of the drop is calculated. Figure 4.12 is directly related to Figure 4.11, it shows the obtained values for $\Delta^D_{m,h}$ by setting the threshold at 50%.

It can be seen on Figure 4.11 that at 4 instances the red or 45 minute dot lays under the threshold. This means that in more than 50% of the cases hours, in which during at

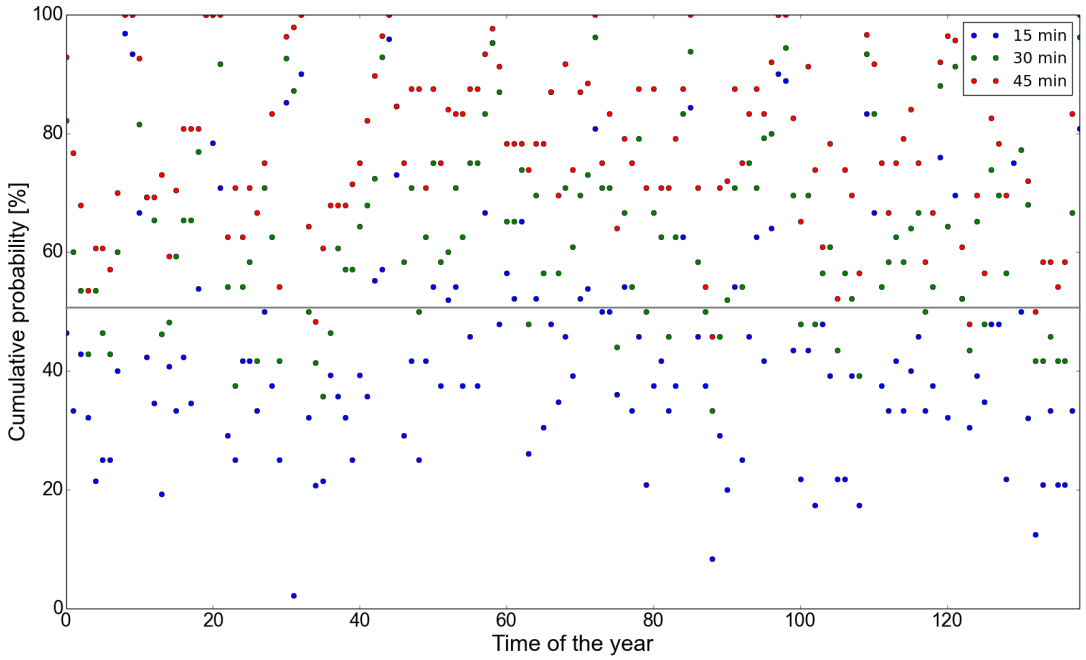

FIGURE 4.11: Cumulative probabilities of durations of the drop in irradiance for a 85% confidence level throughout the year (one daylight hours profile to represent a month) using 15-min data from a site in Moab, Utah

least 15 minutes the irradiance was under the 85%th percentile confidence interval, the irradiance remained the whole hour under that threshold. These 4 red dots are linked with Figure 4.12 by the 4 spikes of 60 minutes. No clear pattern is visible on Figure 4.12. Looking at the average durations of the drops for different confidence intervals the trend is as expected: the higher the confidence interval, thus the higher the magnitude of the drop, the shorter the average duration. This trend is shown on Figure 4.13.

On Figure 4.13 is also the total energy of the drops for a year for the day-type week (and weekend, as it is the same) shown. It should be noted that for the day-type peak the trend would be the same but different absolute values would be obtained. The duration of the drop is modelled as day-type independent but the magnitude as it is relative to the 'expected solar profile' is day-type dependent. The total energy of the drops is calculated as the sum of the products of the drop in irradiance as shown by Figure 4.11 and the durations as shown by Figure 4.12 at each time step. This calculation, shown by Equation 4.13, needs to be done for each confidence interval.

$$\text{Total energy drops}_{,week'} = \sum_{m} \sum_{h} \Delta^{M}_{m,,week',h} * Solar_{m,,week',h} * \Delta^{D}_{m,h} \tag{4.13}$$

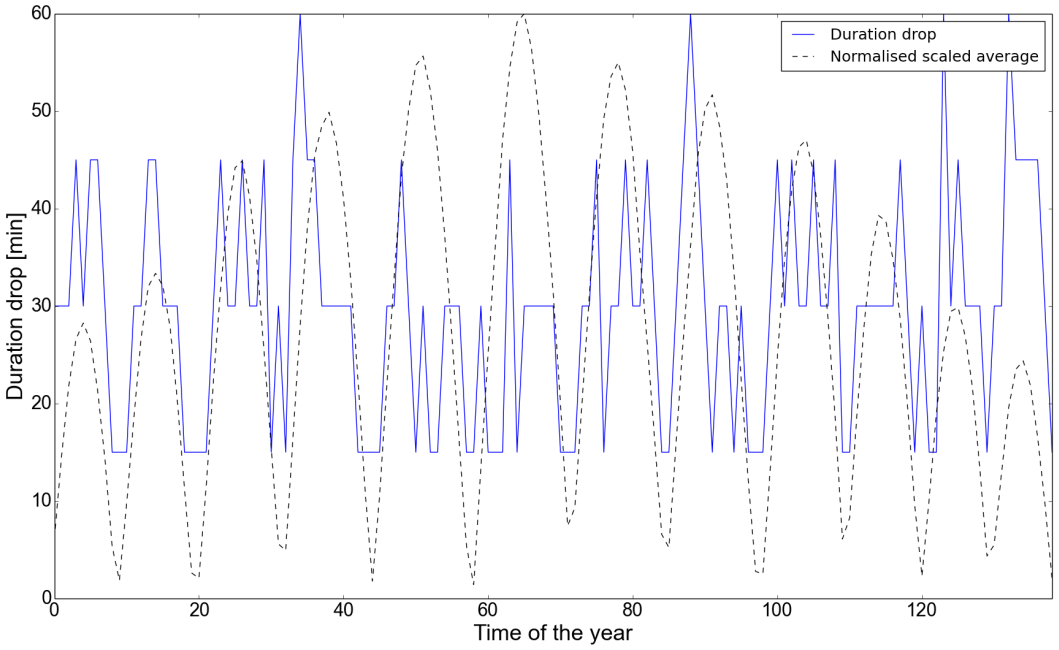

FIGURE 4.12: Final chosen durations $\Delta^D_{m,h}$ in minutes for a 85% confidence level throughout the year (one daylight hours profile to represent a month) using 15-data from a site in Moab, Utah

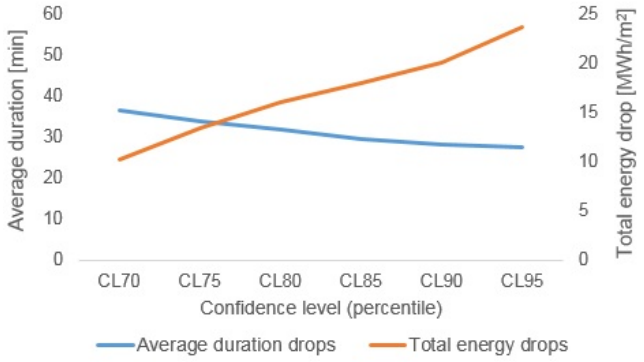

FIGURE 4.13: Average durations of the drop in irradiation and the total energy of the drops for a representative year using 15-data from a site in Moab, Utah

It can be seen on Figure 4.13 that the higher the confidence level the higher the total energy of the drops. The obtained value for the total energy of the drops has no direct physical meaning but its trend shows that by using this approach the magnitude of the drops increases stronger than the duration declines by increasing the confidence interval.

4.7 Remarks

It should be recognised that this modelling approach has its limitations, several of these limitations are listed up in this section.

Variability in demand

In this case demand charges are calculated looking at the maximum electricity purchased during a certain period averaged over 15 minutes. This electricity purchase or net demand is calculated as the electric load minus the electricity generated on-site. This means that not only variability in electricity generated on-site by PV, but also variability in electric load could potentially lead to an underestimation of the demand charges.

In a paper by Marquez et al. (2012) the variability of the load of a school campus and the variability of electricity generated by a PV panel installed at the same site are compared using a one year time series with a 15-min interval. Average demand during daytime for the campus is around 1.25 MW and 1 MW of PV is installed. It is observed that any fluctuation in PV is directly passed to the net demand for which the utility has to compensate. On Figure 4.14 can be seen that the fluctuation patterns in the overall demand are similar to the fluctuations in PV, whereas the fluctuation patterns in the net campus load are relatively constant throughout the year.

One case study is not enough to confirm that variability in PV generation has another order of magnitude than variability in load. Both PV and load variability will be case dependent, but in general it is expected that this statement will hold.

Battery degradation

Currently in DER-CAM the relationship between the dispatch of the battery and battery wear is not taken into account. No capacity loss over the batteries' lifetime time due to its operation is assumed. One of the reasons is that battery degradation is a non-linear function of the energy throughput, depth-of-discharge, the discharge rate and temperature (Wang et al., 2011). This relation could be linearised, but some accuracy will be lost. Even a linearised function of battery degradation would still be hard to implement because of the linear programming nature of DER-CAM. In a simulation

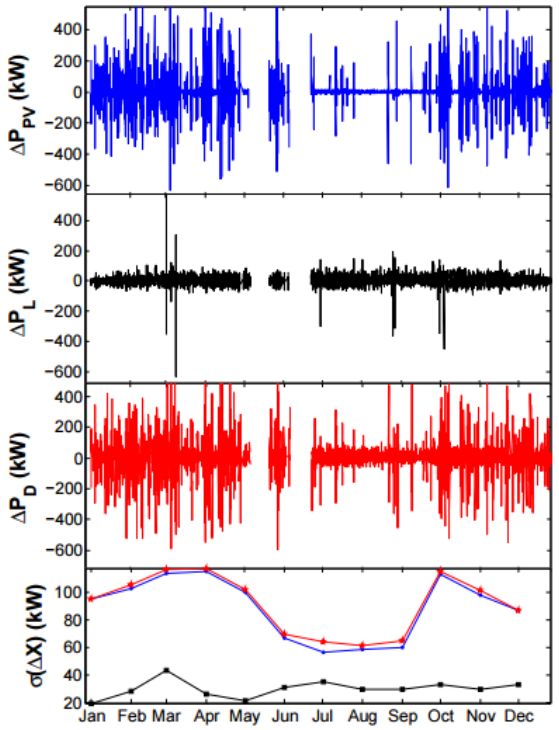

FIGURE 4.14: Time series of 15-min step changes in PV generation, gross demand, net demand and computed standard deviations (Marquez et al., 2012)

approach using time-series capacity fading of the battery is easier to implement. There are alternatives to work around this issue and the development of this feature in DER-CAM is expected soon. In the meantime using a conservative estimate for the battery life in DER-CAM can be used as an approximation to take this effect into account.

In the papers by Sharafi and El-Mekkawy (2014) and Hittinger et al. (2015) the influence of battery wear due to its operation on the optimal dimensioning of a microgrid is investigated. Both confirm that this capacity fade has an impact on the investment decisions and should not be neglected. It is expected by using the battery as the technology to dampen drops in PV generation battery wear becomes even a more important concern.

EVs and demand response

In this work only batteries and fast ramping generators are considered as technologies with the ability to respond fast to changes in PV output. Also electrical vehicles (EVs) connected to the microgrid at the right times could be considered as a technology with

this capability. DER-CAM has the ability to consider EVs as a DER but for simplicity this technology was not considered.

Also from the demand-side actions can be taken in order to take into account these fluctuations and avoid increased demand charges. The condition would be that demand can respond fast enough. Automatic demand response would classify and loads could be either shifted in time or in the worst case curtailed. There will be a trade-off between the cost of load shifting and/or curtailing and the investment and dispatch of the DERs.

Spikes in irradiance

In this analysis of the variability of solar radiation the emphasis is laid on drops in irradiance with respect to the expected irradiance. Next to drops in expected irradiance also spikes in irradiance will occur. These spikes are less importance because of two reasons. First, by looking at for example Figure 4.3 displaying the distributions of 15-min and hourly data of solar radiation conditioned for the hour and the month, it can be seen that these distributions have a long tale to the left. This is generally the case, as also discussed in Appendix A, and implies that percentage-wise, with the average taken as the baseline, the drops are a lot larger than the spikes.

A second reason is the fact that there is no direct cost linked to a higher PV output than expected at a particular time step. Indirectly it can occur that by not taking into account the fact that the PV output will sometimes be higher than expected, more curtailing of PV could occur than is captured by the model. This will only be the case if the PV capacity installed is comparable with the minimum load during daytime and if selling is not allowed. Or if selling is allowed and the PV capacity installed is comparable with the selling limit. If this is the case the added value of PV to the microgrid might be slightly overestimated.

Consideration of islanding or macro grid outages

DER-CAM has the capability to consider outages of the macro grid for grid-connected systems. Even the investment decisions in DERs of a completely islanded microgrid can be optimised, although the model is not often used for this purpose. In this work grid outages are not considered. The analysis of solar radiation data could be helpful

to estimate how much PV installed adds to the reliability of the system if an outage occurs. A similar approach, using confidence levels based on historical data can be used in this case. It is clear that if hourly data would be used for this analysis the potential of PV will be overestimated.

Chapter 5

Case studies

5.1 Setup and key parameters

In this section several case studies are run to test the impact of short-term variability in irradiance, formulated as described in the previous chapter, on optimal microgrid design. Also the sensitivity of the results to the capital cost of stationary electricity storage is investigated. Table 5.1 gives an overview of the case studies.

	Load profile and tariff		Solar data	
	Medium office Tariff A-10	Large hotel Tariff E-19	Utah	Wyoming
Case a	x		x	
Case b	x			x
Case c		x	x	
Case d		x		x

TABLE 5.1: Overview of the considered case studies

Each case is run three times:

- For the first run only the possibility to invest in PV and stationary electricity storage will be considered and selling electricity back to the grid is not allowed;
- The same investment options are considered as in the first run but selling excess electricity generated by PV panels is now possible. Net metering[1] is assumed in this case and the maximum electricity sold is constraint;

[1]The price for buying and selling from and to the grid is the same

- In the third run there is also the possibility to invest in on-site generators next to PV and stationary electricity storage. Selling excess electricity generated by PV panels under net metering is possible and the same constraint regarding selling applies.

5.1.1 Tariffs, load profiles and solar profiles

Tariff design

As already mentioned earlier, from a microgrid owner's perspective the cost of the variability of PV output is expected to be mainly reflected by higher demand charges than in the case when no variability is assumed. Therefore the tariff structure or design to which the microgrid owner is subjected is of crucial in this context.

The way a tariff is structured differs from power system to power system. In some cases consumers have the option to chose between retailers offering different tariffs, in other systems there is no choice possible. Having this choice depends on the degree of liberalisation of the electric power industry of a country (Pérez-Arriaga, 2013). The point where you connect to the macro-grid (high voltage, medium or low voltage) will also be a determinant for the tariff applied as it is the case in California (PG&E, 2015). For different types of consumers, e.g. residential, industrial, commercial or agricultural, different tariffs structure apply. The customer type is strongly correlated to the magnitude of the power requested and even within a certain type different tariffs can apply, dependent on the order of magnitude of the maximum power requested (PG&E, 2015).

In a recent report by the Rocky Mountain Institute (2014), titled 'Rate design on the distribution edge- rate design for a distributed resource future', the structure of an electricity tariff is split up along three axes:

- Attribute unbundling: shifting from fully bundled pricing to rate structures that break apart energy, capacity, ancillary services, and other components;
- Temporal granularity: shifting from basic or inclining block rates to pricing structures that honour the time-based aspects of electricity generation and consumption (e.g., peak vs. off-peak, hourly pricing);

- Locational granularity: shifting from pricing that more or less treats all customers within a distribution network equally to one that recognizes that their location within the system impacts the cost of delivering electricity to them and the value their DERs can provide.

The tariffs used in this work are the A-10 and E-19 tariff for commercial customers, both offered by PG&E (2015). Details about these tariffs can be found in Appendix C. The A-10 tariff applies for customers with a maximum demand between 200 and 499 kW and the E-19 for customers with a maximum demand between 500 and 999 kW.

Both the A-10 and E-19 tariff contain all the elements which were summed up before. Power and energy are unbundled, there is temporal granularity and locational granularity. Although it could be said locational granularity is minimal, only the voltage level of the connection point is taken into account, in the future an even smaller granularity can be expected. The next step on the longer term concerning distribution tariffs would be to move from a static tariff to dynamic location dependent real-time pricing of energy (Rocky Mountain Institute, 2014).

The attractiveness of stationary storage technologies for a microgrid owner is very sensitive to the tariff structure. More specifically mainly two elements of the tariff add value to batteries in a microgrid: demand charges and temporal granularity. The higher the proportion of demand charges in to the total electricity bill and the larger the difference in energy prices between different TOU periods the more attractive the investment in batteries becomes.

Also the attractiveness of the investment in PV is sensitive to the tariff structure. If energy and power prices are higher when solar radiation is expected to be higher, investment in PV will be favoured more strongly. Both installing batteries and PV offers economic synergies from an energy and power perspective. From an energy perspective batteries can transfer energy generated by PV panels during the off or partial peak hours to peak hours. From a power perspective batteries can 'smoothen' the output of PV generation in order to limit demand charges.

As DER adoption grows and changes the manner in which customers rely on the grid, it will become increasingly important for utilities to send clear signals and incentives to customers so they know how to— and are economically motivated to —align DER

deployment with maximizing grid value (for example, reducing peak demand or shifting use) (Rocky Mountain Institute, 2014). Figure 5.1 gives the traditional cost allocation for the mass-market and the larger commercial and industrial customers.

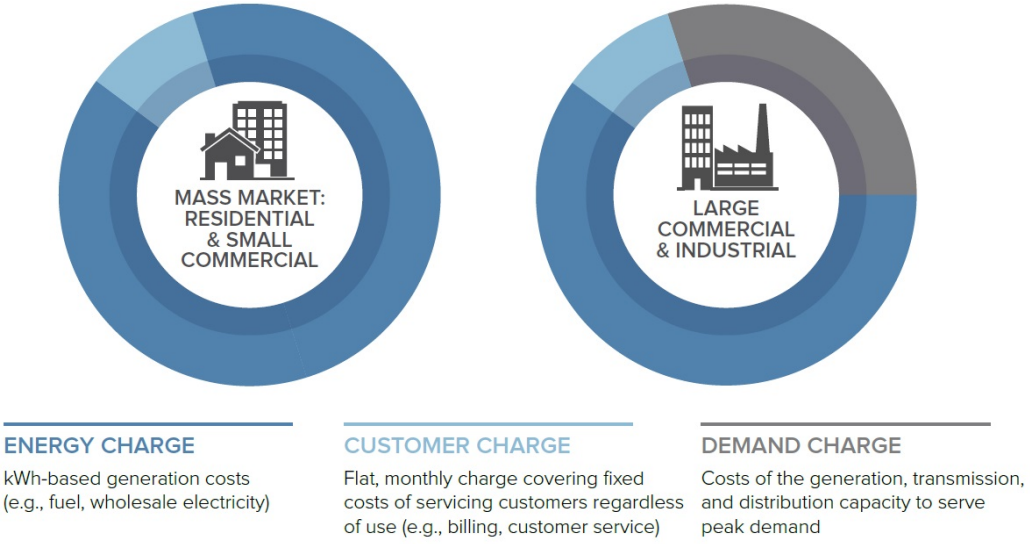

FIGURE 5.1: Traditional cost allocation of the electricity bill (Rocky Mountain Institute, 2014)

It is expected that in the very near future with more penetration of DERs also demand charges will be introduced for residential and small commercial customers to better reflect their real cost. The way demand charges are calculated differs from power system to power system. Most commonly demand charges are calculated on a monthly basis using the highest power demand averaged over 15 minutes. In some cases a longer or shorter interval is used. In summary, the adoption of PV and batteries will be - next to the expected solar radiation and its distribution at the location - highly dependent on:

- The relative importance of demand charges in the electricity bill.
- The interval on which maximum demand is averaged.
- The magnitude of the difference between charges from one TOU period to another.
- The correlation between solar radiation and electricity charges, both power and volumetric charges.

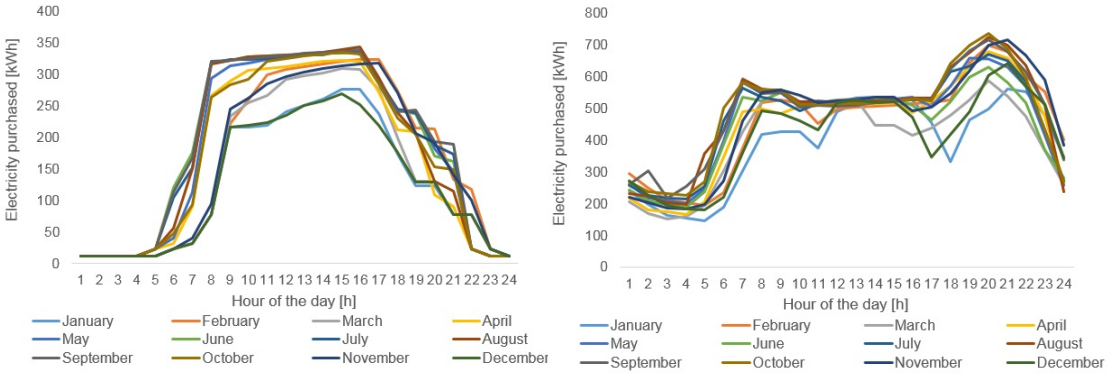

(A) Medium sized office (B) Large hotel

FIGURE 5.2: Electricity purchased on peak days from the utility for different buildings in San Francisco. The data is obtained after running the base case scenario in DER-CAM.

Load profile and solar data

The electricity purchased from the utility by a medium size office in San Francisco[2] on peak days without any investment in distributed energy resources [3] is shown by Figure 5.2a. The annual energy cost for this building in the base case is $ 238000 assuming the A-10 tariff. This tariff is applied because the yearly peak demand of the office is around 344 kW and this tariff applies for commercial customers with a peak demand between 200 kW and 499 kW (PG&E, 2015). The rates for service delivery voltage (or secondary voltage) are used.

It should be noted that the electricity purchased from the utility is an output of the base case run with DER-CAM. The real input inserted in DER-CAM are the different loads of the building during a typical week, weekend day and the peak day of each month. These loads are split up into different end-uses: electricity only, cooling, refrigeration, space heating, water heating and natural gas only. The total annual energy cost obtained in this base case run, also called the base case cost, is important as this cost is used to estimate the operational savings by installing DERs. This operational savings are linked with the payback constraint (Equation 3.23), stating that investments should be paid back by these operational savings within a particular time span.

The electricity purchased from the utility by a large hotel in San Francisco on peak days after running the base case scenario with DER-CAM is shown by Figure 5.2b. In this case the annual energy cost for this building is $ 745000 assuming the E-19 tariff. The

[2]Data obtained from the load database of DER-CAM
[3]This run without considering any investment is called the base case run.

peak demand for a typical year is 736 kW and therefore the E-19 tariff is applied. Also for this building the rates for service delivery voltage (or secondary voltage) are used.

It can be seen from the profiles shown on Figure 5.2 that not only the magnitude of electricity purchased for both buildings differs, but also the shapes of the profiles are very different. For the medium office the consumption is highest between 7 am and 18 pm, while for the hotel the peaks in consumption occur during the early morning and evening. The most import difference between the A-10 and E-19 tariff is the fact that in the E-19 also the demand charges are dependent of the time of occurrence, while for the A-10 only the highest purchase during the whole month is considered for the determination of the demand charge. As the demand charges are additive and also the rates for the demand charges are higher in the E-19 tariff it could be said that this tariff gives a stronger incentive to flatten the load curve for the consumers.

Two different data sets for solar radiation are used, one with data collected from a site in Moab, Utah and the other one with data collected from a site in Green River, Wyoming. Five years of solar radiation with an interval of 15 minutes was used for the analysis [4]. Solar radiation from California was preferred to match the load data and tariff structure, but this data was not easily found. It can be seen from Figure 4.5 in the previous chapter that if we look at average daily insolation throughout the year per m^2 the site in Moab corresponds approximately to central or more southern California, while the site in Green River corresponds approximately to Northern California. After analysing the collected data, it was found that for the site in Green River the average insolation was 4.686 kWh per m^2 per day and for the site in Moab this was 5.189 kW per m^2 per day. These values are in agreement with the heat map shown by Figure 4.5.

These daily averages are important but the focus of this work is on the distributions and variability of irradiance. It is impossible to say if the distributions of this collected data coincides with distributions of irradiance using Californian data without comparing the full data sets. Fernández-Peruchena and Bernardos (2015) state in their paper that the local conditions (atmospheric transparency and proportion, type and variability of clear sky and cloudy conditions) noticeably affect the short-term irradiance distributions, even within the same climate zone. In this work the focus is on the method and qualitative results, using this data does not pose a direct problem but it should be kept in mind.

[4]Source: http://solardat.uoregon.edu/

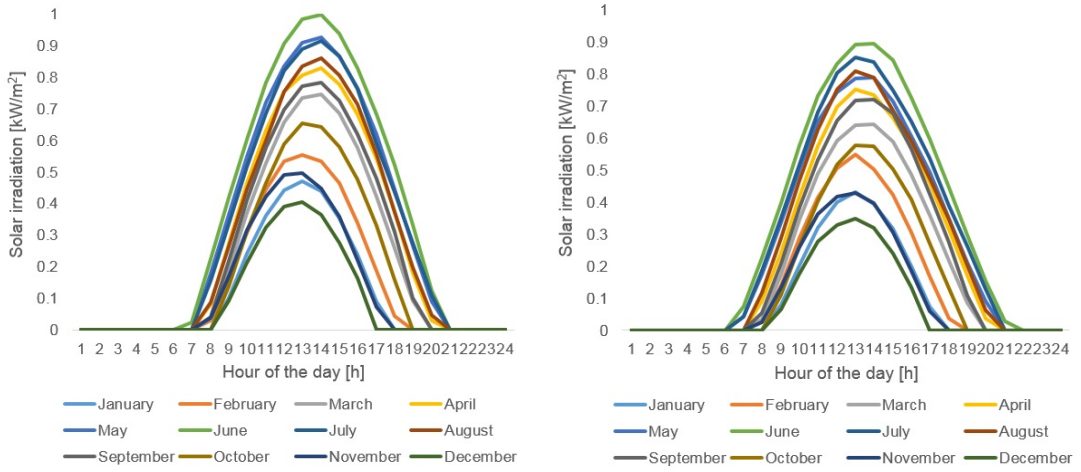

(A) Moab, Utah (B) Green River, Wyoming

FIGURE 5.3: Solar radiation profiles for week and weekend days

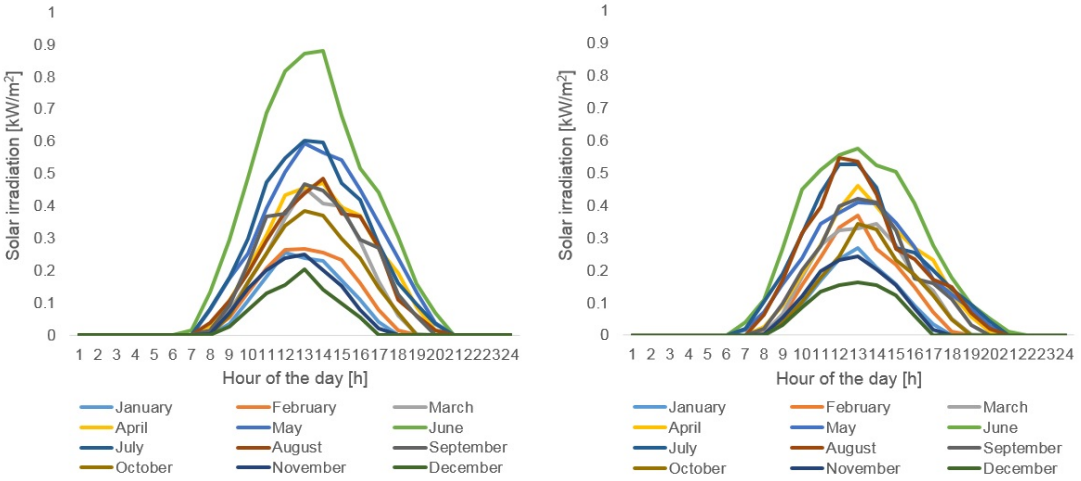

(A) Moab, Utah (B) Green River, Wyoming

FIGURE 5.4: Solar radiation profiles for the peak day

Figure 5.3 and Figure 5.4 show the solar profiles for the two sites for the weekend and weekend days and the peak day respectively. As can be seen from the figures, the site in Moab, Utah is more suitable for PV generation. It can be seen from Figure 5.4a that for that site in June the solar radiation at the peak day, when the 90th percentile of solar radiation data is used, the profile is not very different than the profile used for week and weekend days.

Figure 5.5 shows the values used for the magnitude of the sub-hourly drop in irradiance using a confidence level of 90%. It can be seen that for both sites these values are not very different and not even very dependent of the month. For this confidence level all the drops are between 60% and 70% of the scaled average irradiance during most of the

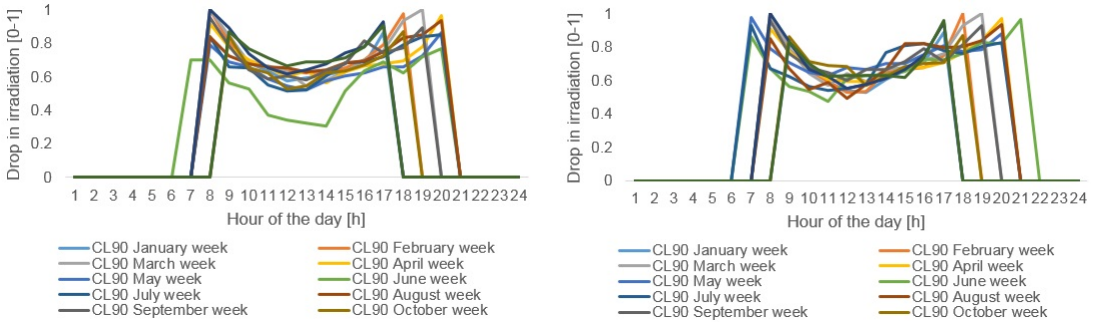

(A) Moab, Utah (B) Green River, Wyoming

FIGURE 5.5: Magnitude of the drops in irradiance as a percentage of the week and week day solar profile for a confidence level of 90%

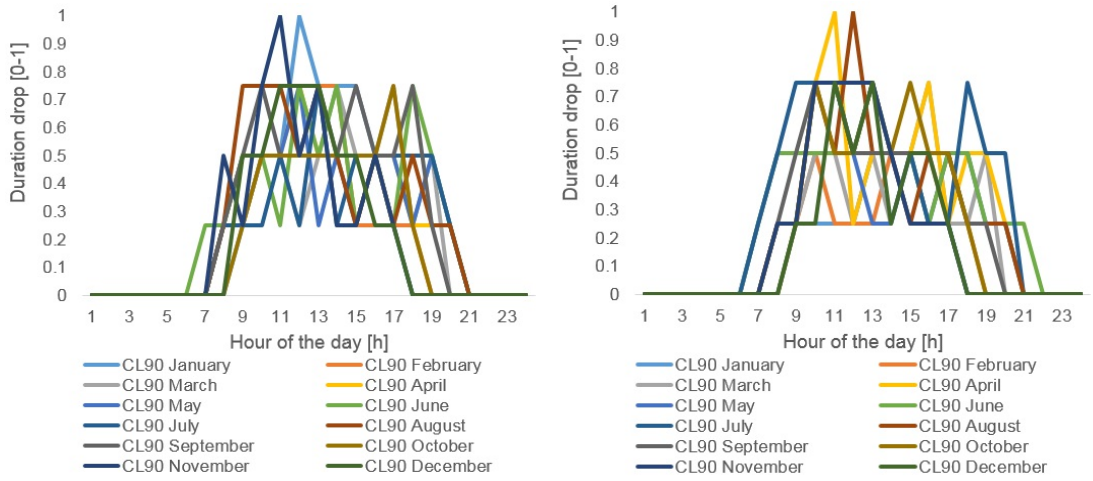

(A) Moab, Utah (B) Green River, Wyoming

FIGURE 5.6: Duration of the drops in irradiance as a fraction of an hour for a confidence level of 90%, independent of day-type

time, as shown by Figure 5.3a. It should be noted that as the scaled average irradiance is slightly higher for the site in Moab, the absolute values for the drop in irradiance will be also slightly higher for this site in this case. The only exception again is the month of June for the site in Moab, it seems that for that month cloud cover, on a longer-term and on the short-term is less present than in other months.

The durations of the sub-hourly drops for a 90% confidence interval are shown by Figure 5.6. A similar pattern is visible on Figures 5.6a and 5.6b namely longer lasting short-term cloud cover before noon than in the after noon, although the months for which this is apparent differ for both sites.

5.1.2 Considered technologies

5.1.2.1 Stationary electricity storage

Today there are several options regarding stationary electricity storage technologies in a microgrid. Fathima and Palanisamy (2015) lists up thirteen technologies, the most important ones being: pump hydro storage, compressed air storage, different types of electrochemical batteries, flow batteries, hydrogen-based systems, flywheel energy storage, superconducting magnetic energy storage and super capacitor energy storage.

The function of stationary storage in a standalone and a grid-connected systems is quite different. In a standalone microgrid stationary storage is mostly used for real and reactive power balancing, it is critical to provide interim power shortfall almost instantaneously due to the unpredictability or malfunctioning of DGs (Fathima and Palanisamy, 2015). In a grid connected system a battery can also be used to maintain power quality, regulate the reactive power and to serve as a back-up and compensate for outages of the central grid. But mainly it will be used as a tool to shift electricity purchase from peak to off-peak periods and to shave the peak demand in order to minimise the electricity bill.

In this work one type of stationary electricity storage is considered, more precisely the lithium-ion battery. Lithium-ion batteries are one of the more costlier types of electrochemical storage but with high energy densities, no memory effect and a slow loss of charge when not used (Fathima and Palanisamy, 2015; Chen et al., 2012). In a recent report by the Rocky Mountain Institute (2015) lithium-ion batteries (in particular LiFePO4) are called efficient, durable and shelf-stable with excellent power characteristics.

Also in Neubauer and Simpson (2015) lithium-ion batteries are used to simulate the impact of operating these batteries under a peak-shaving control algorithm on electricity costs. In that study the cost of the complete installed storage system is assumed to be equal to $300 times the available energy in kWh of the system plus $300 times the power in kW of the system. This is intended to represent the cost of both a battery and inverter, where the cost of the battery scales largely with energy and the inverter with power. Figure 5.7 shows the historical and forecasted prices of lithium-ion battery packs. It can be said that today prices lay between $400 and $ 700 per kWh.

In the executed runs the same reasoning as in the paper of Neubauer and Simpson (2015) is used. The same price applies for the batteries per kWh as per kW and the total price of the battery is the sum of the suggested energy capacity times the price plus the suggested maximum power output times the same price. The maximum power output and input are assumed to be equal. The prices are varying between \$200 and \$500 per kW or kWh in steps of 50\$. This means that the price of a battery with the ratio of energy over power capacity equal to 1 ranges between \$400 and \$1000 dollar. This ratio of the installed battery is restricted between 0.25 and 4 in the executed runs. It should be noted that if no sub-hourly variability in PV is assumed and time steps are hourly it would not make sense to have a battery configuration with an energy capacity over maximum power lower than 1 (not taking into account the discharge efficiency and minimum state of charge).

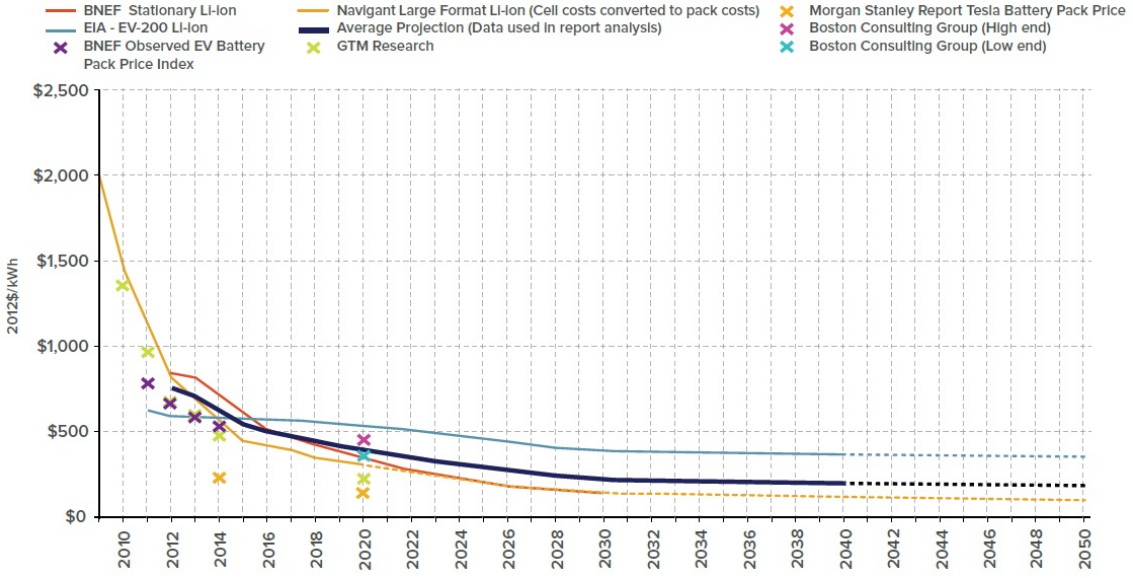

FIGURE 5.7: Lithium-ion battery pack prices: historical and forecasted (Rocky Mountain Institute, 2015)

In Table 5.2 the technical characteristics of the lithium-ion battery are displayed. These values are the default values used in DER-CAM and are in the same line as the values used by the Rocky Mountain Institute (2015) and quoted by Fathima and Palanisamy (2015). Only the estimation of the life time could be labelled conservative, but that compensates for the fact that battery capacity loss due to operation is not taken into consideration in this version of DER-CAM. Also by considering the charging and discharging efficiency of the battery, the optimal solution will minimize the frequency of

charging or discharging for the battery. This will increase the operating life of batteries (Chen et al., 2012).

Characteristic	Value
Efficiency of charging	90 %
Efficiency of discharging	90 %
Decay	0.1 %
Minimum State Of Charge	30 %
Life time	5 years

TABLE 5.2: Technical characteristics of the lithium-ion batteries, default in DER-CAM

In DER-CAM it is possible to consider other energy storage technologies than electrochemical storage. Examples are heat storage, cold storage and flow batteries. Also the interaction between a microgrid and electrical vehicles (EV), a form non-stationary storage, can be taken into account. In this work these other energy storage technologies are not taken into consideration as they are not the core of this work.

5.1.2.2 PV

Three sources were consulted to set a price for the capital cost of PV installed: reports from Lazard (2014), MIT (2015) and the Rocky Mountain Institute (2015). It was chosen to set the cost to 3000 $ per kW PV installed. Figure 5.8 shows historical and forecasted prices for commercial PV. These projections do not disagree with information found in the other two sources.

In Table 5.3 the technical characteristics of the modelled PV panels are shown, these values are used as a default in DER-CAM.

Characteristic	Value
Efficiency of energy conversion	variable, between 15-18 %
Peak PV efficiency	0.1529 kWh per m^2
Available area for PV	Not constraint
Maintenance cost	0.25 $ per kW installed per year
Life time	30 years

TABLE 5.3: Technical characteristics of PV, default in DER-CAM

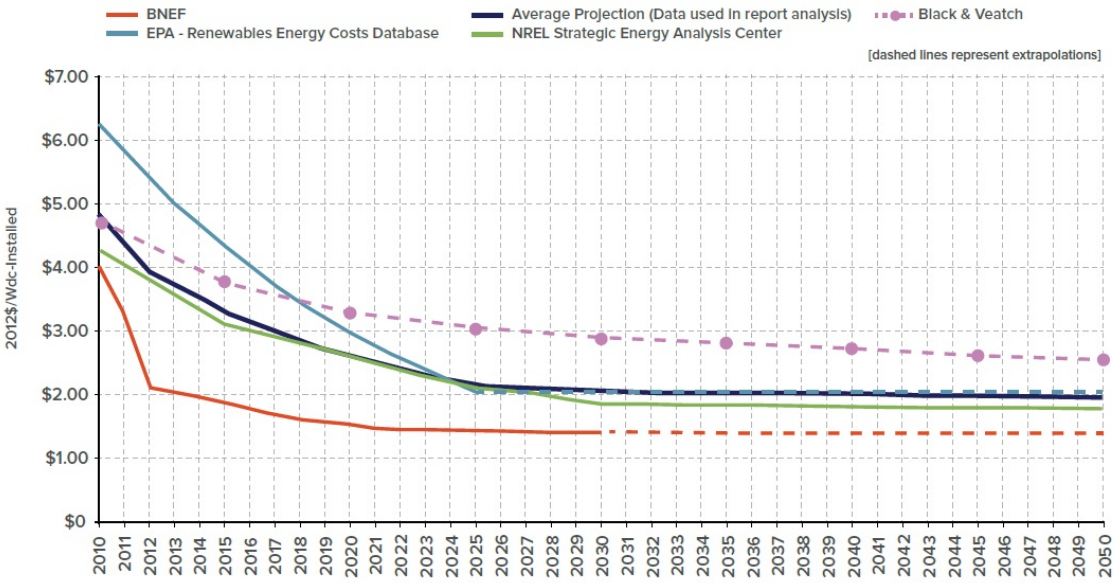

FIGURE 5.8: Commercial PV installed capital costs battery pack prices: historical and forecasted (Rocky Mountain Institute, 2015)

5.1.2.3 On-site generators

Three different types of generators are considered: internal combustion engines (ICE), micro turbines (MT) and fuel cells (FC). All technologies burn natural gas. Two different technologies of fuel cells are included: molten carbonate (MCFC) and phosphoric acid fuel cells (PAFC). All the considered technologies and their characteristics are shown by Table 5.4. Some technologies have the option to deliver power and heat simultaneously (CHP), this increases the total efficiency of the engine but results in a slightly higher investment cost.

From Table 5.4 can be seen that in terms of capital costs fuel cells are relatively expensive while internal combustion engines are the cheapest per kW capacity installed. On the other hand, the fuel cells are the most efficient. The only technology labelled as fast ramping or load following are the internal combustion engines. Because of this load following capability an internal combustion engine (especially when burning diesel) is sometimes coupled with PV panels in an isolated microgrid, as is described in the paper of Dufo-Lopez and Bernal-Agustín (2005). All the other considered generator types are made to run at an as constant as possible power level.

The fuel cost per kWh of primary energy content for natural gas is set to 0.033 $. To estimate this cost information from the U.S. Energy and Information Administration

Technology	MaxP [kW]	Cap. Cost [$/kW]	Lifetime [years]	OMVar [$/kWh]	Fuel	Electric eff. [%]	CHP [0/1]	Heating COP	Min. load [%]
ICE	75	2360	15	0.024	NG	26	0	/	70
ICE	75	3011	15	0.0255	NG	26	1	1	70
ICE	250	2163	15	0.024	NG	27	0	/	70
ICE	250	2704	15	0.0255	NG	27	1	1	70
MT	65	2737	15	0.013	NG	23.8	0	/	75
MT	65	3220	15	0.0145	NG	23.8	1	1.5	75
MT	200	2678	15	0.016	NG	26.7	0	/	75
MT	200	3150	15	0.017	NG	26.7	1	1	75
MT	250	2311	15	0.011	NG	26.1	0	/	75
MT	250	2719	15	0.012	NG	26.1	1	1	75
MCFC	300	10000	20	0.045	NG	42.7	0	/	100
MCFC	300	10750	20	0.046	NG	42.7	1	0.5	100
PAFC	400	7000	20	0.036	NG	38.2	0	/	100
PAFC	400	7300	20	0.037	NG	38.2	1	0.5	100

TABLE 5.4: Technical and financial characteristics of considered on-site generators, default parameters in DER-CAM

was used [5]. The CO_2 emission for natural gas per kWh of primary energy content are set to 0.18 kg. This value is the default value used in DER-CAM. In order to obtain the cost for delivering one kWh electricity this cost per kWh primary energy content needs to be divided by the efficiency of the generator and the variable maintenance cost per kWh needs to be added.

5.1.2.4 Other key parameters

Table 5.5 shows the values of other key parameters. All values for the parameters are the default values in DER-CAM, except for the fixed cost for connection to the electricity grid. The fixed cost for connection to the electricity grid was set using tariff information from PG&E (2015). Less emphasis is laid on the CO_2 related emission parameters as these are not of direct importance for this work.

It should be noted that especially the first two listed parameters in Table 5.5 are of critical importance. Investments will be sensitive to the setting of the interest rate and the maximum payback period. In order to meet the heating and cooling loads it is assumed that a central HVAC system is already present at the building.

[5] More precisely : http://www.eia.gov/dnav/ng/ng_pri_sum_dcu_nus_m.htm and http://www.eia.gov/dnav/ng/hist/n3010us3m.htm

Parameter	Value
Interest rate	5%
Maximum payback period	10 years
Carbon tax	0 %
Ambient temperature	8-25 degrees Celsius, dependent of the hour and month
Marginal CO2 emission of the macrogrid	0.45-0.6 kg per kWh electricity delivered, dependent of the hour and month
Fixed cost for natural gas connection	65 $ per month
Fixed cost for electricity connection	around 140 $ per month, dependent of tariff
Amount of heat generated from 1 kW natural gas (β)	0.8 kW
COP for electrical cooling and refrigeration	4.5

TABLE 5.5: Setting of other key parameters in DER-CAM

5.2 Results

In this section we will refer to the different settings of the input parameters by their case letter as listed up in 5.1. In Table 5.6 the most important metrics for the load, tariff and solar data used in each case are summarized. The average daily electricity purchased, the peak demand and the ratio of power over volumetric charges were obtained by running the base case run for the different cases. As no investment in considered in this run case a and b and case c and d have the same values for these three metrics. It should be noted that the main difference between the A-10 and E-19 tariff is the fact that in the E-19 demand charges are of greater importance, which can also be seen on Table 5.6.

	Average daily electricity purchased [kWh]	Peak demand [kW]	Ratio power charges over volumetric charges	Tariff used [PG&E]	Average daily insolation [kWh/$m2$]
Case a	2705	344	0.32	A-10	5.189
Case b	2705	344	0.32	A-10	4.686
Case c	10636	736	0.54	E-19	5.189
Case d	10636	736	0.54	E-19	4.686

TABLE 5.6: Overview of the main metrics of the considered case studies

The sensitivity for the setting of two parameters is investigated in each run for all cases: the confidence level for the short-term variability in irradiance and the investment cost of batteries. Confidence levels for the short-term variability in irradiance vary between 70%

and 95%, the higher this confidence level the more conservative the attitude towards this variability. Also a 'No drop' case is considered, meaning that for that run this short-term variability is not taken into account. For all runs the battery investment cost per kWh energy and kW maximum power output are set equal. Thus a battery with a energy to power capacity ratio of 1 costs twice the price per kWh. The prices vary between 200 and 500 $ per kWh installed in steps of 50 $.

5.2.1 Allowing for investment in PV and batteries

5.2.1.1 PV sales disabled

Minimised total annual energy cost

On Figure 5.9 the minimised annual total energy cost per case is shown. The annual total energy cost is the objective to be minimised and is defined by Equation 3.1, including the adjustment introduced shown by Equation 4.1. Also the annual total energy cost for the base case is shown as a reference. Selling excess electricity generated by PV is not allowed in this case.

Case a and case c are the cases in which the solar data from the site in Utah is used. It is clear from the results that using this solar data gives more possibilities to reduce the annual costs. It is also seen that the results are sensitive to both the battery investment cost and confidence level of the short-term variability of irradiance, this is especially true for case c. In that case with battery investment cost equal to 200 $ per kWh and assuming no variability in short-term irradiance annual energy savings around 8% with respect to the base case, while assuming the highest capital costs of batteries and the highest confidence level these savings are reduced to only 1% with respect to the base case. Case d is the only case that does not seem to be very sensitive to level of short-term variability of irradiance, in the other cases a trend is visible.

The annual total energy cost does not reveal all the important financial information. Figure 5.10 displays the OPEX over CAPEX ratio for the different cases. The OPEX consists mainly out of cost for electricity purchased (including volumetric and demand charges), fuel cost and maintenance cost. The CAPEX are the annual capital expenses for the technology installed on-site. The lower this ratio, the more investments are

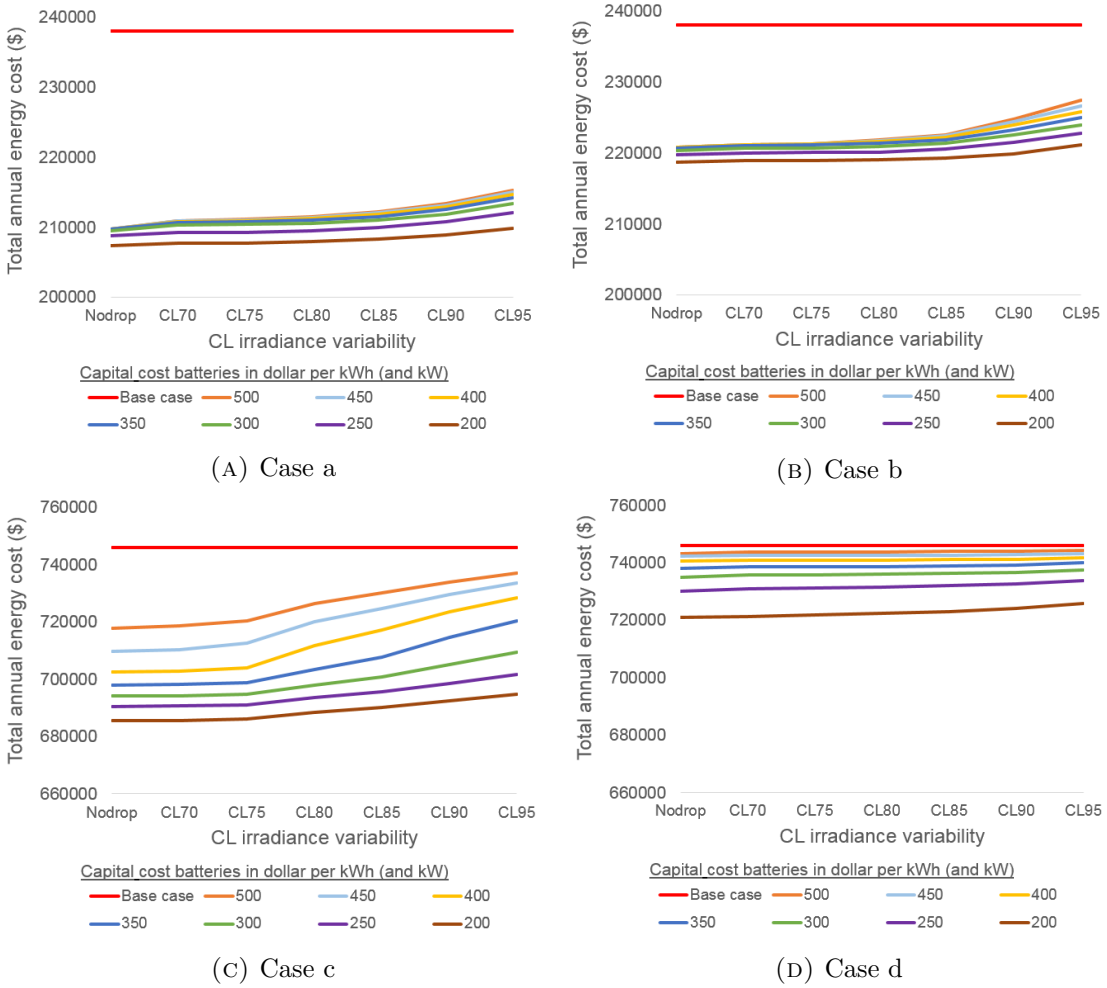

(A) Case a

(B) Case b

(C) Case c

(D) Case d

FIGURE 5.9: Minimised annual energy cost for different confidence levels of short-term variability in solar radiation and battery capital costs

done. It can be seen from Figure 5.10 that this ratio is significantly lower in case a with respect to b and in case c with respect to d, these results are as expected as better solar conditions are assumed in those cases.

It can be seen that for most cases this ratio is only sensitive to battery prices. Only in case c, and less significantly in case b, the ratio increases strongly with higher confidence levels of variability in short-term irradiation. In case c, assuming the highest battery price of 500 $ per kWh, this ratio explodes with higher confidence levels. This means that in this case short-term variability in solar radiation has a strong effect on total capital invested. It seems that under those circumstances investment is discouraged with higher levels of variability.

Figure 5.11 shows the annual volume of electricity purchased for the different cases and different settings of parameters. It can be seen that the annual amount of electricity

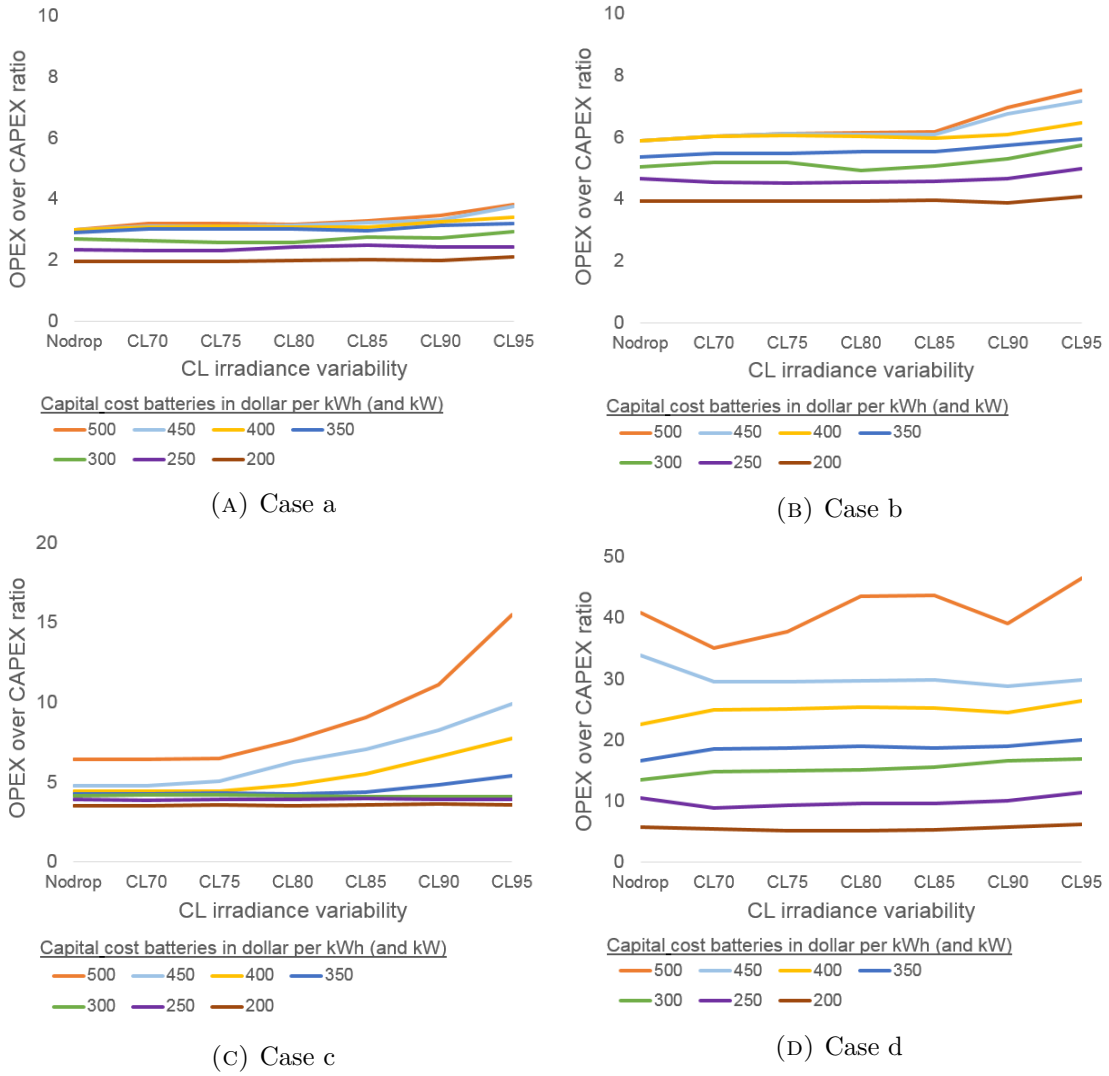

(A) Case a

(B) Case b

(C) Case c

(D) Case d

FIGURE 5.10: OPEX over CAPEX ratio for different confidence levels of short-term variability in solar radiation and battery capital costs

purchased is not very sensitive to the confidence level of variability in irradiance applied. Only in case c is this the case. The increase in electricity purchased for higher confidence levels could already be predicted from the strong increase in OPEX to CAPEX ratio for those same settings shown on Figure 5.9. It can be seen from Figure 5.11 that for all cases, with the exception of case d, the amount of electricity purchased declines significantly if investments in PV and batteries are allowed. Declines are around 55 %, 25 %, 25 % and 10 % for case a, b, c and d respectively. These magnitudes of load defection indicate that the large scale adoption of PV and batteries will have a significant effect on the revenues generated by utilities in the near future. Related to this figure, on Figure 5.12 the peak demand is shown for the cases.

It can be seen from Figure 5.12 that also the maximum electricity purchased over the

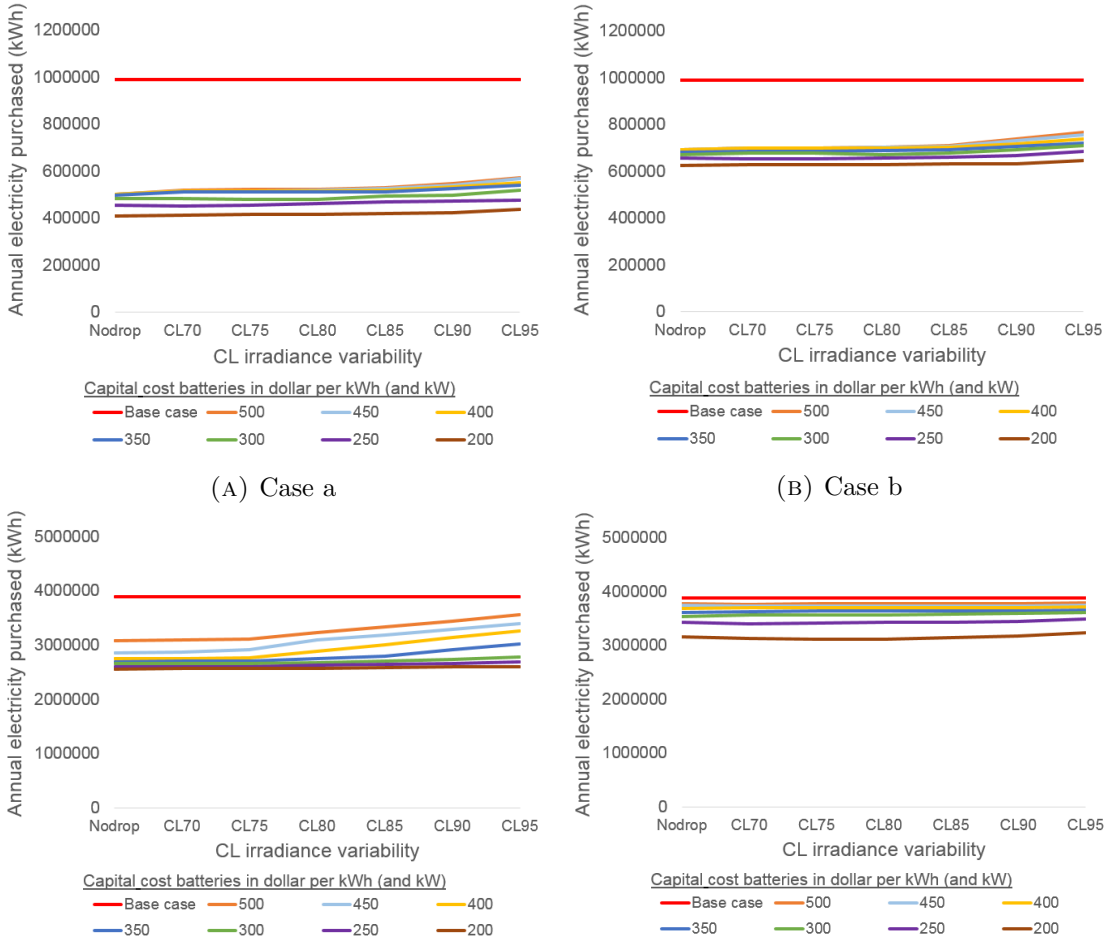

(A) Case a

(B) Case b

(C) Case c

(D) Case d

FIGURE 5.11: Annual electricity purchased for different confidence levels of short-term variability in solar radiation and battery capital costs

year decreases. For case a and b the peak demand decreases between 5 and 15 % dependent of the settings of the parameters investigated and for case c and d the peak demand decreases between 2 and 8%. It can be interfered from these case studies that the adoption of PV and batteries results in a strong decrease in total quantity of electricity purchased, while also the peak demand decreases but less significantly.

Investments in technology

Investment in batteries

The core of this work is to investigate the effect of short-term variability in irradiance on the investments in batteries and PV. Regarding the investments in batteries four metrics are used. The amount of energy capacity installed, the maximum power output of the

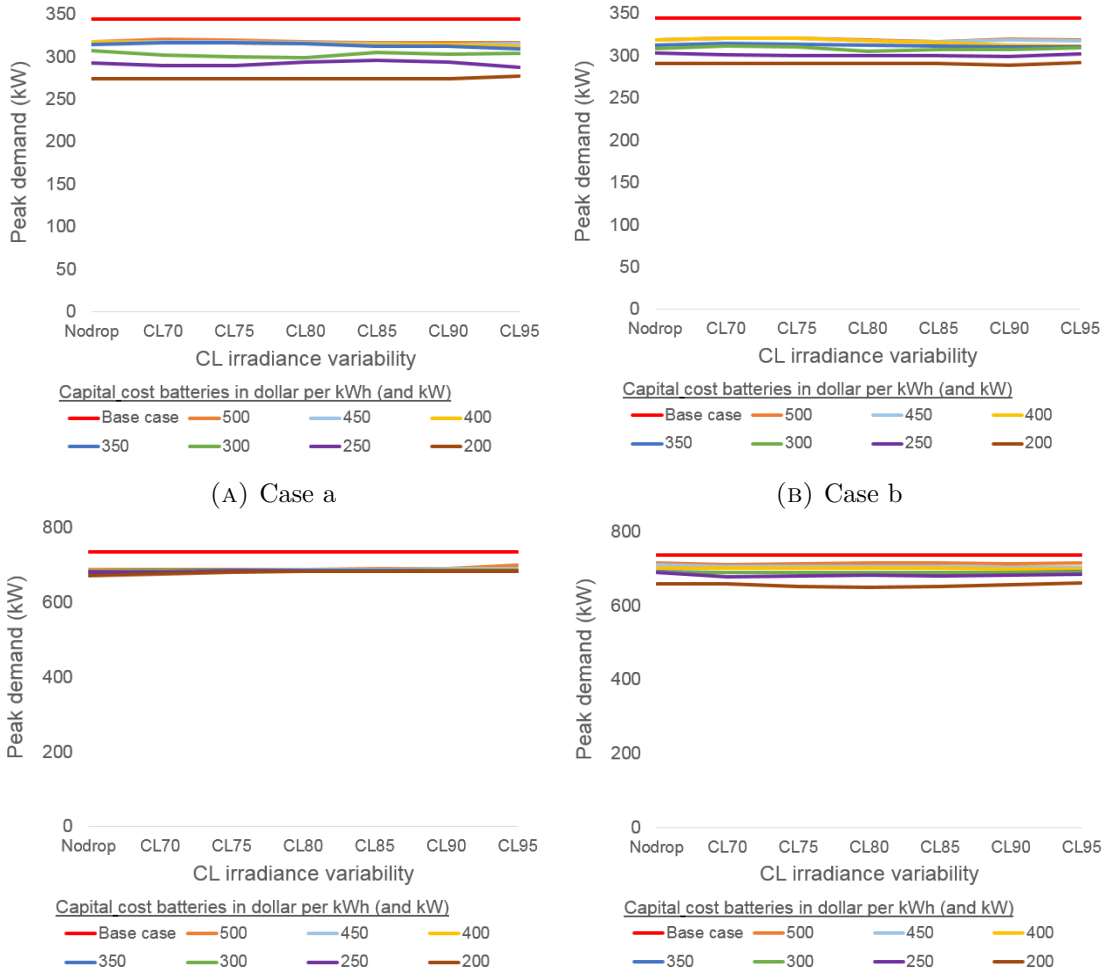

(A) Case a

(B) Case b

(C) Case c

(D) Case d

FIGURE 5.12: Peak demand for different confidence levels of short-term variability in solar radiation and battery capital costs

battery installed, the ratio of energy over power capacity of the battery and the total investment cost of the battery pack. These metrics are shown by Figures 5.13, 5.14, 5.15 and 5.16.

From Figure 5.13 can be seen that for cases a and b the higher the confidence level, the more energy capacity is installed. If batteries are more expensive than 350$ per kWh a small amount are installed with higher confidence levels, while without taking into account this short-term variability batteries would not have been attractive to invest in. The dynamics differ if batteries are 300$ or cheaper per kWh. For case d no real trend is visible, is seems that in this case including short-term variability in irradiance does not affect the investment decision in energy capacity of the battery. In case c something particular happens, the energy capacity of the batteries installed increases with more

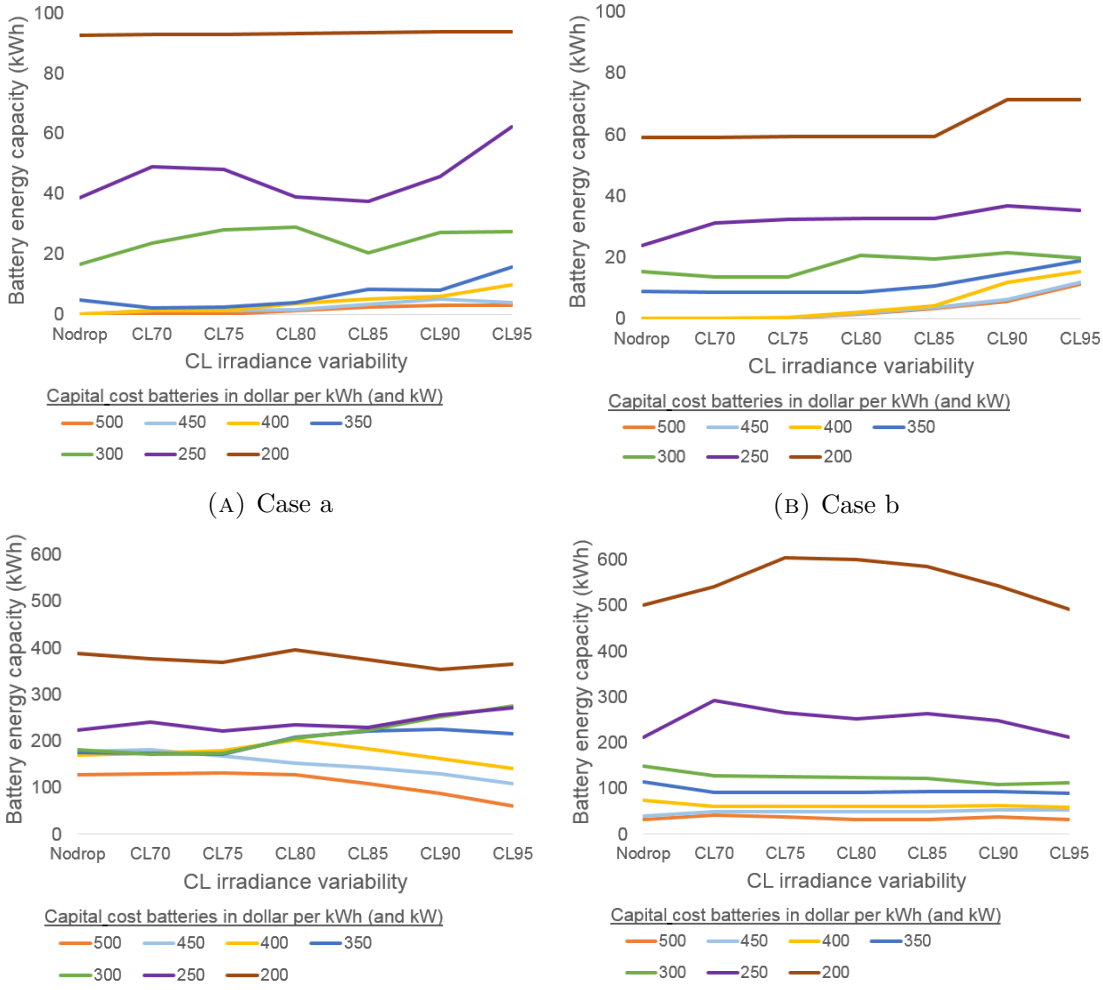

(A) Case a

(B) Case b

(C) Case c

(D) Case d

FIGURE 5.13: Battery energy capacity installed for different confidence levels of short-term variability in solar radiation and battery capital costs

variability if batteries prices are between 250 and 350 $ per kWh, while the energy capacity installed decrease if batteries are more expensive than 350 $ per kWh.

One of the most clear trends is visible on Figure 5.14. In all cases, except case d, there is a clear increase in battery power capacity installed with higher confidence intervals for the short-term variability in irradiance. From this figure it can be interfered that in most cases, if the short-term variability in solar irradiation is not taken into account the optimal power capacity of the batteries will be underestimated. For case a and b the relative increase of battery power with increasing confidence level is the same for all capital costs of batteries. Again for case c the trend is a function of the capital costs of batteries. If batteries are cheaper than 400 $ per kW a strong increase with increasing confidence level is observed, if capital costs are higher than 400 $ per kW the increase

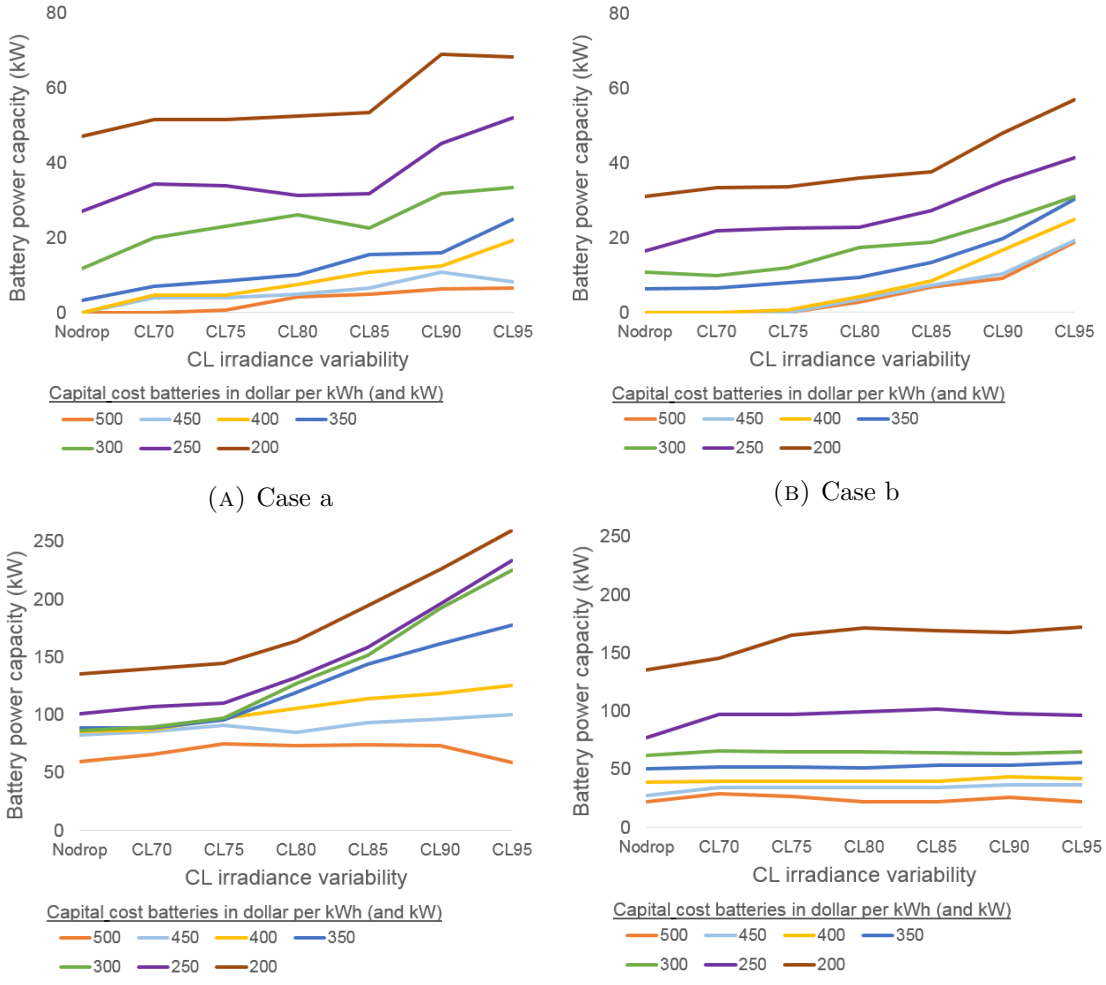

(A) Case a

(B) Case b

(C) Case c

(D) Case d

FIGURE 5.14: Battery power capacity installed for different confidence levels of short-term variability in solar radiation and battery capital costs

is less strong to almost stagnant.

Also on Figure 5.15 trends are visible for cases a, b and c. The trends could already be abstracted from the previous two figures but are more clearly shown on this figure. It can be seen that if short-term variability in irradiance is not taken into account the energy over power ratio of the battery would be overestimated, especially in the case capital costs for batteries are lower.

On Figure 5.16 the total amount of capital invested in batteries for the different cases is shown. For case a and b it is clear to see that including short-term variability in irradiance in DER-CAM makes the investment in batteries more attractive, especially when considering high capital costs for batteries. If batteries are cheaper there is already an investment done in batteries without taken into account this effect, making the

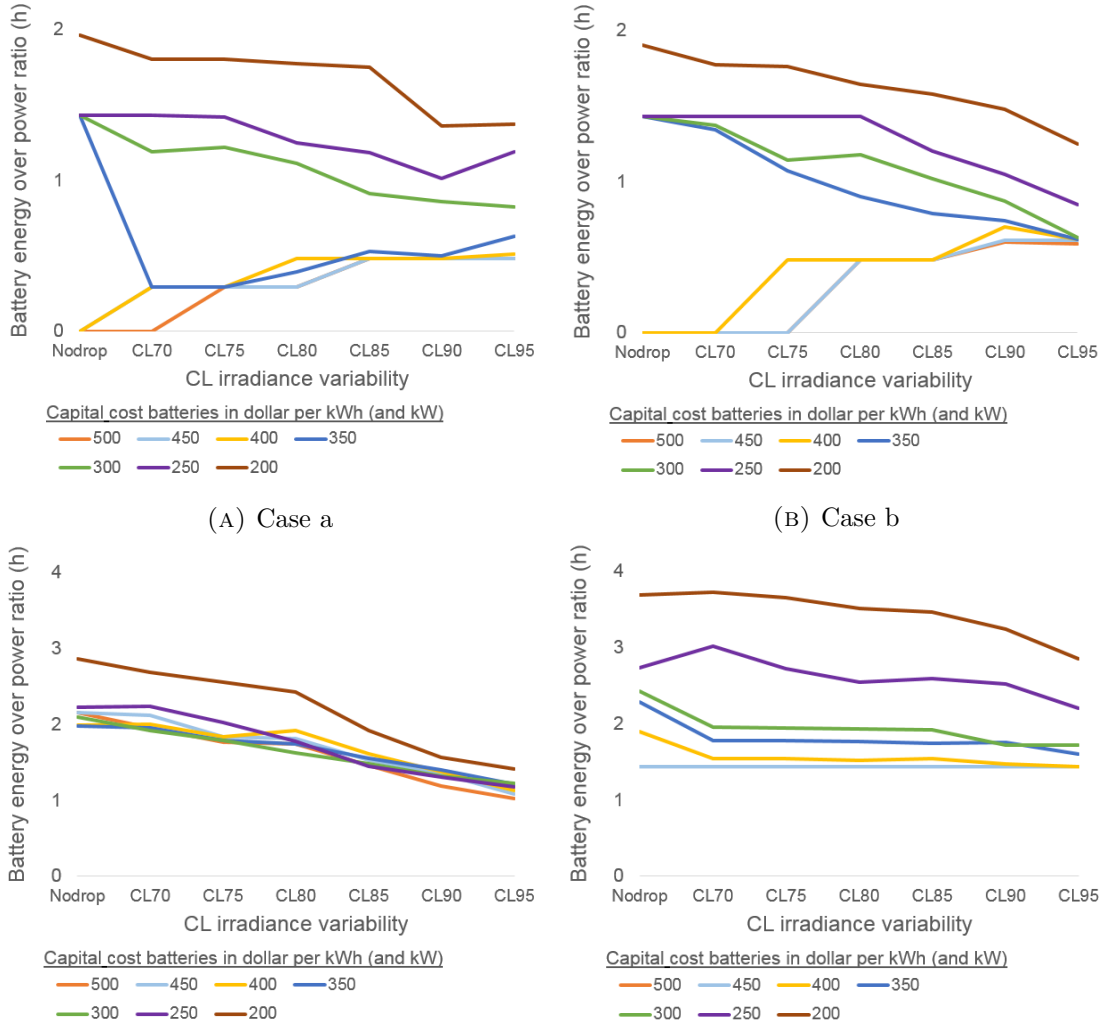

(A) Case a

(B) Case b

(C) Case c

(D) Case d

FIGURE 5.15: Energy over power ratio of the batteries installed for different confidence levels of short-term variability in solar radiation and battery capital costs

increase less significant when this effect is considered. For case c the trend is less clear, the opposite of what is observed in cases a and b happens for the higher battery prices, the more variability assumed, the less attractive the investment in batteries.

The increased attractiveness of the investment in batteries for cases a and b should be looked at in perspective. The total amount of capital invested is around $10000 for the highest confidence interval of short-term solar radiation variability and the more expensive prices battery prices. The lifetime of batteries is assumed 5 years, this means annual capital expenses for the batteries are roughly $ 2000 dollar. The total annual energy cost in these cases is around $ 200 000 dollar, this means that the annual cost for the investment in batteries only represent around 1% of total annual energy cost.

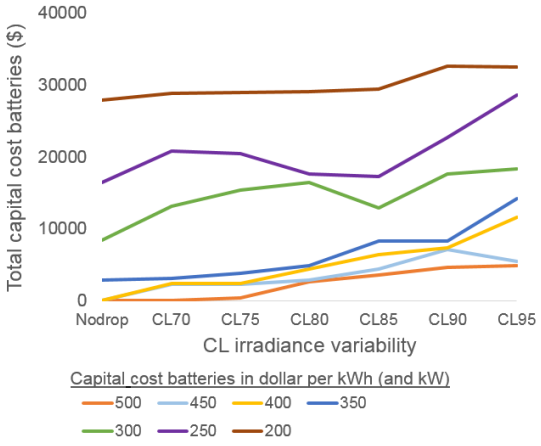

(A) Case a

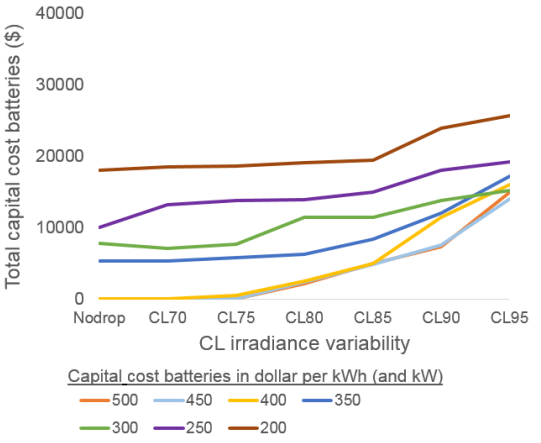

(B) Case b

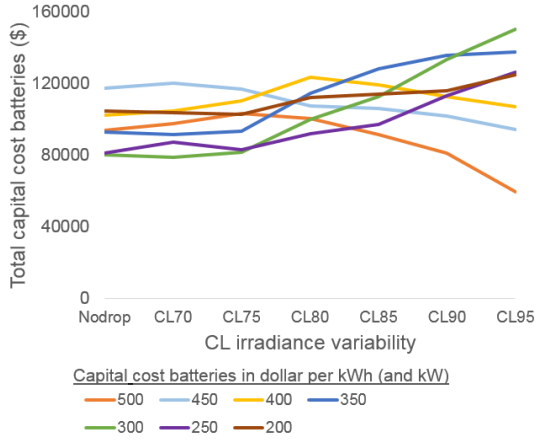

(C) Case c

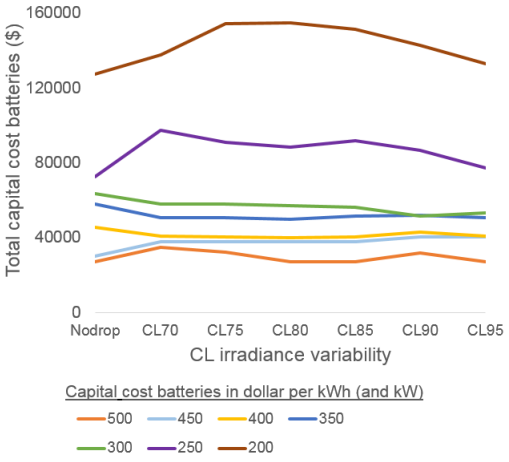

(D) Case d

FIGURE 5.16: Total upfront capital cost of batteries for different confidence levels of short-term variability in solar radiation and battery capital costs

The trend is interesting, but the investment in batteries is still relatively insignificant. For case c, the effect of short-term variability in irradiance is more significant, especially taking into account the trends shown by Figure 5.10.

Investment in PV

On Figure 5.17 the total capacity of PV installed is displayed. As expected the capacity of PV installed is sensitive to the battery prices, but the degree of sensitivity seems to differ strongly from case to case. For cases a and b the capacity of PV installed assuming the cheapest batteries is around 30% higher than the capacity of PV installed assuming the highest battery prices. For case d the capacity of PV installed assuming the cheapest batteries is around 7 times as much as the capacity of PV installed assuming the most

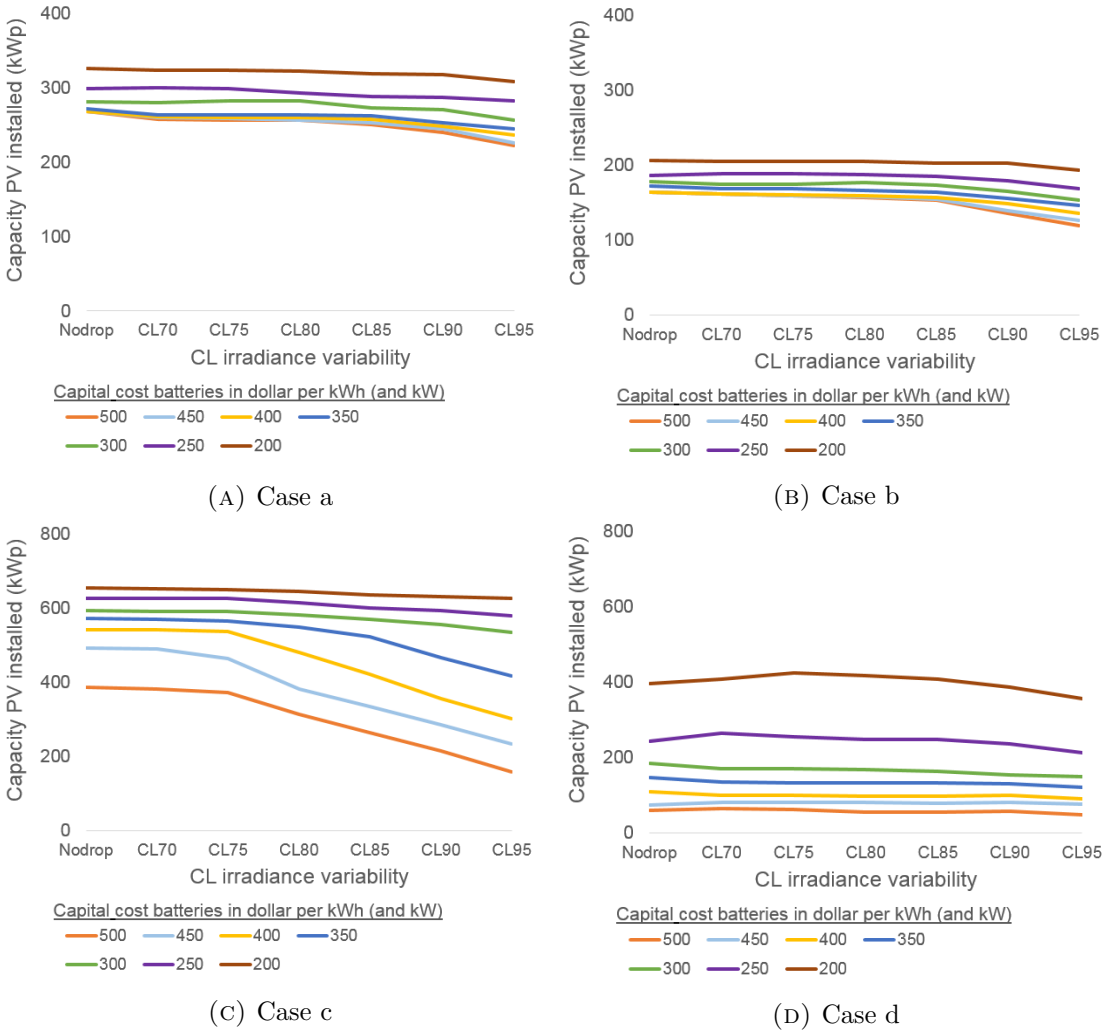

(A) Case a

(B) Case b

(C) Case c

(D) Case d

FIGURE 5.17: Total capacity of PV installed for different confidence levels of short-term variability in solar radiation and battery capital costs

expensive batteries. This switch from investing very little in on-site technologies to investing strongly can also be seen on Figure 5.10d.

Case c seems to be the case witnessing the strongest impact of short-term variability in irradiance. With battery prices over 300 $ per kWh the capacity of PV installed is overestimated strongly when not taking into account short-term variability in irradiance. Decreases around 50% are observed with higher battery prices if this effect is taken into account. This effect is a function of the investment cost of batteries. It seems that in case c by taking this effect into account a lot less capital is invested in on-site technology if batteries are not cheap enough to compensate for it. It can also be argued that if batteries are cheaper, already enough batteries will be installed at the first place and thus cooping with these drops in PV is less an issue.

5.2.1.2 PV sales enabled

In this section the runs for the different cases are discussed with allowing for electricity sales to the utility by the microgrid. The sales are constraint by stating that the maximum power sold cannot exceed half of the yearly peak demand of the building registered in the base case run. Net metering is used, meaning that the price for electricity sold at a time step is the same as the price that would be paid to buy electricity at that time step. The metrics for the different cases are not that extensively covered in this section as in the previous section. The emphasis is laid on the cases where results differ significantly from the previous section. On Table 5.7 an overview is given of the decrease in annual total energy cost and annual total electricity purchased in each case by investing in DERs with and without allowing for sales. The decrease in total annual energy cost and electricity purchased are calculated with respect to the base case. The lower boundary of savings are the savings incurred with the highest battery cost (500 $/kWh) and the highest confidence level for short-term solar irradiance (95%). The upper boundary are the savings made with the cheapest capital cost for batteries (200$ /kWh) and the 'No drop' case, thus not including short-term variability in PV generation.

	Decrease in annual total energy cost		Decrease in annual electricity purchased	
	without sales	with sales	without sales	with sales
Case a	9.5 - 13 %	23 - 25 %	42 - 58 %	70 %
Case b	4.5 - 8 %	11.5 - 19 %	22 - 37 %	50 - 68 %
Case c	1.2 - 8 %	1.2 - 12 %	8 - 34 %	8 - 40 %
Case d	0.2 - 3.3 %	0.2 - 3.3 %	2 - 19 %	2 - 19 %

TABLE 5.7: Overview of savings and decrease in electricity purchased for the different cases and settings

The impact of allowing for sales differs for each case as can be seen on Table 5.7. The strongest increase in savings is made in case a, an increase of around 15 percentage points is observed. At the same time for case d the savings remained constant. In this case it is not financially attractive to install more PV when sales are allowed. In case c, the lower boundary remained unchanged while the upper boundary of savings increased. It was only interesting to install more PV if batteries were cheaper than 400 $/kWh and the confidence level of sub-hourly drops in irradiance was lower than 80%.

Regarding the decrease in total annual electricity purchased from the utility the strongest decrease was observed for case a and b, this decline in energy purchased is directly related to the increased capacity of PV installed. Only in case b a slight decrease in peak demand is observed, in the other cases the peak demand remained approximately the same.

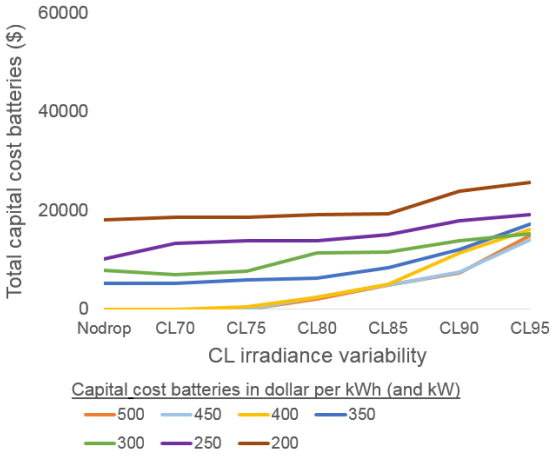

(A) Case b: Upfront capital cost batteries - sales disabled

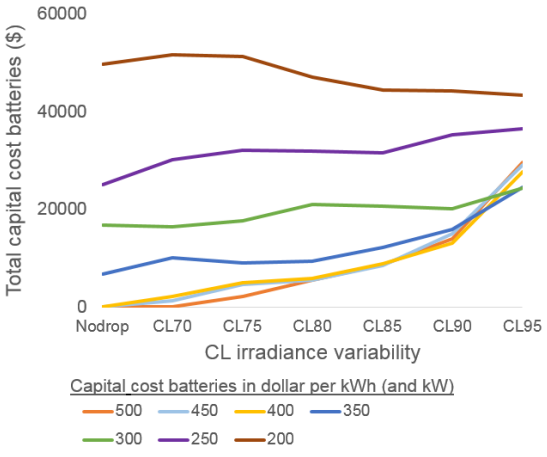

(B) Case b: Upfront capital cost batteries - sales enabled

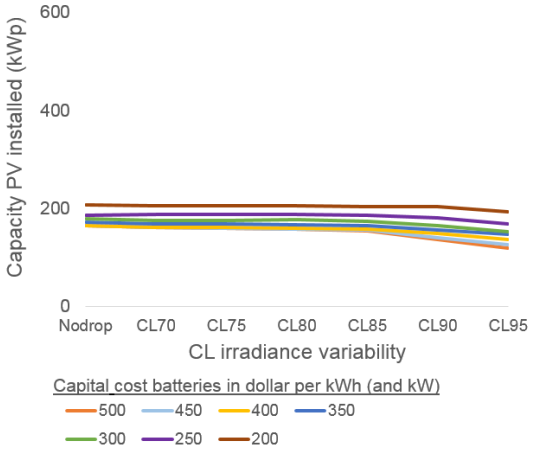

(C) Case b: PV capacity - sales disabled

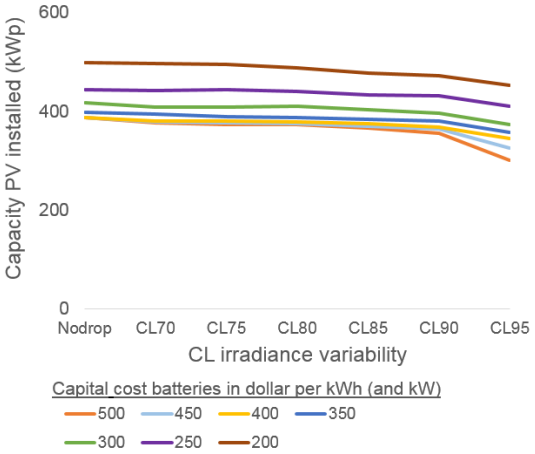

(D) Case b: PV capacity - sales enabled

FIGURE 5.18: Total upfront capital cost of batteries and capacity of PV installed for different confidence levels of short-term variability in solar radiation and battery capital costs for case b

For case a investment in PV becomes very attractive by allowing for sales. In this case the amount of PV installed for all runs is approximately 505 kW. This capacity installed is insensitive to battery price or confidence levels of sub-hourly variability of irradiance and is constrained by the fact that not more can be sold than half of the peak demand in the base case. In terms of the investment and optimal configuration of batteries the same dynamics as when sales were not allowed are observed. The optimal energy over power ratio decreases if more variability in irradiance is introduced. Slightly less

capital is invested in batteries than in the case sales where not allowed, with battery prices higher than 400 $/kWh no investment in batteries is done even for the highest confidence levels of variability in irradiance.

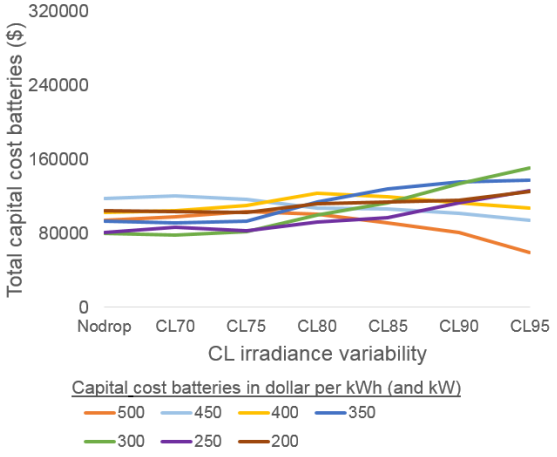

(A) Case c: Upfront capital cost batteries - sales disabled

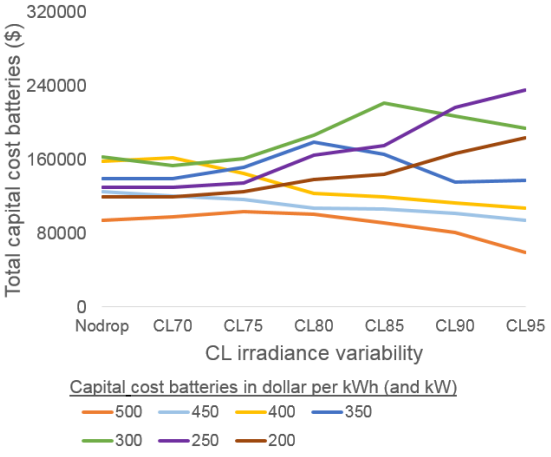

(B) Case c: Upfront capital cost batteries - sales enabled

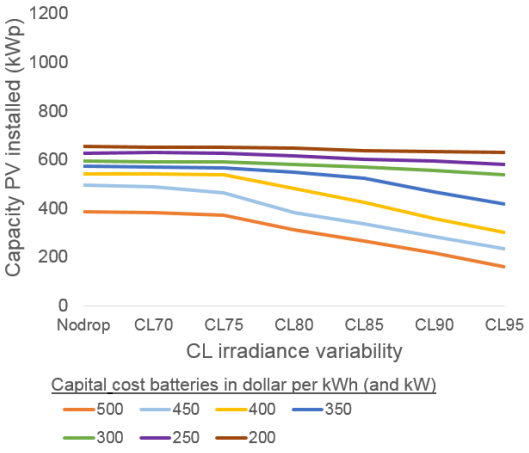

(C) Case c: PV capacity - sales disabled

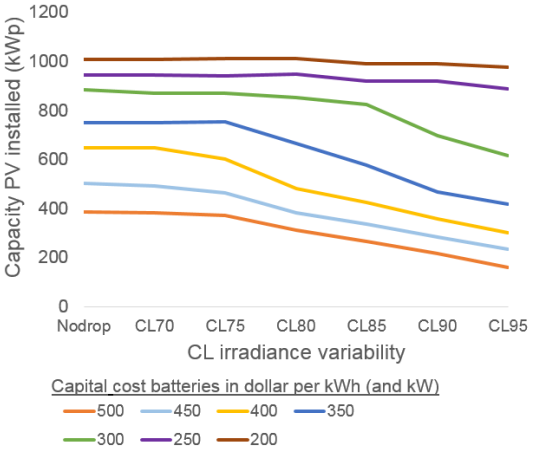

(D) Case c: PV capacity - sales enabled

FIGURE 5.19: Total upfront capital cost of batteries and capacity of PV installed for different confidence levels of short-term variability in solar radiation and battery capital costs for case c

Exactly the opposite happens in case b, investment in batteries become more attractive now sales to the grid are allowed. On Figure 5.18 the capacity of PV installed and the total capital invested in batteries is shown for the runs when sales are disabled and when sales are enabled. Two forces explain the increase in attractiveness of the investment in batteries. Firstly, the compatibility of PV and batteries. And secondly, by investing more in PV and selling more electricity the operational savings increase, this way more capital can be invested in batteries while still complying with the payback constraint.

On Figure 5.22 the same metrics for the runs for which sales are not allowed and allowed are shown, but now for case c. It can be seen that the investment decisions do not change if batteries cost are 450-500 $ per kWh when allowing for sales. At the same time more PV and more batteries are installed when batteries are cheaper by allowing for sales. Again the same forces are at work: if more PV is installed batteries become more attractive and by installing more PV there are more operational savings thus there is also more budgetary space for investing in batteries.

Again in this case the results show the most sensitivity for the variability in irradiance. Investment in PV decreases strongly for the more expensive batteries with increasing variability. And investment in batteries increases significantly for the cheaper batteries and increasing variability. Also the energy over power capacity of the batteries installed declines from values between 2-2.5 in the case no variability is assumed to 1-1.5 for the highest confidence level of sub-hourly variability in PV.

5.2.2 Allowing for investment in PV, batteries and generators

In these runs investments in the generator sets shown on Table 5.4 is possible. Also selling of electricity is allowed in these runs, the same tariff and constraint hold as in the previous section. Table 5.8 shows the results for several metrics for cases c and d. Cases a and b are not included in this table because for those datasets no investment in generators are suggested and thus the results remain the same.

	Decrease in total annual energy cost		Decrease in electricity purchased		Decrease in peak demand	
	with sales	with sales and generators	with sales	with sales and generators	with sales	with sales and generators
Case c	1.2 - 12 %	9 - 12 %	8 - 40 %	44 - 62 %	5 - 10 %	19 - 46 %
Case d	0.2 - 3.3 %	6 - 9.5 %	2 - 19 %	54 - 64 %	3 - 11 %	41 - 54 %

TABLE 5.8: Overview of savings, decrease in electricity purchased and decrease in maximum power demand for the different cases and settings

It should be noted that in the previous two sections the optimization is run with a maximum optimally gap of 0.01%, while in this case an optimality gap of 1% is allowed. A higher optimality gap is allowed in order to keep the computational time reasonable. The disadvantage is that if the area around the optimal solution is very flat, which is

sometimes the case, the investment decisions might not seem very robust. This indicates that the eventual impact of several investment portfolios on the annual total energy cost is very similar. The same principle for the total annual energy cost is still valid: the lower boundary incurs when batteries are the most expensive and the highest confidence level for sub-hourly variability is used and the upper boundary when batteries are the cheapest and there is no sub-hourly variability is assumed. This principle does not hold any more for the other metrics.

As can be seen on Table 5.8 an increase in savings is observed in both cases by allowing for investment in generators, especially the lower bound of savings went up significantly. The most spectacular metrics are the decrease in annual electricity purchased and the decrease in peak demand. It seems that by allowing for investments in generators these buildings become a lot more independent from the utility. These numbers confirm that with an increased adoption of DERs utilities will have to change their business models (Rocky Mountain Institute, 2015). The electricity bill decreased between 50 to 63% for case b and between 60 to 68 % for case d, due to investment in on-site generation.

All generators installed on-site are microturbines with CHP capability. One or more microturbine with a capacity of 65 kW, one microturbine with a capacity of 250 kW or a combination of both types is installed. These generators are not labelled as fast ramping thus cannot be used to compensate for the drops in PV generation. It must be that, although in terms of capital cost and operational cost the internal combustion engines are very similar to the microturbines, the added value of being able to react faster was not enough for the internal combustion engines to be preferred over the microturbines. One of the reasons might be that because the minimum load for all types of on-site generators is already high (in the order of 70-75% of the maximum output), the remaining power to ramp up above the minimum load to dampen the drop is rather small. The capacities installed for the different runs are shown by Figure 5.20 and Figure 5.21.

Two trends are visible on the tables shown by Figure 5.20 and Figure 5.21: the lower the capital cost of the batteries the smaller the capacity of microturbines installed and the higher the confidence level of sub-hourly variability in irradiance the higher the capacity of microturbines installed. This second trend suggests that if the short-term variability

Capital cost of batteries in $ per kWh (or kW)	Confidence level of the sub-hourly variability in irradiance: Nodrop	CL70	CL75	CL80	CL85	CL90	CL95
500	250	250	315	250	250	315	315
450	250	250	250	250	250	315	315
400	250	250	250	250	250	250	250
350	250	250	250	250	250	250	250
300	250	250	250	250	250	250	250
250	130	130	195	250	250	250	250
200	65	130	250	130	130	130	195

FIGURE 5.20: Total capacity of microturbines with CHP installed in case c [kW]

Capital cost of batteries in $ per kWh (or kW)	Confidence level of the sub-hourly variability in irradiance: Nodrop	CL70	CL75	CL80	CL85	CL90	CL95
500	315	380	315	380	315	380	380
450	315	315	315	315	315	315	380
400	315	315	315	315	315	315	380
350	315	315	315	315	315	315	315
300	315	315	315	315	315	315	315
250	250	250	250	250	250	315	315
200	250	250	250	250	250	250	315

FIGURE 5.21: Total capacity of microturbines with CHP installed in case d [kW]

in irradiance is not taken into account in the optimization, the optimal capacity of on-site generators to install might be underestimated. More case studies with different load and solar profiles need to be run in order to verify this claim, but there are clear indications that this might be the case.

On Figure 5.22 the OPEX over CAPEX ratio is shown for case c and b, without and with the investment possibility in generators. It can be seen that the sensitivity of this ratio to sub-hourly variability in irradiance and battery prices in case c and to battery prices in case d is decreased strongly by allowing for the investment in generators. It should be noted that the fuel burned by installed generators is accounted for as OPEX. It might be that in the case investment in generators is allowed the CAPEX increased strongly because of investing in the generators, but at the same time the OPEX does increase slightly or remains constant because of more natural gas being burned.

The capacity of PV installed for the same cases and settings is shown on Figure 5.23. Also on this figure it can be seen that the sensitivity of case c to the sub-hourly variability of irradiance decreases strongly by allowing for generators. At the same time case d was almost completely insensitive to this variability when no investment in generators was allowed, but by allowing investment in them a slight influence is visible. Also remarkable is that by allowing for the investment in generators in general the capacity of PV installed

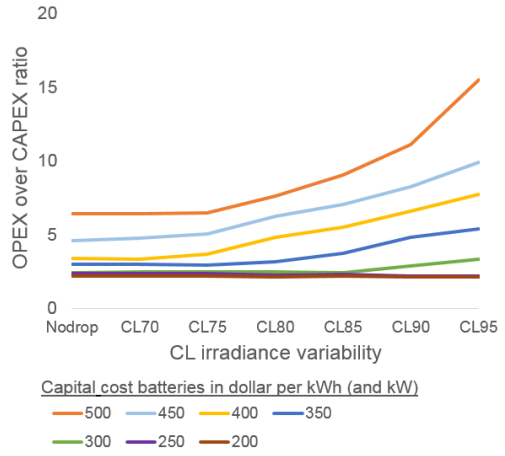

(A) Case c: OPEX over CAPEX ratio - sales enabled

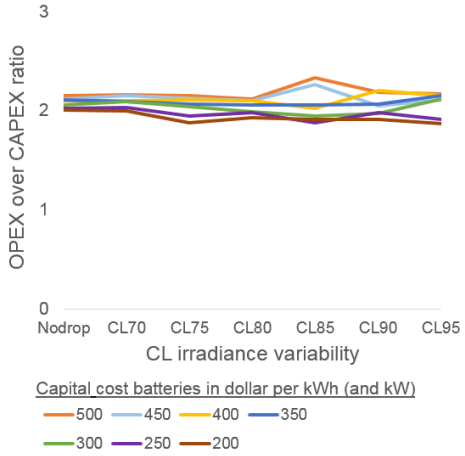

(B) Case c: OPEX over CAPEX ratio - sales and generators enabled

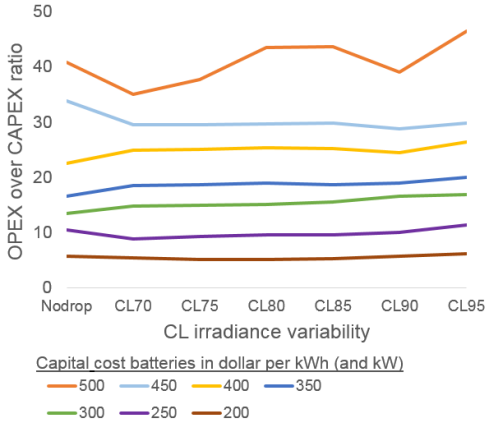

(C) Case d: OPEX over CAPEX ratio - sales enabled

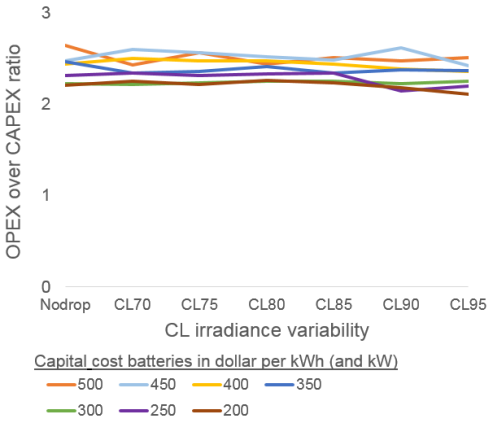

(D) Case d: OPEX over CAPEX ratio - sales and generators enabled

FIGURE 5.22: OPEX over CAPEX ratio for different confidence levels of short-term variability in solar radiation, battery capital costs and settings for cases c and d

increased strongly. For example for case d, with a battery price of 500 $ per kWh the capacity of PV installed increased with about a factor of 8. Again two forces are working here: the compatibility of on-site generators with PV and by installing generators there are more operational savings generated thus there is more budgetary space for investing in PV.

The maximum power output of the batteries installed is shown by Figure 5.24. On this figure it can be seen clearly that case d is sensitive to changes in the confidence level of sub-hourly variability in irradiance when investment in generators is allowed. This sensitivity is linked with the fact that the capacity of PV installed in this case is much higher than the capacity of PV installed if only investments in PV and batteries are considered. For case c the maximum power output of the battery does not differ

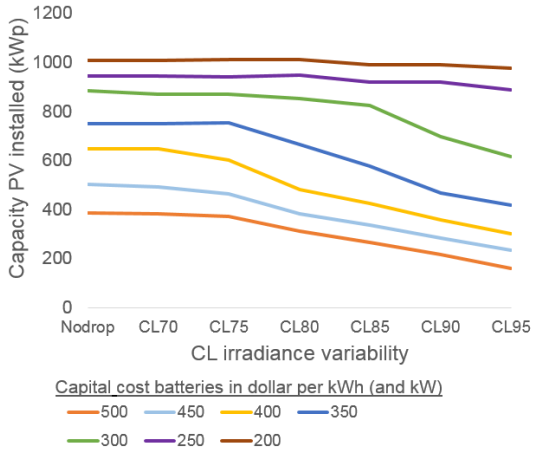

(A) Case c: PV capacity installed - sales enabled

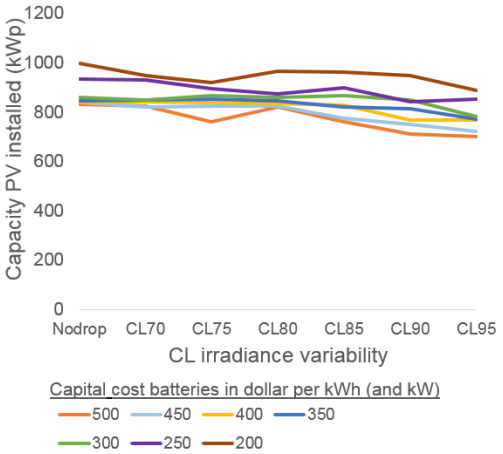

(B) Case c: PV capacity installed - sales and generators enabled

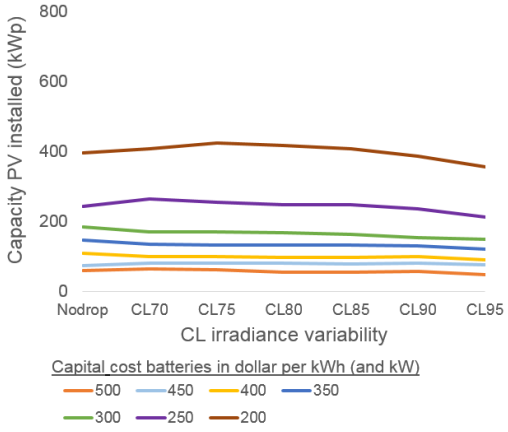

(C) Case d: PV capacity installed - sales enabled

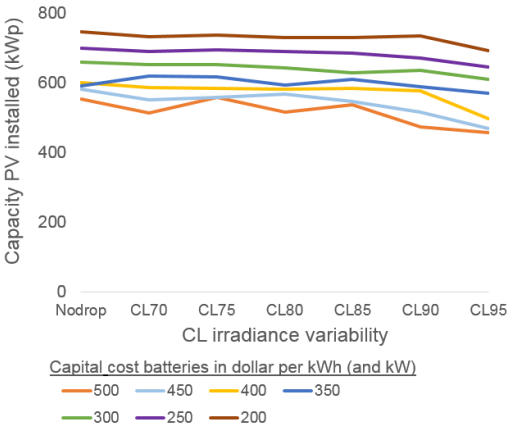

(D) Case d: PV capacity installed - sales and generators enabled

FIGURE 5.23: PV installed for different confidence levels of short-term variability in solar radiation, battery capital costs and settings for cases c and d

significantly with and without generators installed, the maximum power even declines slightly in the case investment in generators is considered.

Figure 5.25 shows the amount of PV generation curtailed per capacity of PV installed for case c. This figure is related to Figure 5.24b. As can be seen on Figure 5.24b the increase in the maximum power of the battery with increasing confidence level of sub-hourly variability is less strong than on Figure 5.24a. Another way to dampen the drop in PV generation next to compensation by a battery or a fast ramping generator is to increase selling or curtailing of PV generation. A trend is visible on Figure 5.25, more curtailment per capacity of PV installed occurs for higher confidence levels of sub-hourly variability of irradiance. It must be said that this trend is not equally clear for all battery price levels.

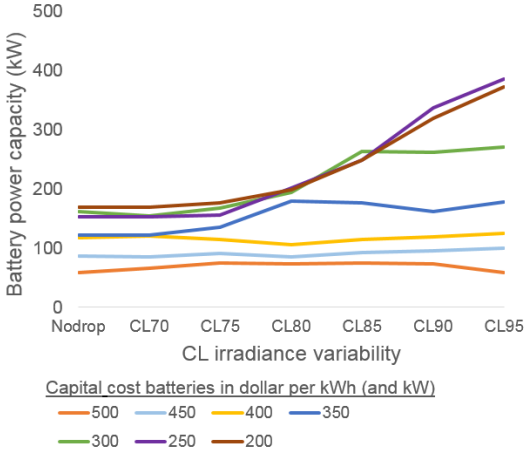

(A) Case c: maximum power output of the battery - sales enabled

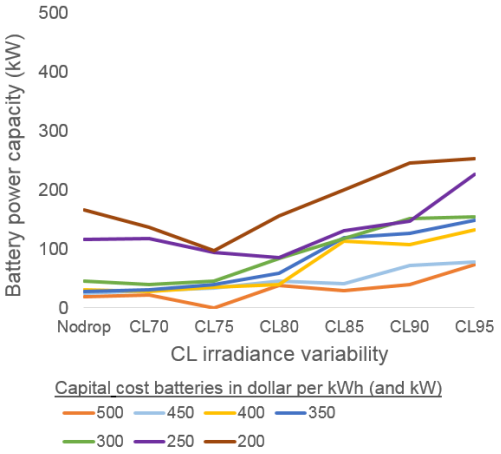

(B) Case b: maximum power output of the battery - sales enabled

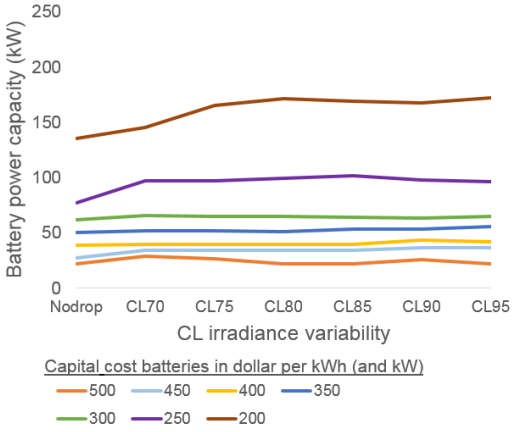

(C) Case b: maximum power output of the battery - sales disabled

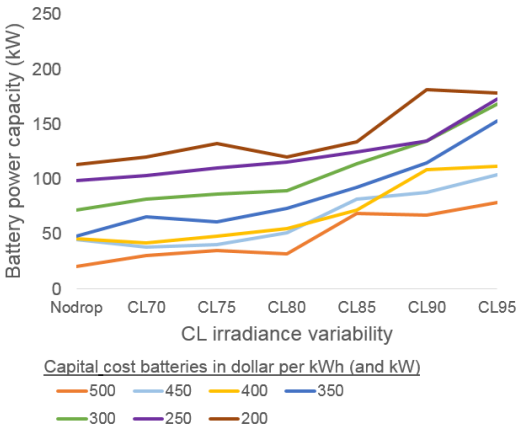

(D) Case b:maximum power output of the battery - sales enabled

FIGURE 5.24: maximum power output of the battery for different confidence levels of short-term variability in solar radiation, battery capital costs and settings for cases c and d

The explanation is that in this case curtailment is used next to a battery as the tool to dampen these drops in PV. Curtailment will especially occur if generators are online. Although electricity generated by PV is 'free' (marginal cost is zero) it is still preferred in some cases to use the generators in order to minimise the total electricity bill, including the demand charges. These on-site generators when online 'shift' the electricity generated by PV 'upwards' closer to the limit where they will be curtailed. This principle is visualised by the dispatch shown by Figure 5.27. There is a trend on Figure 5.25, but these numbers should also be looked at from perspective; the total annually electricity generated by PV sold is in this case around 600 MWh, more than 50 to 100 times the annual amount of PV curtailed.

Clear differences between the dispatch shown by Figure 5.26 and 5.27 can be observed.

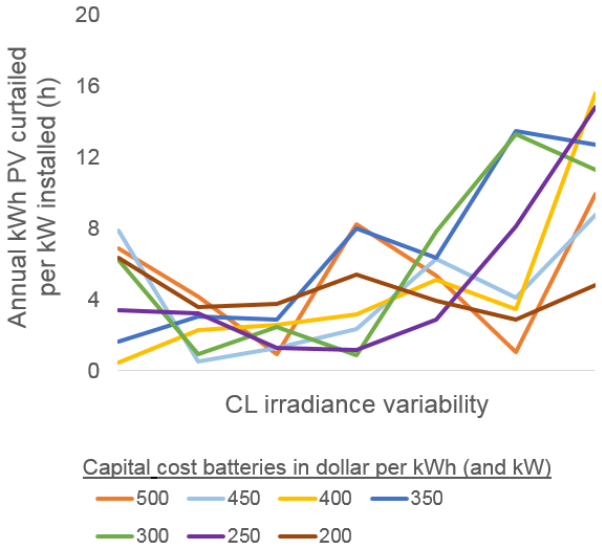

FIGURE 5.25: Curtailment per capacity of PV installed in case c

The only difference in input for both optimizations is the incorporation of sub-hourly variability (90% confidence level) for the dispatch shown on Figure 5.27, while for the dispatch shown on Figure 5.26 no sub-hourly variability was assumed. Two main differences can be noted between the dispatches. Firstly, without taking into account sub-hourly variability the amount of PV energy used for self consumption is higher, this also has to do with the fact more PV is installed. By taking into account sub-hourly variability the generators are used more. Secondly, the state of charge of the battery between 12 am and 8 pm is a lot higher for the case sub-hourly variability is included versus when not. Similar observations are done looking at dispatches of other day-types and months. It is expected that the reason for these two observations is the inclusion of sub-hourly variability. The dispatch shown on Figure 5.27 could be called a more conservative dispatch towards fast changes in PV output. It should be noted that a lot of variables and their interactions determine the dispatch and that it is not always straightforward to draw conclusions.

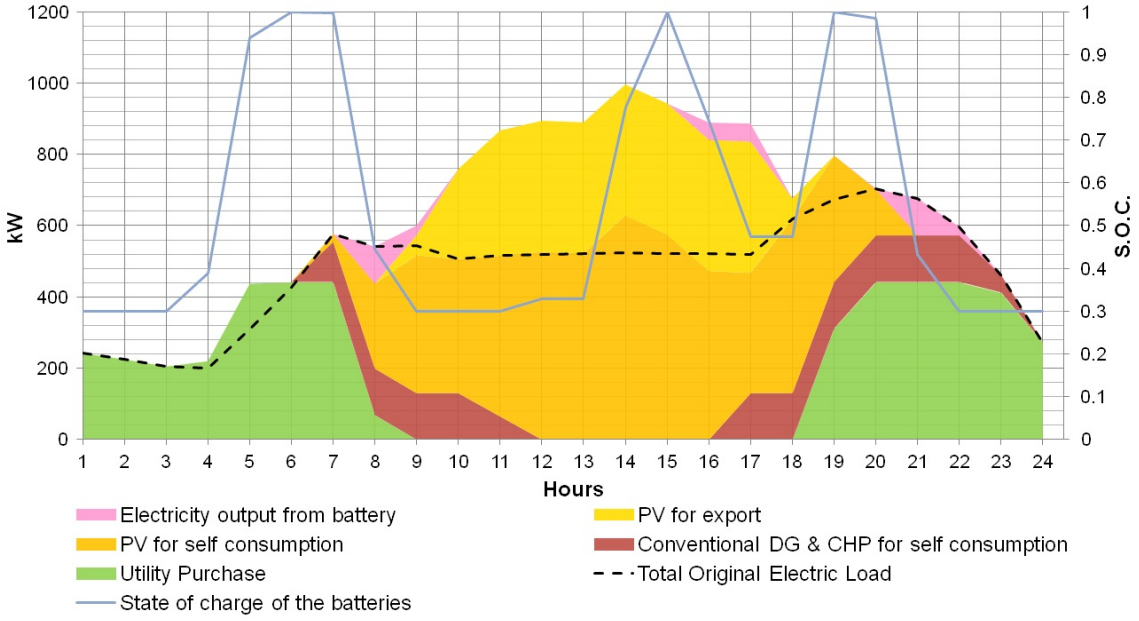

FIGURE 5.26: Dispatch on a weekday in June for case c with battery capital cost of 250 $ per kWh (and kW) and no sub-hourly variability in solar radiation assumed. Battery energy capacity: 210 kWh / Battery maximum power output: 116 kW / PV capacity: 935 kW / Capacity MT with CHP: 2x 65 kW

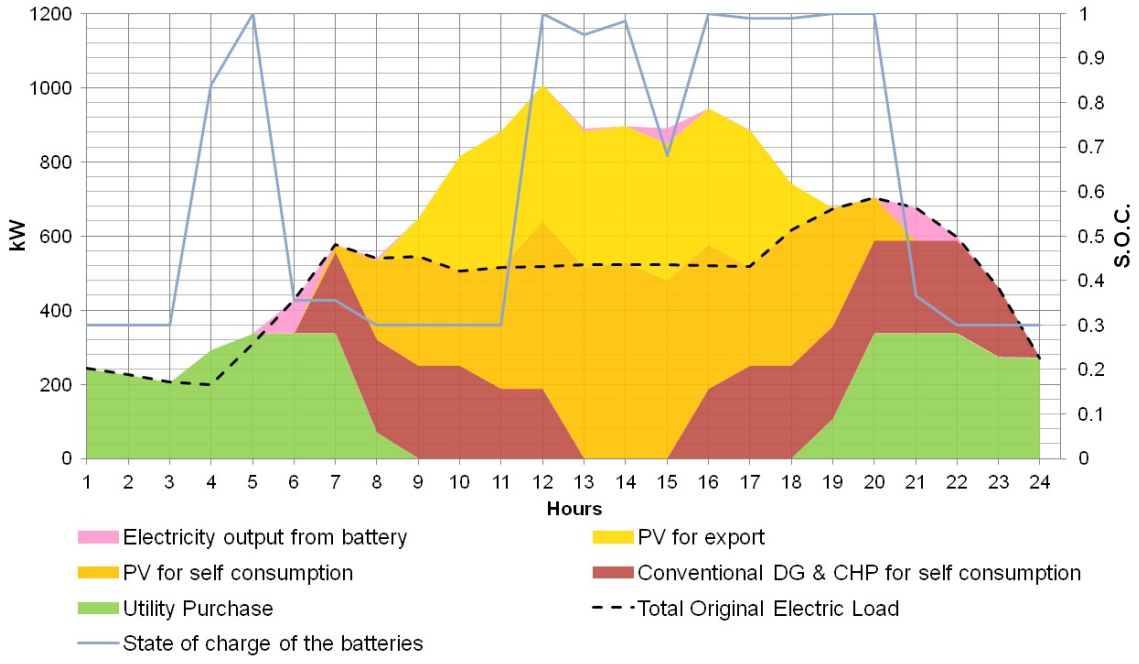

FIGURE 5.27: Dispatch on a weekday in June for case c with battery capital cost of 250 $ per kWh (and kW) and the 90th percentile confidence level for sub-hourly variability of solar radiation set. Battery energy capacity: 156 kWh / Battery maximum power output: 153 kW / PV capacity: 842 kW / Capacity MT with CHP: 1x 250 kW

Chapter 6

Conclusion and future work

Conclusion

In this work a methodology is proposed to incorporate the variability of solar radiation on a sub-hourly scale into the investment and planning version of DER-CAM. Because the considered version of DER-CAM is formulated as a deterministic mixed integer linear program making use of hourly time steps and 3 typical days to represent a month, this can be considered as a non-trivial task.

From the results of the four case studies it can be interfered that the impact of including short-term variability of solar radiation on the optimal microgrid design is very case dependent. The objective function, more precisely the annual total energy cost, does not increase significantly by taking into account sub-hourly variability in PV. Only an increase of a couple of percentage points is observed. At the same time, the underlying investment decisions can -in some cases- be significantly impacted. This agrees with the results observed in the paper of Hittinger et al. (2015), wherein is found that by using a higher resolution of the time steps the LCOE of the system does not increase drastically but the investment decisions (in that case stationary storage) are affected.

A general trend that can be seen is that by taking into account this variability the configuration of the optimal battery to be installed changes, more precisely the energy capacity over maximum power output ratio of the battery pack installed declines. In most cases the maximum power output of the batteries increases, while the energy

capacity installed remains fairly constant. This trend is present in all case studies with only one exception.

In the cases subjected to tariff A-10, in which a less strong emphasis is laid on demand charges and the yearly peak demand is 344 kW before investment, DER-CAM suggest investment in expensive batteries when short-term variability in PV is taken into account when before it was not. The investment in batteries is still relatively small with respect to the total annual energy cost. In these cases a strong additional increase in savings is made by allowing for sales to the grid of excess energy generated by PV. By allowing for selling energy to the grid the annual energy purchased decreases in both cases with more than 50 % relative to the business-as-usual scenario for all settings of the parameters. At the same time the peak demand only decreases with 5 to 15 %.

In the cases subjected to tariff E-19, with a yearly peak demand of 736 kW before investment, the impact of including short-term variability in PV generation seems to be dependent of the solar data and the consideration of investment in generators. From the results it can be concluded that by not taking into account sub-hourly variability of solar radiation the optimal amount of PV to be installed can be strongly overestimated if: demand charges constitute an important part of the electricity bill, the yearly average insolation is high and batteries are expensive. Under the same circumstances the optimal maximum power output of the battery pack will be underestimated if the investment cost of batteries is low.

Another finding was that the optimal amount of PV to be installed is very sensitive to battery prices. For example in a case it was found that if battery prices decrease from 500 $ per kWh to 250 $ per kWh the capacity of PV installed increases by a factor 5. This result demonstrates the compatibility of PV with batteries. Not exactly the same analysis is done, but this result seems to contradict with findings in the paper of Neubauer and Simpson (2015). In that paper is said that the optimal configuration of the battery pack (which is only used for peak shaving in that work) is found to be insensitive to the presence or not of PV at the same site.

When investments in generators are considered there are indications that by not taking into account the sub-hourly variability of solar radiation the optimal total capacity of the generators to be installed might be underestimated, while the capacity of PV to be installed might be slightly overestimated. In all cases where investment in on-site

generators was profitable microturbines with CHP capabilities were preferred. These microturbines were not labelled as fast ramping enough to dampen the drops in PV generation, instead slightly increased curtailment and batteries with a higher maximum power output were used for this purpose. Also important to note was that by allowing for the investment in generators, the capacity of PV installed increased. Two reasons are found for this: the compatibility of on-site generators with PV and that fact that by installing generators more operational savings are generated thus more budgetary space is created for investing in PV without the payback constraint is being violated.

For the cases subjected to tariff E-19 by allowing for investment in PV, batteries, generators and sales, the annual amount of electricity purchased declines with around 50 %. At the same time also the peak demand decreases very strongly, for some settings of the parameters declines of around 40 to 50 % are observed. This implies that in the near future these medium large customers with an original peak demand between 500 and 1000 kW will become more and more grid independent if they opt for a microgrid. Especially during peak-times no electricity is bought any more in most cases, instead electricity flows from these microgrids to the macro-grid. It is important to remark that actually these customers now belong to the A-10 tariff scale and not the E-19 tariff scale any more because the peak demand declined that strongly. For simplicity this analysis does not include this switch to another tariff scale which complicates the optimization.

A policy implication distilled from this work can be that if demand charges would constitute a larger portion of the electricity bill in the future, growth in PV capacity installed in microgrids might be stifled while investing in generators becomes more attractive. This statement holds as long as battery technology has not matured enough.

Also simulations were done to look at what happens with the total annual energy cost when the design of a microgrid is optimized without taking into account these short-term fluctuations in solar radiation. This was done by fixing the investment suggested in the 'NoDrop' case and then running the optimization including short-term variability. It is observed that the objective function remained approximately the same but that the payback constraint was violated. Now instead of the investments being paid back by operational savings in less or equal than 10 year, more than 10 to maximum 12 years would be needed. The reason for this is that the operational savings are lower than expected due to increased demand charges.

Future work

The remarks made at the last section of chapter 4 sum up some potential lines of future work. It is expected that battery technology will gain more importance in the coming years, because of this reason modelling variable efficiency and capacity fade of batteries due to its operation is soon to be expected in DER-CAM. It will be interesting to look at how these two features would affect the investment in batteries, especially taking into account the interaction with demand charges and the variability of PV.

In the paper of Hittinger et al. (2015) is investigated which type of battery performs better under which circumstances, also here the link could be made with the topic of this work. Maybe a particular type of battery is better suited to discharge deep and infrequently in order to dampen the drop in PV generation due to fast moving clouds. Another type of battery could be used as a tool for arbitrage.

Another interesting research line would be to investigate the correlation between demand and solar radiation. Both demand and solar radiation are sources of uncertainty in optimal microgrid design. It would be interesting to see if both enforce or partially cancel each other out. Directly related with this discussion is how demand response could be used as a tool to 'flatten' the load curve taking into account uncertainty in PV output on a short time scale.

In this work no test is conducted to look at what the implications are of demand charges calculated by the highest demand averaged over 5 minutes instead of over 15 minutes. Already in some tariffs this is the case and it is intuitive to expect the impact of not including this short-term variability to be even stronger.

The ultimate test of the proposed formulation would be to build a validation model with shorter time steps and more days to represent a month. In that model energy and power generated by PV would not need to be decoupled any more, it could be investigated how accurate the assumptions made in this work are. More computational power than available today is needed in order to build such a precise model. Implementing the same generic approach in the stochastic 7-day version would be a first attempt, although also in that model time steps are still hourly.

Appendix A

Detailed literature review of statistical analysis of solar radiation

The backbone of this appendix is the chapter 'Modelling the statistical properties of solar radiation and proposal of a technique based on Boltzmann statistics' by Tovar-Pescador (2008) of the book 'Modeling Solar Radiation at the Earth's Surface'. To analyse solar radiation time series are used, of which the considered interval between the data points are dependent of the time scale of interest. Most methods of time series analysis assume stationarity of the data, implying that the mean and autocorrelation function of the data series do not change in time. However, many atmospheric processes, such as solar radiation, are distinctly not stationary. When studying solar radiation, we expect stationarity conditions to be met only in its annual or diurnal cycles. A way is to deal with this stochasticity is to stratify the data. That is, to conduct separate analyses for different subset of the data that are short enough to be regarded as nearly stationary, for instance monthly subsets of daily solar radiation values (Tovar-Pescador, 2008).

The seasonal and diurnal variations of solar radiation are described by well established astronomical relationships and thus can be be accurately predicted at any time (Iqbal, 1983; Ettoumi et al., 2002; Woyte et al., 2007). At the short-term, the behaviour of solar radiation is mainly ruled by the stochastic parameters: frequency and height of the

clouds and their optical properties, atmospheric aerosols, ground albedo, water vapour and atmospheric turbidity (Woyte et al., 2007; Tovar-Pescador, 2008; Mills and Wiser, 2010). Variability in solar radiation can be split up in two components: a deterministic and a stochastic component. This deterministic component is already taken into account in DER-CAM, the stochastic component is the subject of this work.

The most important metric used in the following subsections is the global instantaneous clearness index $k_t(t)$. The deterministic and stochastic factor in the solar radiation G can easily be isolated by definition of this metric originally formulated by Iqbal (1983):

$$k_t(t) = \frac{G}{I_0 E_0(t) cos(\theta_i(t))} = \frac{G}{G_0} \tag{A.1}$$

$$\text{and } k_t(t) = k_d(t) + k_b(t) \tag{A.2}$$

The index t stands for total or global, d for diffuse and b for beam or direct irradiance; the variable t stands for time; I_0 is equal to 1367 W/m2, the solar constant; E_0, the eccentricity correction factor (Iqbal, 1983; Wong and Chow, 2001) and θ_i, the angle of incidence on an arbitrarily oriented surface (equal to the zenith angle for a horizontal panel). In other words this index gives the ratio of the actual energy on the ground to that initially available at the top of the atmosphere and therefore accounts for the transparency of the atmosphere. This index can be averaged out on a minutes, hourly, daily or monthly basis.

It is important not to confuse the clearness index with the global clear sky index, which is sometimes used as well as in the paper of Mills and Wiser (2010). Both indexes, the clearness and clear sky index are used for the same purpose but the way actual global radiation is normalised is different (Brownson, 2014). The global clear sky index is defined as the ratio of the actual global insolation measured at the site to the global insolation expected if the sky were clear, and thus will always higher than the clearness index because the denominator is smaller. Figure A.1 shows the global clear sky index for intervals averaging 1 minute and 60 minutes. Even looking at the 60-min averaged intervals, the deviations can be very significant during the day. The global clear sky index can be higher than one because of additional diffuse irradation because of reflection by clouds.

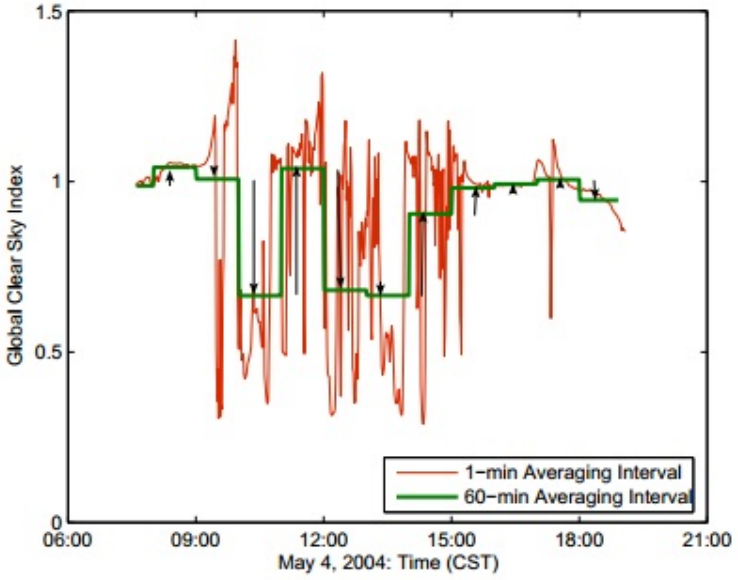

FIGURE A.1: Example of 1-min global clear sky index, 60-min average of the clear sky index, and arrows representing magnitude and direction of 60-min deltas (Mills and Wiser, 2010)

A.1 Daily data

Among all the solar radiation measurement, the daily global values have been studied the most frequently (Tovar-Pescador, 2008). Papers by Liu and Jordan (1960), Bendt et al. (1981), Hollands and Huget (1983) and Olseth and Skartveit (1984) discuss this matter and try to fit probability distributions for the global daily clearness index $\bar{k_t}^D$ conditioned for a monthly mean clearness value $\bar{k_t}^M$. In all these studies there are two big questions that arise. The first one being the question if the probability density functions are unimodal or bimodal, an example of unimodel probility density functions (PDFs) are given on Figure A.2. Ibanez et al. (2003) studies this question by analysing data of 50 locations in the USA. This study concluded that 60% of the distributions showed a bimodal behaviour. The modality of the distribution seems to be locational specific. This bimodality has a physical explanation, the lower maximum accounts for cloud covered days, while the higher maximum accounts for days with a clear sky within a month.

The second question that arises is if the distributions used to fit the models are universal. Tiba et al. (2007) concluded that the cumulative distribution functions (CDFs) do not

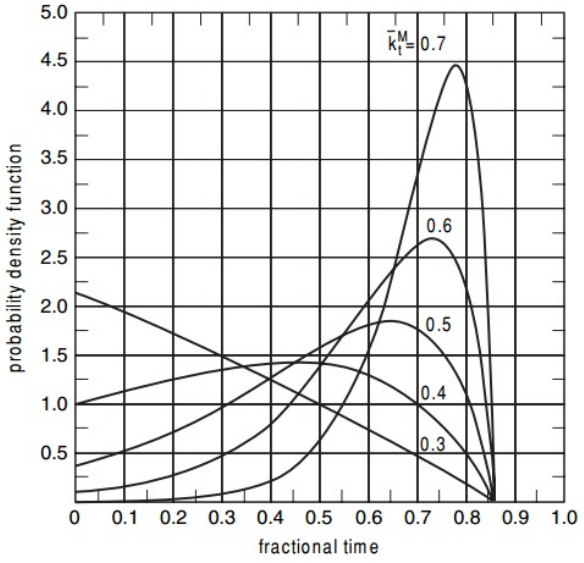

FIGURE A.2: The density distribution functions proposed by Hollands and Huget (1983). All the curves are unimodal (Tovar-Pescador, 2008).

have a universal character, as previously was stated by other authors, after analysing the CDFs for 23 sites located in the Southern hemisphere.

A.2 Hourly data

There is less literature available commenting on distributions of hourly solar radiation. An interesting study has been done by Dizqah et al. (2012). In their paper they model hourly solar radiation as Beta distributions, as has been done by Karaki et al. (1999); Ettoumi et al. (2002). On this time scale depending on the hour and the location the frequency distributions can be bimodal. Ettoumi et al. (2002) propose to use a linear combination of two Beta distributions to model bimodality.

Also artificial intelligence techniques can be used to forecast hourly solar radiation, methods using several of these has techniques has been tested in the paper of Sfetsos and Coonick (2000). The results indicate that at that time the developed artificial intelligence models predict the solar radiation time series more effectively compared to the conventional procedures based on the clearness index.

A.3 Sub-hourly data

The distributions that can be considered as instantaneous (less than 10-minutes) show a different shape, since the transient effects caused by clouds are now evident and contribute to the increase of the bimodality (Tovar-Pescador, 2008). Vijayakumar et al. (2005) analysed the instantaneous distributions, with the aim of exploring the differences between hourly and instantaneous distributions. They concluded that the variations in solar radiation within an hour cannot be considered negligible when conducting performance analyses of solar energy systems. And depending on the critical level, location and month, an analysis using hourly data rather than short-term data can underestimate the performance between 5% and 50%.

An important parameter to be introduced here is the optical airmass m_a, the optical airmass is defined as:

$$m_a = \frac{1}{cos(\theta_z)} \tag{A.3}$$

θ_z in this formula is the solar radiation incident relative to the normal to the Earth's surface (or zenith angle) and thus location and time dependent. The optical airmass actually is a measure for the distance between the sun and the Earth's surface and has an influence on the distributions of the clearness index on sub-hourly intervals. Because the altitude of the location also can play an important role it is sometimes incorporated, the metric incorporating the altitude is called the relative optical airmass and defined as follows (Assuncao et al., 2003):

$$m_{a_{rel}} = \frac{1}{cos(\theta_z)} * e^{-0.0001184\Delta z} \tag{A.4}$$

Δz stands for the station altitude in meters above sea level. In the literature it is very common that the instantaneous clearness index is conditioned for the (relative) optical airmass. There are also papers conditioning the instantaneous clearness index for the hourly clearness index k_T and in other ones conditioning is done for both combined. Table A.1 and A.2 give an overview of the different datasets and methods used in papers discussing distributions of sub-hourly solar irradation data.

	Interval		Conditioned on			Type of radiation		
	1 min	5 min	m_a	k_T	Both	k_d	k_d	k_t
Skartveit and Olseth (1992)		X		X			X	X
Gansler et al. (1995)	X			X	X			X
Tovar-Pescador et al. (2001)	X			X				X
Assuncao et al. (2003)		X	X			X	X	X
Vijayakumar et al. (2005)	X	X			X	X	X	X
Woyte et al. (2007)	X				X			X
Tovar-Pescador (2008)	X		X	X		X	X	X
Zhang (2014)	X							X
Fernández-Peruchena and Bernardos (2015)	X		X	X	X			X

TABLE A.1: Summary of the data of papers analysing sub-hourly solar radiation

Most of the studies make use of solar radiation averaged over a one-min interval and fewer use longer time intervals. Skartveit and Olseth (1992) argue that if a finer time resolution than 1 h is required there is an obvious gain in going down to a five-min averaging time, but no significant additional gain in going further down. They stress the important fact that even during hours with high variability the distribution of instantaneous values differs only slightly from that of five-min averages.

It can be seen that so far, the analyses of the solar radiation variability followed very different approaches. Nevertheless, one shared pitfall for most of them is that they were carried out using local data bases (Tovar-Pescador, 2008). This implies that the proposed models are site dependent and when a new analysis needs to be done a lot of data is required to validate the selected approach.

An important remark was made by Vijayakumar et al. (2005), namely that his research supports the conclusion of Gansler et al. (1995) that frequency distribution correlations for short-term radiation data should be developed as functions of air mass and hourly clearness index. Using this methodology would allow locations, where short-term data is unavailable as is mostly the case, to use available hourly averages to predict the distribution of short-term clearness indices. The first part of this statement, namely that short-term radiation data should be developed as functions of air mass and hourly clearness index is agreed upon by the most recent paper listed up in Table A.1, but the second part of the statement is proven to be not the case by Fernández-Peruchena and Bernardos (2015). Considering this issue it is interesting to discuss in more depth the results obtained by Fernández-Peruchena and Bernardos (2015).

	Distributions/method used
Skartveit and Olseth (1992)	Global radiation is modelled by a Weibull distribution and beam radiation by a Beta distribution. Also a first order autoregressive model is presented.
Gansler et al. (1995)	A Weibull distribution is used to model global irradiance.
Tovar-Pescador et al. (2001)	Boltzmann statistics are used to model one-minute global irradiance data on the hourly average radiation, the distributions are unimodal.
Assuncao et al. (2003)	Linear combinations of Beta distributions are used. A combination of two Beta distributions is used to model global irradiance, three Beta distributions were combined to model direct irradiance and one was used to model diffuse irradiance. Conditioning is done for the relative optical air mass.
Vijayakumar et al. (2005)	Different older approaches are compared, the paper is more focused on the utilizability concept to evaluate the long-term performance of solar energy systems.
Woyte et al. (2007)	Localised spectral analysis based on wavelet basis is applied on measurements with an interval of 1 min and shorter.
Tovar-Pescador (2008)	Linear combinations of Boltzmann (and Delta) functions are used to model global, beam and diffuse radiation conditioned on air mass or the hourly average clearness index.
Zhang (2014)	A whole different approach is used in this paper, a simulation model employing the Gaussian kernel density estimator is proposed to reconstruct short-term solar radiation. Different models are fit conditioned for the season, cloudiness and the hour of the day.
Fernández-Peruchena and Bernardos (2015)	Boltzmann statistics are used to model global irradiance conditioned for air mass, the hourly average clearness index and the combination of both.

TABLE A.2: Summary of methods used in papers analysing sub-hourly solar radiation

In their paper Fernández-Peruchena and Bernardos (2015) use data of nine sites located in five different climate zones, listed up by Table A.3, to compare the distributions of one-minute k_t conditioned on different parameters. Their results and methods are summarized in Table A.4. They conclude that all distributions, except very few, are location dependent. This statement holds independently of the parameter(s) the distributions are conditioned on. It can be said that the local conditions (atmospheric transparency and proportion, type and variability of clear sky and cloudy conditions) noticeably affect the one-minute k_t distributions, even within the same climate zone.

Figure A.3 shows the PDFs obtained for different location by using a Boltzmann function

Location(ID)	Country	Elevation(m)	Years	Climate
Ilorin (ILO)	Nigeria	350	1999–2001	Tropical savannah
Alice Springs (ASP)	Australia	547	2006–2008	Hot desert
Tamanrasset (TAM)	Algeria	1385	2007–2009	Hot desert
Boulder (BOU)	United States	1577	2006–2008	Cold semi-arid
Camborne (CAM)	England	88	2003–2005	Oceanic
Carpentras (CAR)	France	100	2007–2009	Mediterranean
Florianopolis (FLO)	Brazil	11	2003–2005	Humid subtropical
Toravere (TOR)	Estonia	70	2007–2009	Humid continental
Georg von Neumayer (GVN)	Antarctica	42	2006–2008	Polar

TABLE A.3: Radiometric stations selected for the study of Fernández-Peruchena and Bernardos (2015)

Conditioned for	Modality	Distribution used	Similarity of distributions
m_a	Mostly bimodal	Linear combination of two Boltzmann functions	No coincidence
k_t^H	Unimodal	One Boltzmann function	No coincidence
Both	Unimodal	One Boltzmann function	5% of the cases

TABLE A.4: Summary of result obtained by Fernández-Peruchena and Bernardos (2015) studying 1-min k_t measurements

conditioned for a certain value for k_t^H and m_a . It can be seen that the PDFs are fairly different, even within a climate zone. It is not a surprise that the distribution found for the polar climate (GVN) is very different from the other distributions.

Figure A.4(a) shows two distributions of one-minute k_t conditioned for the same value of the optical air mass m_a, but conditioned for different values of the average hourly solar radiation k_t^H. It can be seen that the shape of two distributions is very different in terms of width, height and degree of asymmetry. Also can be seen that the Boltzmann functions allow a good approximation of the histograms shown on the same graph. The other three graphs on Figure A.4 show the fit parameters for the Boltzmann distribution for several locations. Trends are visible for the different parameters but it is clear that they cannot considered to be the same for all locations.

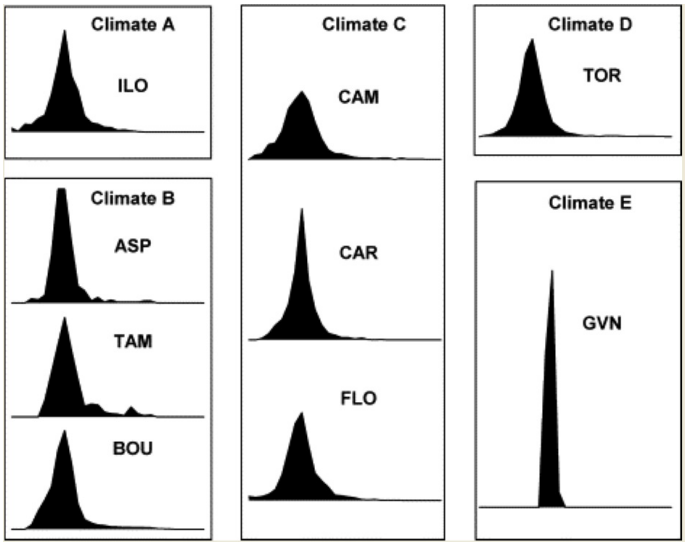

FIGURE A.3: Distributions of one-minute k_t conditioned of to m_a equal to 2.0 and k_t^H equal to 0.30 (normalised to 1), different distributions are observed depending on the location (Fernández-Peruchena and Bernardos, 2015)

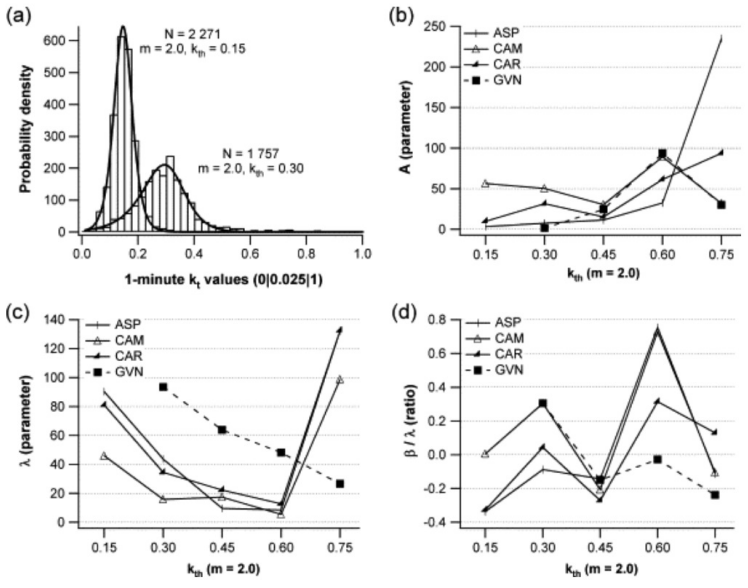

FIGURE A.4: PDFs for one-minute k_t conditioned to different k_t^H and m_a (a). Comparison of the fit parameters at the four sites (b–d) (Fernández-Peruchena and Bernardos, 2015).

Appendix B

Modelling of the efficiency of PV generation

This appendix gives a more detailed explanation how the efficiency of the PV module is calculated at every time step. The efficiency is time dependent and is modelled as a function of the (global) solar irradiance ($Solar_{m,h}$), the ambient temperature ($AT_{m,h}$) and the wind speed (WS) at that particular time step and the technical characteristics of the panel. The PV efficiency model in DER-CAM is based on 'Comparison of Predicted to Measured Photovoltaic Module Performance' by Fanney et al. (2009). It was adapted by Nico Hotz, postdoc at the Mechanical Engineering department at UC Berkeley, hotz@berkeley.edu. Please note some parameters from the original model are not used in this simplified model. The description of this modelling approach can also been found in the handbook of DER-CAM version 3.9.4.m (Le Gall and Stadler, 2013).

The PV panel used is Sanyo H168 PSEL2115 PV with cell characteristics from http://photovoltaics.sandia.gov/docs/Database.htm:

- Area = 1.19m^2, (35.2" x 51.9"). Weight = 23 kg (51 lb).
- Bifacial module with 96 large-area (100 cm^2) HIT (heterojunction with intrinsic thin layer)
- High-efficiency crystalline silicon cells connected in series.
- Aluminum frame, tempered glass front sheet, glass backsheet, module laminated with EVA encapsulant. Pre-production.

The parameters from PV settings are listed below.

$E0$	1000	$T0$	25
A	1.19	$a1$	0.062356
$a2$	-0.010119	$a3$	0.00067031
$a4$	-0.000016221	$Isc0$	4.104
αIsc	0.000458	aPV	-3.27
b	-0.107	$Imp0$	3.819
αImp	0.000082	$c1$	0.0019
$c2$	-0.30396	$c3$	-9.22773
$Voc0$	67.1	n	1.165
Ns	96	βVoc	-0.1915
$Vmp0$	53.98	βVmp	-0.1682
AMa	1.5	$kBYq$	0.0000861738

In DER-CAM the distinction between the diffuse and the beam radiation is not made because in most cases only the global irradiance on a tilt surface, which is inserted by parameter $Solar_{m,h}$, is known.

$$f1AMa = a0 + a1 * (AMa) + a2 * (AMa)^2 + a3 * (AMa)^3 + a4 * (AMa)^4 \tag{B.1}$$

$$\begin{aligned} Tc_{m,h} &= Solar_{m,h} * E0 * exp(aPV + b * WS) \\ &+ AT_{m,h} \ \forall\, m, h \end{aligned} \tag{B.2}$$

$$\begin{aligned} Isc_{m,h} &= Isc0 * f1AMa * Solar_{m,h} * (1 + \alpha Isc * (Tc_{m,h} - T0)) \\ &\forall\, m, h \end{aligned} \tag{B.3}$$

$$Ee1_{m,h} = \frac{Isc_{m,h}}{Isc0} * (1 + \alpha Isc * (Tc_{m,h} - T0)) \ \forall\, m, h \tag{B.4}$$

$$Ee_{m,h} = \frac{(Ee1_{m,h} + abs(Ee1_{m,h}))}{2} + 10^{-12} \ \forall\, m, h \tag{B.5}$$

$$Imp_{m,h} = Imp0 * c0 * Ee_{m,h} + c1 * Ee_{m,h}^2 * (1 + \alpha Imp * (Tc_{m,h} - T0)) \ \forall\, m, h \tag{B.6}$$

$$\delta_{m,h} = n * kBYq * (Tc_{m,h} + 273.15) \ \forall\, m, h \tag{B.7}$$

$$Voc_{m,h} = Voc0 + Ns * \delta_{m,h} * log(Ee_{m,h}) + \beta Voc * (Tc_{m,h} - T0) \ \forall\, m, h \tag{B.8}$$

$$\begin{aligned} Vmp_{m,h} &= Vmp0 + c2 * Ns * \delta_{m,h} * log(Ee_{m,h}) + c3 * Ns * (\delta_{m,h} * log(Ee_{m,h}) * (-1))^2 \\ &+ \beta Vmp * (Tc_{m,h} - T0) \ \forall\, m, h \end{aligned} \tag{B.9}$$

$$Wmp_{m,h} = Imp_{m,h} * Vmp_{m,h} \quad \forall\, m, h \tag{B.10}$$

$$ScEff_{PV,m,h} = \frac{Wmp_{m,h}}{A * (Solar_{m,h} * E0 + \epsilon)} \quad \forall\, m, h \tag{B.11}$$

$$ScEff_{PV,m,h} = \frac{(ScEff_{PV,m,h} + abs(ScEff_{PV,m,h}))}{2} \quad \forall\, m, h \tag{B.12}$$

Equations B.11 and B.12 are the most relevant for this thesis. In Equation B.11 the efficiency of the PV module is calculated as the ratio of the estimated power output of the module and sum of the solar radiation and a correction factor multiplied by a another correction factor. Equation B.12 ensures that the estimated efficiency will always be positive. The obtained value for $ScEff_{PV,m,h}$ is used in Equation 3.8 to calculate the energy generated by the PV installation.

Appendix C

Tariffs

Two tariff structures are used in this work, the tariff A-10 and E-19 both offered by PG&E (2015). Additional to volumetric charges and demand charges there is also a fixed charge. This fixed charge is sometimes called the meter or connection charge.

Schedule A-10 is a demand metered rate schedule for general service customers. If a customer is new and PG&E believes that the customer's maximum demand will be between 200 through 499 kilowatts and that the customer should not be served under an agricultural or residential rate schedule, PG&E will serve the customer's account under the provisions of time-of-use rate schedule A-10. If the customer's demand exceeds 499 kW for three consecutive months, the customer's account will be transferred to schedule E-19 or E-20. Table C.1 displays the tariff.

The E-19 schedule is a medium general demand-metered TOU tariff. A customer will be served under this tariff is a customer's maximum demand is 500 through 999 kW and that the customer should not be served under a time-of-use agricultural schedule. The tariff is displayed by Table C.2.

Season	Demand charge $ per kW			TOU	Volumetric charge $ per kWh		
	2nd	1st	Transm.		2nd	1st	Transm.
Summer	16.23	15.22	10.85	Peak	0.17891	0.16420	0.13481
				Part Peak	0.17087	0.15846	0.12958
				Off Peak	0.14642	0.13650	0.10973
Winter	8.0	8.2	6.29	Part Peak	0.12750	0.11949	0.10392
				Off Peak	0.10654	0.10231	0.08816

Summer Period A (May-October)		
Peak	12 am to 6 pm	Weekdays
Partial-Peak	8:30 am to 12 am	Weekdays
	6 pm to 9:30 pm	Weekdays
Off-Peak	9:30 pm to 8:30 am	Weekdays
	All day	Weekend and holidays
Winter Period B (November-April)		
Partial-Peak	8:30 am to 9:30 pm	Weekdays
Off-Peak	9:30 pm to 8:30 am	Weekdays
	All day	Weekend and holidays

Fixed cost: $4.59959 per meter per day

TABLE C.1: Tariff A-10 TOU offered by PG&E (2015)

Season	TOU	Demand charge $ per kW			TOU	Volumetric charge $ per kWh		
		2nd	1st	Transm.		2nd	1st	Transm.
Summer	Peak	19.04	18.91	17.03	Peak	0.16233	0.14861	0.09129
	Part Peak	4.42	4.06	3.78	Part Peak	0.10893	0.10219	0.08665
	Maximum	15.07	12.08	7.87	Off Peak	0.07397	0.07456	0.07043
Winter	Part Peak	0.24	0.46	0.0	Part Peak	0.10185	0.09696	0.08500
	Maximum	15.07	12.08	7.87	Off Peak	0.07797	0.07787	0.07214

Summer Period A (May-October)		
Peak	12 am to 6 pm	Weekdays
Partial-Peak	8:30 am to 12 am	Weekdays
	6 pm to 9:30 pm	Weekdays
Off-Peak	9:30 pm to 8:30 am	Weekdays
	All day	Weekend and holidays
Winter Period B (November-April)		
Partial-Peak	8:30 am to 9:30 pm	Weekdays
Off-Peak	9:30 pm to 8:30 am	Weekdays
	All day	Weekend and holidays

Fixed cost: $19.71 per meter per day for connection to secondary

TABLE C.2: Tariff E-19 offered by PG&E (2015)

Bibliography

Al-Hasan, A., Ghoneim, A., and Abdullah, A. (2004). Optimizing electrical load pattern in Kuwait using grid connected photovoltaic systems. *Energy conversion and management*, 45(4):483–494.

AssignmentPoint (2015). Assignment on solar radiation. Available at http://www.assignmentpoint.com/other/assignment-on-solar-radiation.html, Retrieved 05/03/'15.

Assuncao, H., Escobedo, J., and Oliveira, A. (2003). Modelling frequency distributions of 5 minute-averaged solar radiation indexes using beta probability functions. *Theoretical and Applied Climatology*, 75(3-4):213–224.

Awerbuch, J. (2015). Homer support discussing the battery dispatch method. Information available at http://support.homerenergy.com/index.php?/Knowledgebase/Article/View/523/0/10517---why-wont-my-batteries-discharge-charge-andor-operate-how-i-want.

Bendt, P., Collares-Pereira, M., and Rabl, A. (1981). The frequency distribution of daily insolation values. *Solar Energy*, 27(1):1–5.

Bourges, B. (1987). A simple conversion factor for the computation of monthly solar global irradiation on tilted planes. *International journal of solar energy*, 5(3):171–184.

Bourges, B. (1991). *European simplified methods for active solar system design*. Kluwer Academic Publisher, Dordrecht.

Brownson, J. (2014). Decoupling beam and diffuse: Clearness and clear sky indices. Available at https://www.e-education.psu.edu/eme810/node/471, Slides of the e-course: Solar Resource Assessment and Economics.

Cardoso, G., Stadler, M., Bozchalui, M. C., Sharma, R., Marnay, C., Barbosa-Póvoa, A., and Ferrão, P. (2014). Optimal investment and scheduling of distributed energy resources with uncertainty in electric vehicle driving schedules. *Energy*, 64:17–30.

Chen, C., Duan, S., Cai, T., Liu, B., and Hu, G. (2011). Optimal allocation and economic analysis of energy storage system in microgrids. *Power Electronics, IEEE Transactions on*, 26(10):2762–2773.

Chen, S., Gooi, H. B., and Wang, M. (2012). Sizing of energy storage for microgrids. *Smart Grid, IEEE Transactions on*, 3(1):142–151.

Dahmani, K., Dizene, R., Notton, G., Paoli, C., Voyant, C., and Nivet, M. L. (2014). Estimation of 5-min time-step data of tilted solar global irradiation using ann (artificial neural network) model. *Energy*, 70:374–381.

Dizqah, A. M., Maheri, A., and Busawon, K. (2012). An assessment of solar irradiance stochastic model for the uk. In *Environment Friendly Energies and Applications (EFEA), 2012 2nd International Symposium on*, pages 670–675. IEEE.

Dufo-Lopez, R. and Bernal-Agustín, J. L. (2005). Design and control strategies of pv-diesel systems using genetic algorithms. *Solar energy*, 79(1):33–46.

Ettoumi, F. Y., Mefti, A., Adane, A., and Bouroubi, M. (2002). Statistical analysis of solar measurements in algeria using beta distributions. *Renewable Energy*, 26(1):47–67.

Fanney, A. H., Dougherty, B. P., and Davis, M. W. (2009). Comparison of predicted to measured photovoltaic module performance. *Journal of Solar Energy Engineering*, 131(2):021011.

Fathima, A. H. and Palanisamy, K. (2015). Optimization in microgrids with hybrid energy systems–a review. *Renewable and Sustainable Energy Reviews*, 45:431–446.

Fernández-Peruchena, C. M. and Bernardos, A. (2015). A comparison of one-minute probability density distributions of global horizontal solar irradiance conditioned to the optical air mass and hourly averages in different climate zones. *Solar Energy*, 112:425–436.

Gamarra, C. and Guerrero, J. M. (2015). Computational optimization techniques applied to microgrids planning: a review. *Renewable and Sustainable Energy Reviews*, 48:413–424.

Gansler, R., Klein, S., and Beckman, W. (1995). Investigation of minute solar radiation data. *Solar Energy*, 55(1):21–27.

Gitizadeh, M. and Fakharzadegan, H. (2014). Battery capacity determination with respect to optimized energy dispatch schedule in grid-connected photovoltaic (pv) systems. *Energy*, 65:665–674.

Greentechmedia (2014). New York plans $40m in prizes for storm-resilient microgrids. Available at: http://www.greentechmedia.com/articles/read/new-york-plans-40m-in-prizes-for-storm-resilient-microgrids.

Hafez, O. and Bhattacharya, K. (2012). Optimal planning and design of a renewable energy based supply system for microgrids. *Renewable Energy*, 45:7–15.

Hittinger, E. (2013). Understanding microgrid operation and economics with the energy system model. Blog available at http://blog.aquionenergy.com/understanding-microgrid-operation-and-economics-with-the-energy-system-model.

Hittinger, E., Wiley, T., Kluza, J., and Whitacre, J. (2015). Evaluating the value of batteries in microgrid electricity systems using an improved energy systems model. *Energy Conversion and Management*, 89:458–472.

Hollands, K. G. T. and Huget, R. (1983). A probability density function for the clearness index, with applications. *Solar Energy*, 30(3):195–209.

HOMER (2015). Website HOMER energy. http://support.homerenergy.com/.

Ibanez, M., Rosell, J., and Beckman, W. (2003). A bi-variable probability density function for the daily clearness index. *Solar energy*, 75(1):73–80.

Iqbal, M. (1983). An introduction to solar radiation. *Vancouver: Academic*.

Karaki, S., Chedid, R., and Ramadan, R. (1999). Probabilistic performance assessment of autonomous solar-wind energy conversion systems. *Energy Conversion, IEEE Transactions on*, 14(3):766–772.

Koohi-Kamali, S., Rahim, N., and Mokhlis, H. (2014). Smart power management algorithm in microgrid consisting of photovoltaic, diesel, and battery storage plants considering variations in sunlight, temperature, and load. *Energy Conversion and Management*, 84:562–582.

Lambert, T., Gilman, P., and Lilienthal, P. (2006). Micropower system modeling with homer. *Integration of alternative sources of energy*, 1(15):379–418.

Lazard (2014). Lazard's levelized cost of energy analysis — version 8.0.

LBNL Grid Integration Group (2015). Website grid integration group. Retrieved 27/02/'15.

Le Gall, L. and Stadler, M. (2013). DER-CAM version 3.9.4.m handbook.

Litchy, A., Young, C., Pourmousavi, S., and Nehrir, M. (2012). Technology selection and unit sizing for a combined heat and power microgrid: Comparison of webopt and homer application programs. In *North American Power Symposium (NAPS), 2012*, pages 1–6. IEEE.

Liu, B. Y. and Jordan, R. C. (1960). The interrelationship and characteristic distribution of direct, diffuse and total solar radiation. *Solar energy*, 4(3):1–19.

Logenthiran, T., Srinivasan, D., Khambadkone, A. M., and Raj, T. S. (2012). Optimal sizing of distributed energy resources for integrated microgrids using evolutionary strategy. In *Evolutionary Computation (CEC), 2012 IEEE Congress on*, pages 1–8. IEEE.

Mahapatra, S. and Dasappa, S. (2012). Rural electrification: optimising the choice between decentralised renewable energy sources and grid extension. *Energy for Sustainable Development*, 16(2):146–154.

Marnay, C., Venkataramanan, G., Stadler, M., Siddiqui, A. S., Firestone, R., and Chandran, B. (2008). Optimal technology selection and operation of commercial-building microgrids. *Power Systems, IEEE Transactions on*, 23(3):975–982.

Marquez, R., Davis, B., Kaur, A., and Coimbra, C. F. (2012). Characterization and cost analysis for the uc merced campus load including effects of solar farm variability. In *ASME 2012 6th International Conference on Energy Sustainability collocated with*

the ASME 2012 10th International Conference on Fuel Cell Science, Engineering and Technology, pages 997–1007. American Society of Mechanical Engineers.

Mendes, G., Ioakimidis, C., and Ferrão, P. (2011). On the planning and analysis of integrated community energy systems: A review and survey of available tools. *Renewable and Sustainable Energy Reviews*, 15(9):4836–4854.

Milan, C., Stadler, M., Cardoso, G., and Mashayekh, S. (2015). Modeling of non-linear CHP efficiency curves in distributed energy systems. *Applied Energy*, 148:334–347.

Miller, M., Johns, M., Sortomme, E., and Venkata, S. (2012). Advanced integration of distributed energy resources power and energy society general meeting. *IEEE Power and energy society general meeting*, pages 1–2.

Mills, A. (2010). Understanding variability and uncertainty of photovoltaics for integration with the electric power system. *Lawrence Berkeley National Laboratory*.

Mills, A. and Wiser, R. (2010). Implications of wide-area geographic diversity for short-term variability of solar power. *Lawrence Berkeley National Laboratory*.

MIT (2015). The future of solar energy.

NERC (2009). Accommodating high levels of variable generation. North American Electric Reliability Corporation, White paper.

Neubauer, J. and Simpson, M. (2015). Deployment of behind-the meter energy storage for demand charge reduction. Technical Report: NREL/TP-5400-63162 http://www.nrel.gov/docs/fy15osti/63162.pdf.

Olseth, J. A. and Skartveit, A. (1984). A probability density function for daily insolation within the temperate storm belts. *Solar Energy*, 33(6):533–542.

OpenEI (2015). Definition of ghi. Available at http://en.openei.org/wiki/Definition:Global_horizontal_irradiance, Retrieved on 11/03/'15.

Perez, R., Hoff, T., Herig, C., and Shah, J. (2003). Maximizing pv peak shaving with solar load control: validation of a web-based economic evaluation tool. *Solar Energy*, 74(5):409–415.

Perez, R., Kivalov, S., Schlemmer, J., Hemker, K., and Hoff, T. (2011). Parameterization of site-specific short-term irradiance variability. *Solar Energy*, 85(7):1343–1353.

Pérez-Arriaga, I. J. (2013). *Regulation of the Power Sector*. Springer.

PG&E (2015). Electric schedule a-10: Medium general demand-metered service. Information available at http://www.pge.com/tariffs/tm2/pdf/ELEC_SCHEDS_A-10.pdf.

PG&E (2015). Tariff structure. http://www.pge.com/tariffs/.

Roberts, B. (2008). Photovoltaic resource of the US. Data used from NREL, www.solreliable.com.

Rocky Mountain Institute (2014). Rate design for the distribution edge. http://www.rmi.org/elab_rate_design#pricing_paper.

Rocky Mountain Institute (2015). The economics of load defection:. Available at www.rmi.org.

Sargosis (2014). Difference between irradiance and insolation. Available at http://sargosis.com/articles/science/intro-guide/irradiance-vs-insolation/, Retrieved on 11/03/'15.

Sfetsos, A. and Coonick, A. (2000). Univariate and multivariate forecasting of hourly solar radiation with artificial intelligence techniques. *Solar Energy*, 68(2):169–178.

Sharafi, M. and El-Mekkawy, T. Y. (2014). Multi-objective optimal design of hybrid renewable energy systems using pso-simulation based approach. *Renewable Energy*, 68:67–79.

Skartveit, A. and Olseth, J. (1992). The probability density and autocorrelation of short-term global and beam irradiance. *Solar Energy*, 49(6):477–487.

Stadler, M., Groissböck, M., Cardoso, G., and Marnay, C. (2014). Optimizing distributed energy resources and building retrofits with the strategic der-camodel. *Applied Energy*, 132:557–567.

Stadler, M., Kloess, M., Groissböck, M., Cardoso, G., Sharma, R., Bozchalui, M. C., and Marnay, C. (2013). Electric storage in California's commercial buildings. *Applied Energy*, 104:711–722.

Steen, D., Stadler, M., Cardoso, G., Groissböck, M., DeForest, N., and Marnay, C. (2015). Modeling of thermal storage systems in milp distributed energy resource models. *Applied Energy*, 137:782–792.

Tiba, C., Siqueira, A. N., and Fraidenraich, N. (2007). Cumulative distribution curves of daily clearness index in a southern tropical climate. *Renewable energy*, 32(13):2161–2172.

Tovar-Pescador, J. (2008). Modelling the statistical properties of solar radiation and proposal of a technique based on boltzmann statistics. In *Modeling Solar Radiation at the Earth's Surface*, pages 55–91. Springer.

Tovar-Pescador, J., Olmo, F., Batlles, F., and Alados-Arboledas, L. (2001). Dependence of one-minute global irradiance probability density distributions on hourly irradiation. *Energy*, 26(7):659–668.

Türkay, B. E. and Telli, A. Y. (2011). Economic analysis of standalone and grid connected hybrid energy systems. *Renewable energy*, 36(7):1931–1943.

Vijayakumar, G., Kummert, M., Klein, S. A., and Beckman, W. A. (2005). Analysis of short-term solar radiation data. *Solar energy*, 79(5):495–504.

Villarreal, C., Erickson, D., and Zafar, M. (2014). Microgrids: A regulatory perspective. Report from the California Public Utilities Commission Policy & Planning Division.

Wang, J., Liu, P., Hicks-Garner, J., Sherman, E., Soukiazian, S., Verbrugge, M., Tataria, H., Musser, J., and Finamore, P. (2011). Cycle-life model for graphite-lifepo 4 cells. *Journal of Power Sources*, 196(8):3942–3948.

WashingtonPost (2015). Why Teslas announcement could be such a big deal. http://www.washingtonpost.com/news/energy-environment/wp/2015/04/30/why-teslas-announcement-could-be-such-a-big-deal/.

Wong, L. and Chow, W. (2001). Solar radiation model. *Applied Energy*, 69(3):191–224.

Woyte, A., Belmans, R., and Nijs, J. (2007). Fluctuations in instantaneous clearness index: Analysis and statistics. *Solar Energy*, 81(2):195–206.

Zhang, X. (2014). A statistical approach for sub-hourly solar radiation reconstruction. *Renewable Energy*, 71:307–314.